INFORMATION TO USERS

This manuscript has been reproduced from the microfilm master. UMI films the text directly from the original or copy submitted. Thus, some thesis and dissertation copies are in typewriter face, while others may be from any type of computer printer.

The quality of this reproduction is dependent upon the quality of the copy submitted. Broken or indistinct print, colored or poor quality illustrations and photographs, print bleedthrough, substandard margins, and improper alignment can adversely affect reproduction.

In the unlikely event that the author did not send UMI a complete manuscript and there are missing pages, these will be noted. Also, if unauthorized copyright material had to be removed, a note will indicate the deletion.

Oversize materials (e.g., maps, drawings, charts) are reproduced by sectioning the original, beginning at the upper left-hand corner and continuing from left to right in equal sections with small overlaps. Each original is also photographed in one exposure and is included in reduced form at the back of the book.

Photographs included in the original manuscript have been reproduced xerographically in this copy. Higher quality 6" x 9" black and white photographic prints are available for any photographs or illustrations appearing in this copy for an additional charge. Contact UMI directly to order.

UMI

A Bell & Howell Information Company
300 North Zeeb Road, Ann Arbor MI 48106-1346 USA
313/761-4700 800/521-0600

Ventilation Impact on Indoor Air Quality Problems in Partitioned Offices

Yan Huo

A Thesis

in

The Centre

for

Building Studies

Presented in Partial Fulfillment of the Requirements
for the Degree of Doctor of Philosophy at
Concordia University
Montreal, Quebec, Canada

February 1997

ABSTRACT

Ventilation Impact on Indoor Air Quality Problems
in Partitioned Offices

Yan Huo, Ph.D.
Concordia University, 1997

Complaints of many indoor air quality problems occur in partitioned offices. Ventilation is one way to control the contaminant distribution and to provide better indoor air quality within the office. A comprehensive research of the ventilation impact on indoor air quality problems in partitioned offices was conducted in this thesis. Experimental measurement and computational fluid dynamics (CFD) simulation methods were applied.

The study results show that, the supplied air was uniformly distributed in the ventilated area under various conditions. At the same time, the contaminant distribution was influenced by almost all kinds of parameters in the office. It was the room air flow pattern but not the uniformity of the supplied air distribution which influenced the contaminant distribution in the office. The results also indicate that the contaminant distribution in a mechanically ventilated

partitioned office need to be studied individually according to the different cases. CFD simulation is an efficient tool for such kind of studies.

The air inflow condition is one of the most important parameters affecting the air flow pattern and contaminant distribution in a mechanically ventilated room. Because of the complex geometry of the supply air diffuser and computer capacity, the conventional method of describing the supply air diffuser boundary conditions in CFD simulation may not well define the air inflow condition. The inaccurate description to the air inflow condition could lead to a totally unrealistic simulation result of the air flow inside the office. A new method to correctly describe the diffuser boundary conditions in CFD simulation was proposed in this thesis. The model prediction was validated with the experimental data in a literature and the results from the experimental part of this thesis. The CFD predictions applying the new method were in good agreement with the experimental results.

ACKNOWLEDGEMENT

I would like to express my greatest gratitude to my supervisor, Dr. F. Haghighat, for his continued guidance, support, encouragement and patience, for his lively and fruitful discussions regarding this research.

Extended thanks go to Dr. C.Y. Shaw and Dr. J.S. Zhang of National Research Council, Canada, for their helpful suggestions and valuable advises.

Dr. Z. Li from the University of Illinois kindly provided the detailed measurement data for the diffuser validation. His support is highly appreciated.

The financial assistance from Natural Science and Engineering Research Council of Canada is gratefully acknowledged.

Finally, I would like to thank my wife and my parents, for their love, support and patience while I finished this thesis.

Table of Contents

List of Figures

List of Tables

Nomenclature

A	Gross area of diffuser
A_{eff}	Effective area of diffuser
Ar	Archimedes number
C	Contaminant (tracer gas) concentration at sampling location
C_s	Contaminant (tracer gas) concentration at the supply duct
C_{ra}	Contaminant (tracer gas) concentration at the exhaust air duct
C_{std}	Standard deviation of contaminant (tracer gas) tracer gas concentration
C_{avg}	Average contaminant (tracer gas) concentration
E	Contaminant removal efficiency
g	Gravitational acceleration
H_0	Effective width of the linear diffuser jets
h	Heat generation rate
K	Thermal diffusivity
K_1	Diffuser centerline velocity decay constant
K_2	Diffuser centerline temperature decay constant
k	Turbulent kinetic energy
L	Length scale
U_m	Uniformity of the contaminant (tracer gas) concentration

u	Air velocity
u_0	Average air velocity at the diffuser discharge
u_m	Air velocity on the diffuser centerline
V	Mean air velocity
V_s	Supply air velocity
PD	Percentage of dissatisfied people due to draught
Q_s	Supply air flow rate
r	Radial distance
T	Mean temperature of the room air
T_a	Outdoor air temperature
T_0	Supply air temperature
T_m	Temperature on the diffuser centerline
T_r	Return air temperature
t	Time
ε	Dissipation rate of the turbulent kinetic energy
ν	Kinematic viscosity of the air
ν_t	Eddy viscosity of the air
θ	Temperature difference
ρ	Density of air
τ_p	Local mean age of air at point p

CHAPTER 1

INTRODUCTION

1.1 INDOOR AIR QUALITY (IAQ) PROBLEMS

Indoor Air Quality (IAQ) refers to the effect, good or bad, of the contents of the air inside a structure, on its occupants. Usually, temperature (too hot or too cold), humidity (too dry or too damp), and air velocity (draftiness or motionlessness) may also make someone uncomfortable inside a structure. Most IAQ professionals will take these factors into account in investigating air quality situations.

Good IAQ is the quality of air which has no unwanted gases or particles in it at concentrations which will adversely affect someone. Poor IAQ occurs when gases or particles are present at an excessive concentration so as to affect the satisfaction or health of occupants.

It is important to note that the concentration of the contaminant or contaminants is crucial. Potentially infectious, toxic, allergenic, or irritating substances are always present in the air. There is nearly always a threshold level below which no effect occurs (Namiesnik 1992).

According to the World Health Organization 1984 report, approximately 30% of all commercial buildings have significant IAQ problems (Byrd 1995). IAQ problems are increasingly realized in office and commercial buildings, which are usually mechanically ventilated or air-conditioned by a HVAC system.

Many people working in office or commercial occupations suffer from symptoms of illness caused by working in buildings with bad indoor climate conditions. These symptoms are referred to as "Sick Building Syndrome". When more people than expected suffer from these symptoms and they appear to be related to staying in the building, the building is often considered "Sick". These symptoms usually appear after a short stay in the building and gradually increase during the day. In general, the symptoms quickly disappear after people leave the building.

The uncomfortable working environment could significantly influence the productivity of workers. For some allergic persons, the sickness caused by IAQ problems could be very strong.

1.2 CAUSES OF IAQ PROBLEMS

IAQ is a new field in many ways. Much of the current knowledge is less than 20 years old, and there is a great deal that is not known about it. In fact, it is safe to say that far more is unknown than is known about the field at this time (Byrd 1995).

It is rarely possible to explain the cause of IAQ problems through the influence of a single factor. Usually more than one factor may cause the same problem. The causes of IAQ problems could be divided into physical, chemical, biological and psychological factors (Valbjorn 1990).

Physical factors include temperature, humidity, air flow velocity and amount of outdoor air in a room, etc. They are influenced by the HVAC system of the room. According to his study, Woods et al (1988) found that unsatisfactory ventilation or poor maintenance of the HVAC system were the common denominator in many buildings which had IAQ problems. When the HVAC system does not work properly, the harmful contaminants in the room cannot be efficiently removed. Sometimes, the contaminants in the HVAC system itself can cause the IAQ problems. Poor maintenance of the HVAC systems is also a well known cause of indoor air pollution and its health consequences (Collett et al 1988).

Ventilation is an important parameter in air quality. All the harmful contaminants need to be exhausted by using the ventilation system. The ventilation system should be effective in

removing all possible pollutants. There is a minimum outdoor air supply to provide outdoor air to the occupants. The more outdoor air is supplied, the more energy is needed. How much outdoor air should be designated as the minimum outdoor air supply is important. This value is not easy to decide.

Chemical factors include tobacco smoke, formaldehyde, volatile organic compounds (VOC), combustion gases, radon, odors and other gaseous substances present in the room. New building materials and some office machines release these types of contaminants. If they are not removed or diluted efficiently, they become sources which produce IAQ problems.

Biological factors such as allergies and some psychological factors also affect the occupants' feeling about the indoor environmental comfort. About 20% of the human population displays one or more inhalant allergies. An insignificant problem with the indoor air may have significant influence on allergic people. Some allergic people can hardly stay a moment in a room with IAQ problems.

1.3 IAQ PROBLEM STUDIES

Indoor air quality experts generally agree that the two most effective means of achieving acceptable indoor air quality are by controlling the release of contaminants into the

air at their sources and by removing or diluting the contaminated air. Research about indoor air quality problems could be divided into two different categories: controlling the contaminant source and providing better ventilation.

Studies show that 28% of the indoor air pollution in investigated areas come from occupants, while the other pollution originates from building materials and HVAC systems (Zhang Y. et al 1996). Over the last few years, considerable work has been conducted on studying building materials emissions and controlling other contaminant sources. Although the emission of the pollutant could be controlled as little as possible, there are always some pollutant sources that cannot be controlled. The building ventilation system is the last line of defense against indoor pollutants. As a result, a detailed knowledge of source characteristics and local ventilation system performance is required to ensure that the ventilation system provides pollutant control at reasonable ventilation rates.

Tightly constructed buildings, such as most modern commercial buildings, depend on outdoor air supplied by the ventilation system to dilute contaminants normally generated and present within a building. There are always some contaminants, when outdoor air supplied is insufficient, they can build up to a point where they become a problem for people.

Ventilation systems can cause pollutants to flow from one location in a building to another. Improper pressure relationships can direct pollutants where they do not belong, or

they can fail to dilute or remove pollutants from a building or a portion of it. A major cause of IAQ problems is an improperly designed, installed, operated, or maintained ventilation system.

The amount of outdoor air introduced into the room and the distribution and mixing of outdoor and contaminated air determine the air quality at different locations within the room. Air distribution systems can be designed and operated to provide clean air in some areas of a room while people are working with hazardous airborne materials in other areas of the same room. Opportunities exist to expand the technologies for controlling airflow and air mixing within rooms to achieve the desired air quality in the occupied parts of rooms, even though air quality may be less than desired in the unoccupied parts.

Considering that a lot of complaints about indoor air quality problems come from people working in office and commercial buildings, especially in partitioned offices, the work in this thesis will concentrate on the ventilation impact on indoor air quality problems in partitioned offices.

1.4 PROPOSED CONTRIBUTIONS

Nowadays, indoor air quality and thermal comfort problems in buildings are becoming increasingly important. In particular that many indoor air quality complaints come from people

working in partitioned offices that are mechanically ventilated. Indoor air quality and thermal comfort conditions in this type of office are strongly influenced by the ventilation air distribution in the room. It is very important to carefully study the ventilation air distribution and indoor air quality problems in such an office.

There are many parameters that influence the air distribution and indoor air quality in a mechanically ventilated partitioned office. To obtain acceptable indoor air quality and thermal comfort levels, all these parameters need to be taken into account and studied in detail. It is necessary to accurately predict the air distribution and ventilation effectiveness. This will aid engineers to design, diagnose and analyze ventilation systems and office arrangements in partitioned offices.

Predicting and assessing the indoor air distribution and air quality can be achieved by two main methods: experimental investigation and numerical prediction. These methods have different advantages and disadvantages, and may be used under different conditions.

The most reliable information regarding a physical process is often given by actual measurement. Such measurements involving full scale equipment, are usually expensive, time consuming and complicated. It is impractical, if not impossible, to apply this method to each case with which one is concerned. However, the measurement method is valuable when the general information about the relationship between the indoor air distribution and air quality in partitioned offices is desired. The measurement results will also provide an indication of the

kinds of parameters and geometry that most critical for the analysis of indoor air distribution and air quality. This could help simplify the consideration of the boundary conditions in numerical prediction.

The numerical prediction method is inexpensive than measurement. It can be applied to any case with which one is concerned. More information can be obtained from numerical prediction. Computational Fluid Dynamics (CFD) simulation is a numerical prediction method to assess the air and contaminant distribution in a room. This method has been well recognized in air movement analysis. Extensive powerful commercial software has been developed. It is a very useful tool for assessing indoor air distribution and air quality problems in partitioned offices. CFD simulation results can provide the guidelines to help in the design and analysis of ventilation systems and office arrangements. It can also be applied for the on-line analysis of a given special case with which one may concern at a given time.

The supply diffuser (supply outlet) boundary conditions is one of the most important parameters affecting the air distribution in a mechanically ventilated room. Real supply diffusers often have very complicated geometry. Because of the complex geometry of the supply air diffuser and computer capacity, the conventional method of describing the supply air diffuser boundary conditions in CFD simulation is difficult and may give incorrect results for some cases. When the supply diffuser boundary is not well defined to correctly express the air inflow condition, the simulation of the air flow inside the office could lead to a totally wrong result. An accurate specification method is needed.

A comprehensive study of the ventilation impact on indoor air quality problems in partitioned offices was conducted in this thesis. Experimental measurement and CFD simulation methods were applied. The experimental study was conducted to identify the parameters which significantly influence the air and contaminant distribution in an office. The CFD study was conducted to predict the air flow pattern in an office which is difficult to achieve by experiment. A new method to correctly describe the diffuser boundary conditions in CFD simulation was proposed to make the IAQ analysis more accurate when applying the CFD simulation method.

The expected contributions of this thesis are :

1. Experimental and computational data for identifying the important parameters which influence the indoor air distribution and contaminant distribution in partitioned offices, and
2. Proposing the new jet main region specification method to describe the complicated diffuser boundary conditions for CFD simulation.

CHAPTER 2

LITERATURE REVIEW

2.1 TOPICS TO BE REVIEWED

The literature about the research applied in this thesis is reviewed in this chapter. The topics are experimental studies, CFD simulation method, diffuser boundary conditions specification in CFD simulation. They showed the conditions and potentials of ventilation effect on IAQ problems in partitioned offices.

2.2 REVIEW OF THE EXPERIMENTAL STUDIES

Supplied air distribution in an office has been studied by many researchers. Miller (1971) studied the room air distribution performance using different types of supply diffusers. Int-Hout (1981) studied indoor air diffusion in actual office environments to predict the thermal

comfort. The study of contaminant distribution and indoor air quality problems in a partitioned office was just started.

Ventilation systems have traditionally been designed to provide odor control and thermal comfort under the assumption that the air in a building is perfectly mixed. Increased concern over the health impacts of indoor air pollutants has led to the need for more accurate methods of determining indoor pollutant transport and exposure (Davidge et al 1990).

ASHRAE standard 62-1989 "Ventilation for Acceptable Indoor Air Quality" states that "Acceptable indoor air quality is achieved by providing ventilation air of specified quality and quantity to the space" (ASHRAE 1989).

For most buildings, the quality and quantity of ventilation air can be determined by measuring the minimum ventilation rate, air distribution patterns, contaminant flow patterns and re-entrainment of exhaust air (Shaw 1992).

Age of air methods can be used to detect spatial variations of air distribution by comparing the residence time of the air as a function of room location. The spatial average age of room air can be used to define a measure of air exchange efficiency. The air change efficiency is a measure of how quickly the air in a space is replaced. There are two definitions for this term. European researchers (AIVC 1990) define the air exchange efficiency as the ratio between the nominal time constant and the air exchange time for the location. ASHRAE

defines the air exchange efficiency as the ratio between the mean age of air at the breathing height of one location and average age of all the air in the room.

Ventilation efficiency is an important parameter in diagnosing indoor air quality problems and in designing spaces capable of providing acceptable indoor air quality in an energy efficient manner. Poor ventilation efficiencies can lead to the local buildup of contaminants that may affect the health or comfort of the occupants. Investigation of ventilation efficiencies in a building, therefore, becomes a useful procedure for evaluating the performance of a building HVAC system.

Ventilation systems that selectively remove pollutants will have higher average concentrations in the exhaust than in the room. Systems that are not very efficient at removing pollutants will have lower average concentrations in the exhaust than in the room. To quantify this effect, AIVC (1991) defined ventilation efficiency to be the ratio of the concentration in the exhaust to the average room concentration at steady state.

Tracer gas methods were usually used for studying the mean age of air and ventilation efficiency (Shaw 1992, Takai et al 1996). Since more IAQ complaints come from offices with partitioned workstations, some experimental work have been concentrated in this research area.

Eftekhari (1996) studied the mean age of air and air changes efficiency using SF_6 tracer gas. Doi (1996) measured the multi-zone air flow and Takai et al (1996) studied the accuracy of multiple tracer gas techniques.

Bauman et al (1991) experimentally investigated the air quality in workstations formed by partitions using the tracer gas technique. They found that heat sources have a strong influence on the air movement. The other parameters they studied did not have a significant effect on the air distribution. Shaw et al (1993a, 1993b), also using tracer gases, examined the air distribution, mean age of air and ventilation efficiency for workstations considering the partition gap, surrounding areas and other parameters. They found that the parameters studied have minimal effects on the air distribution at the workstation. Menzies et al (1993) reported considerable differences in the concentration of indoor contaminants, temperature, relative humidity, and air velocity between workstations on the same floor. Scheller et al (1990) also experimentally examined the air movement and thermal comfort in partitioned offices.

Research of the ventilation impact on partitioned offices is still in its initial stage. Only cases with simple geometry and room layout were studied by the above mentioned researchers.

2.3 REVIEW OF THE CFD SIMULATION METHOD

Numerical modeling is one way to assess the air distribution in a ventilated room. The numerical prediction method is relatively inexpensive, can be applied to any case, and more information can be obtained. Computational Fluid Dynamics (CFD) is a good prediction method to assess the air distribution in a room. This method has been highly recognized in air movement analysis. Powerful commercial software have been developed (Kurabuchi 1989). They had been used to study the air temperature and air velocity distributions in industrial applications and were seen as a potential tool to predict and model time dependent distribution in enclosed spaces (Guthrie 1996).

The turbulence model applied in the CFD simulation software is important. Problems in turbulence model closure have been studied by many researchers. The two-equation k-ε model is primarily used for IAQ analysis (Haghighat et al 1991, and Chaturvedi et al 1989).

Turbulent flow models consist of many assumptions and experimental constants. The empirical constants used in the k-ε model are described by Rodi and Spalding (1983). Many studies on these constants have been conducted (Ohishi et al 1989). While evaluating the degree of approximation for different types of flows, one must consider the actual phenomena in question. A model can be made to agree with the actual phenomena by adjusting different constants.

The current k-ε two-equation model has been found to work well when simulating a fully developed and isotropic turbulent flow, but is expected to fail for flow with weak turbulence. The model also has some problems accurately simulating air flow in the area adjacent to a wall. This model can however be used in the IAQ analysis. The offices studied for IAQ analysis were usually mechanically ventilated and the turbulence was strong. Furthermore, the mainly concerned study in IAQ analysis for offices was the air flow pattern inside the room, but not that near the walls.

Some researchers, such as Peng et al (1996), Murakami et al (1996) and Davidson and Nielsen (1996), are working to improve the turbulence models in CFD simulation. Some other researchers, such as Brohus et al (1996), are studying the detailed model of people and furniture in the studied room when applying the CFD simulation method.

Tools are still needed to study certain aspects of modeling complicated airflow fields. As computational power increases, it will be possible to study very complex flow models and boundary conditions by using future super-computers.

There are different numerical methods to solve the k-ε two-equation model. Some CFD programs use the finite difference method (FDM). The finite difference method uses a orthogonal coordinate system with equally and/or unequally spaced grids. Equations are solved by iteration or by the successive over-relaxation (SOR) method (Kurabuchi 1989).

The finite element method (FEM) is another numerical method. While the finite difference method uses a orthogonal grid network, in the finite element method it is possible to use elements of any shape. However, equations to describe boundary conditions in FEM are more complicated than in the FDM. In addition, programming the FEM for a fluid dynamics problem is much more complicated. The computer memory and computer time required to solve the FEM representation of flow equations are much larger than in the FDM.

Other advanced numerical methods like large eddy simulation (LES) and direct numerical simulation (DNS) exist for CFD simulation. They are more complicated. The large-scale eddy simulation method promises to provide statistically realistic indications of the eddying nature of ventilation air movement, but it needs a much longer simulation time. Only very simple geometry was applied when these kinds of methods were used for ventilation related simulation (Davidson and Nielsen 1996).

Considering the complicated geometry and three dimensional, non-isothermal cases simulated in this thesis, the FDM method is applied. Given the status of computer power today, the complicated methods have difficulties to practically simulate these complicated cases in an acceptable simulation time.

The boundary conditions to be considered for the calculation of airflow in a room may be the air inlet, air outlet, walls, interior furnishings, symmetric planes, heat and contaminant sources, as well as sinks. It is necessary to set the values or gradients of independent variables

at these boundaries. The boundary conditions in actual rooms are extremely complicated. Data are needed for simplifying the boundary region calculation and for simulating simplified boundary models.

CFD codes have been successfully applied by expert users to analyze practical problems in a research environment. However, HVAC engineers do not generally find these codes useful in supporting alternative design assessments. Particularly limiting are the difficulties in modeling the complex geometry in rooms for real case IAQ analysis. Handling complex geometry in a real office will dramatically increase the simulation time and take the big risk of unstable solutions.

CFD software nowadays, including the very good commercial software, are relatively difficult to use. It regularly takes about half a year for the user to feel comfortable with the software (Chen and Jiang 1992b).

Numerical computation can easily become unstable. If attempts are made to improve the stability, accuracy may be sacrificed. The running of a CFD simulation could be very time consuming. Realistic problems require expert adjustments for a converged numerical solution. This prompts some new users to develop their own code so as to be knowledgeable about the adjustable built-in parameters.

Because orthogonal grids are used, the finite difference method has difficulties in specifying the complicated geometry. The most important problem that could occur when simulating a realistic case is the correct specification of the supply diffuser boundary conditions. The simplification of the diffuser boundary conditions could cause large discrepancies.

In a mechanically ventilated room, the supply air flow condition is a very important parameter affecting the air flow distribution in the room. It dominates the air flow in the room. Real supply diffusers often have very complicated geometry. Because of the complex geometry of the supply air diffuser and computer capacity, the conventional method of describing the supply air diffuser boundary conditions in CFD simulation is difficult and may give incorrect results for some cases. When the supply diffuser boundary is not well defined to correctly express the air inflow condition, the simulation of the air flow inside the room could lead to a totally unrealistic result.

Recent advances in computational fluid dynamics and computer power have provided tools that can accurately predict some features of airflow within ventilated spaces (Albright 1989). The CFD method has been successfully applied for air flow analysis in relatively complicated conditions, like non-isothermal, three dimensional conditions and furniture inside the room. Haghighat et al (1991) numerically studied the effect of door locations in a partition on contaminant removal efficiency and thermal comfort in a two-zone enclosure. Haghighat et al (1994b) also numerically studied the indoor air quality in a newly painted office and assessed the effects of ventilation rate and partition layout on the pre-ventilation time required to allow

the contaminant concentration level to drop to an acceptable level. Zhang et al (1992a) evaluated a numerical simulation model for predicting room air velocity, turbulence kinetic energy and temperature. Chen and Jiang (1992a) numerically studied the indoor air quality and thermal comfort in a classroom filled with people and furniture.

2.4 THE DIFFUSER BOUNDARY CONDITIONS SPECIFICATION

The supply diffuser (supply outlet) boundary conditions specification has become a key factor to correctly simulate the air flow distribution in a room for IAQ analysis using CFD simulation method.

For a real diffuser, the geometry of the diffuser could be very complicated. Considering the ability of the CFD simulation software nowadays, it is not realistic to use many small grids to accurately describe all the details of the diffuser geometry. Usually a simplified opening area is used for the supply area.

While the conventional method, widely used in CFD simulation for room air flow analysis, is applied, the description of the supply diffuser boundary conditions is as follows:

1. Consider the supply diffuser as a simple free opening.
2. The supply velocity component perpendicular to the free opening plane is calculated as the ratio of the supply air flow rate and the area of the free opening, Q_s/A.

3. The supply velocity component parallel to the free opening plane is neglected or calculated based on manufacture's data.

Even though many validations of this method have been studied, the cases studied used only diffusers with simple geometry that the free opening area equals to the effective diffuser area. This method may cause errors for diffusers which have complicated geometry.

In reality, the supply diffuser could be very complicated. If the diffuser has complicated geometry, such as louvered or perforated face, with vane, or curved surface, the real effective diffuser area will be different with the diffuser opening area.

The supply diffuser could look like the one shown in Figure 2.1. The supply air flow rate and supply air velocity have the following relationships:

$$V_s = \frac{Q_s}{A_{eff}} \qquad (2.1)$$

$$A_{eff} = C_d * A \qquad (2.2)$$

Where, Q_s is the supply air flow rate,

V_s is the supply air velocity,

A_{eff} is the effective area of diffuser,

A is the gross area of diffuser, and

C_d is the coefficient of discharge.

rate is constant, the supply air velocity vector will be smaller than the real situation. It leads to the wrong prediction of the velocity in the entire room.

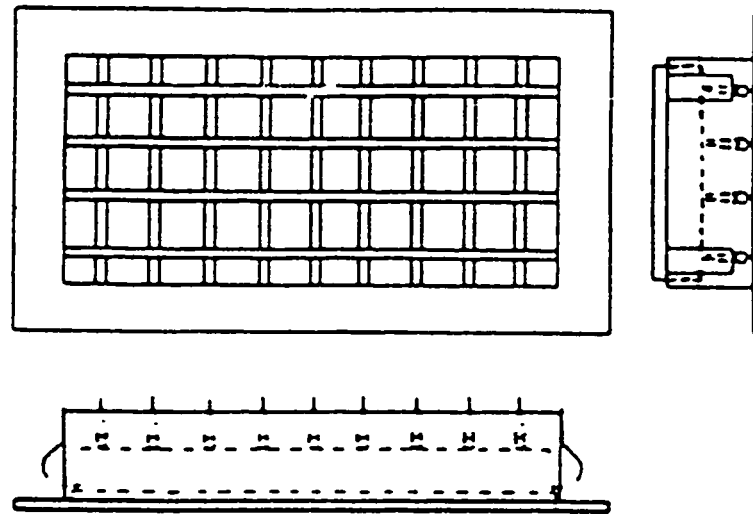

Figure 2.1 A Real Diffuser Geometry

Some researchers have encountered problems when using the conventional simplification method in their research work.

Kurabuchi (1989) studied the air flow pattern in a ventilated room. The diffuser he used had a complicated geometry. He simplified it using the conventional method. The diffuser was considered as an opening. The measured supply velocity was used in the simulation. The supply area was considered as the area of free opening. His simulation results showed that the

free opening. The simulation results showed that the supply air went straight to the opposite wall. But in the measurement, the air flow started to turn back in the middle of the room. The reason for this difference is that a higher supply air flow rate was used in the simulation than occurred in reality.

Some other researchers found similar problems in their simulation work (Chen et al, 1991a). They tried another way of using the conventional description method. The supply area was simplified as an opening which has the same area as the effective diffuser area and is smaller than the real one. The supply air velocity can then be calculated correctly by using the actual supply area. But the results showed that the prediction of the velocity around the diffuser is not in agreement with the measurement results. Both the simplified and the real diffuser are supplying the same amount of air flow but the profile is different for the two cases. This method cannot work well either. The smaller diffuser opening area used in the simulation than occurred in reality caused the problem.

The problem of diffuser boundary conditions simplification does not only occur for a diffuser whose supply opening area is different from its effective supply area. The boundary conditions for square or round diffusers, widely used in office buildings, are also difficult to simplify. Figure 2.2 shows a square diffuser. From the dimension list of the square diffuser series, the connecting duct to the square diffuser could have different diameters for the same diffuser. It means that the same diffuser under the same flow rate could have different supply conditions. The conventional method definitely cannot handle this type of diffuser.

IMPERIAL

INCHES

SIZE	A	B	C	D	E	F
5	5	—	11¾	4	¾	5½
6	6	—	11¾	4	¾	5½
7	7	—	11¾	4	¾	5½
8s	8	—	11¾	4	¾	5½
8	8	—	23¾	4	2¼	7
10	10	—	23¾	4	2¼	7
12	12	—	23¾	4	2¼	7
15s	15	—	23¾	4	2¼	7

METRIC

MILLIMETERS

SIZE	A	B	C	D	E	F
5	127	—	298	102	19	140
6	152	—	298	102	19	140
7	178	—	298	102	19	140
8s	203	—	298	102	19	140
8	203	—	603	102	57	178
10	254	—	603	102	57	178
12	305	—	603	102	57	178
15s	381	—	603	102	57	178

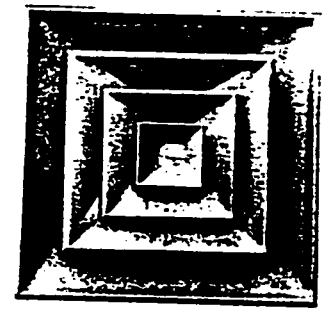

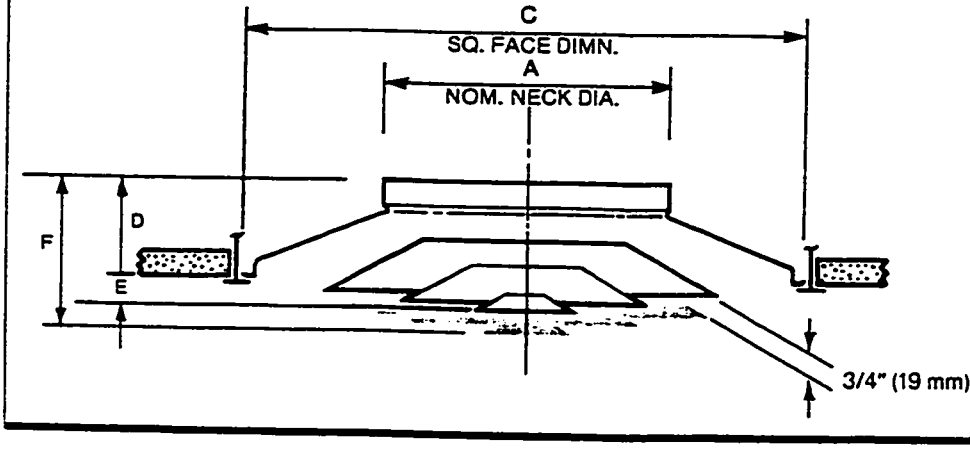

Figure 2.2 A Series of Square Diffusers

The swirl diffuser is also widely used in office buildings. Like the square diffuser, Christianson (1994) found that the baffle, placed in either the lower or upper position for the same swirl diffuser, could result in an absolutely different air flow pattern (Figure 2.3). The round geometry of the swirl diffuser is also a big problem when orthogonal grids are used in the simulation.

Currently, there are several modeling methods to describe the complicated boundary conditions at the supply openings.

Chen (1991a) proposed a new momentum method to overcome the problem in the conventional description method. In his method, the supply opening area was considered the same as in the conventional method. The velocity vector was calculated based on the effective area, not the opening area, in order to have the correct velocity description. To keep the right supply air flow rate and to introduce the same amount of air into the room, the boundary conditions for the continuity equation and the momentum equations are separately described. Chen (1991b) and Jiang (1992) simulated diffusers with complicated geometry using the momentum method. The results showed this method is applicable for the diffuser studied. Most of the commercial CFD software do not support the separate boundary conditions description for continuity and momentum equations. This method also needs to be validated for more diffusers.

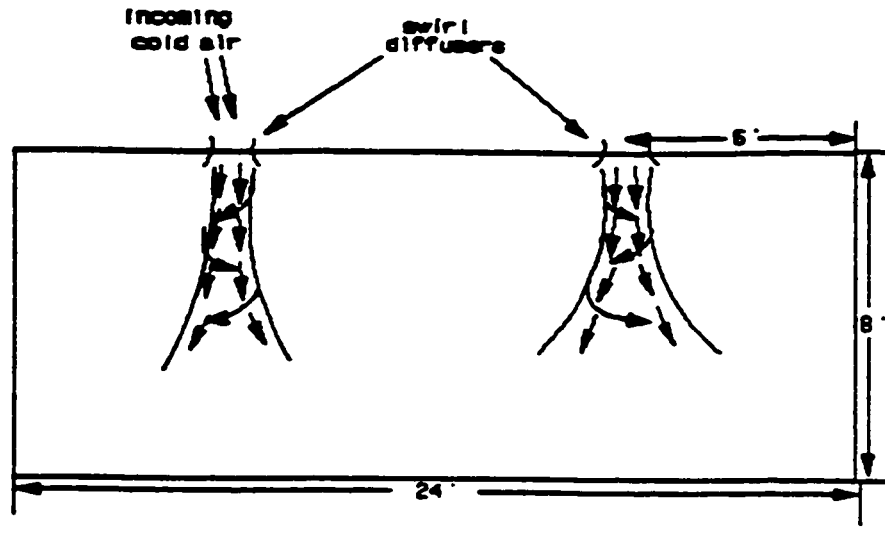

(a) with baffles up

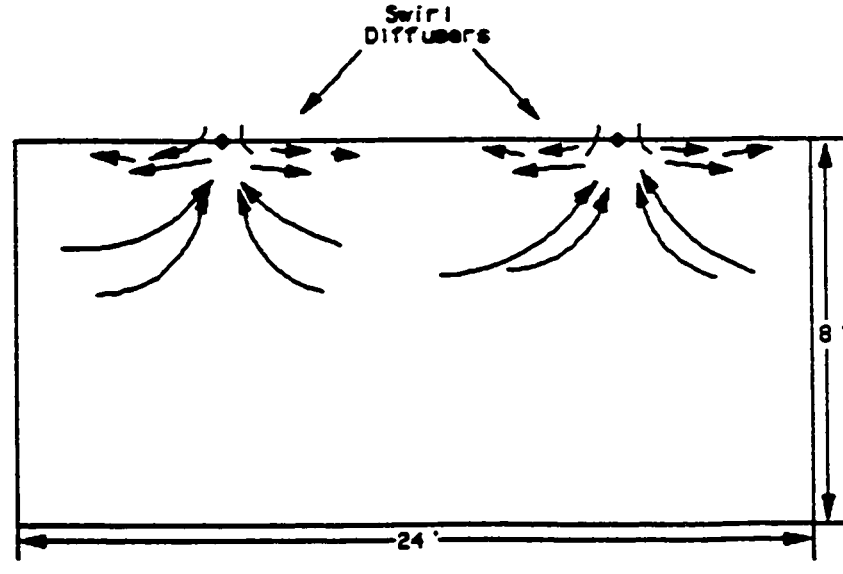

(b) with baffles down

Figure 2.3 Schemes of the Swirl Diffuser Jet

Nielsen (1978) proposed a box method for diffuser description in which he assumed a box located around the diffuser. The description of the diffuser boundary conditions is transferred to the description of the box boundary conditions. The boundary conditions at the box surface parallel to the supply opening surface were decided by measurement. The boundary conditions at the box surface perpendicular to the supply opening surface were considered as $\partial\Phi/\partial n=0$. n is the direction parallel to the studied surface. Φ is velocity u, v, kinetic energy k and the dissipation rate of kinetic energy ε etc. Compared with his measurement data, good results were obtained for this method. Considering the detailed measurements that have to be conducted for every diffuser studied, this method is not very practical.

Nielsen (1992) proposed another new method called the velocity prescription method. It improved his earlier box method. This time, the diffuser boundary conditions were specified using the conventional method. At the same time, one component of the velocity was measured inside his assumed box area. The velocity component values inside the box were prescribed as extra boundary conditions to correct the unsatisfied velocity prediction around the diffuser area. It was said the results were very good for the diffuser studied. Applying this method, measurement for every diffuser studied is still needed. The boundary conditions description for the complicated supply diffuser cannot be avoided.

Chen and Jiang (1996) simulated a two-dimensional diffuser with complex geometry. The diffuser was presented in detail in the simulation. They used the finite volume method and

tried different coordinates and grid systems. They demonstrated it is possible to present the very detail of a complex diffuser in CFD simulation using state-of-art techniques. They also presented the difficulties of this kind of diffuser presentation in CFD simulation and great demand for computer capacity.

Emvin and Davidson (1996) reviewed the different diffuser description methods. They found that the full representation of the supply diffuser is accurate but expensive and very time consuming. The momentum method can give qualitative results but cannot properly represent the entrainment of the supply diffuser and may only works on coarse meshes. The box model is consistent and should perform as well as the full representation, but will require measurements.

There is still a considerable amount of researchers using the conventional method to present complex diffusers in their recent CFD simulations. It is important to propose a supply diffuser boundary conditions specification method to present the real supply diffuser correctly without performing any measurements or sacrificing accuracy. This will make the CFD simulation more practical in HVAC design and IAQ analysis.

CHAPTER 3

DESCRIPTION OF EXPERIMENTAL STUDY

3.1 OBJECTIVES OF THE EXPERIMENTAL STUDY

Experimental study was conducted first to obtain more general information about the ventilation effect on indoor air quality problems in partitioned offices since little research work had been accomplished in this area.

Many factors affect the airflow pattern, contaminant removal efficiency and indoor air quality in partitioned offices. The objectives in ventilating a building are to efficiently distribute ventilation air to the occupied zones and to remove or dilute indoor contaminants. The performance of a ventilation system is judged by its local mean age of air, contaminant removal effectiveness and the thermal conditions. The distribution of ventilation air within buildings is influenced by many parameters, such as the type of supply air diffuser, the dimension and location of the supply and exhaust openings, the geometry of the room, the thermal condition, and the room lay-out.

A detailed experimental work was conducted to study the effect of ventilation supply and return, office furniture design and workstation layouts on ventilation performance, contaminant removal effectiveness and occupants' comfort in workstations (Huo et al 1995). The range of furniture configurations and environmental parameters investigated included:

1) partition heights,

2) partition air gap size at the bottom,

3) diffuser type,

4) air supply diffuser positions relative to workstation,

5) air return grille positions relative to workstation,

6) heat source influence,

7) furniture influence,

8) supply air temperatures,

9) influence between workstations,

10) contaminant source locations,

11) supply air flow rates, and

12) outdoor air flow rates.

The tracer gas technique was used to experimentally study the relative impact of these parameters on the air distribution and ventilation performance, as well as

contaminant removal effectiveness. Thermal environmental parameters, such as air velocity and temperature, were monitored at several locations to characterize the impact of these parameters on the occupants' thermal comfort (Haghighat et al 1996).

3.2 EXPERIMENTAL PROCEDURE

The experiment was conducted in a controlled environment at the Institute for Research in Construction of the National Research Council Canada. The controlled environment consists of two interconnected rooms, the dimensions of each room are 4.9m*4.8m*2.9m high. These two rooms could be connected to form one large space by removing the wall between them. Each room was equipped with an independent HVAC system, and furnished with two basic designs of supply air outlets and return air inlets: recessed air light fixtures (slot diffusers, 1.2 m or 4 ft long) and square ceiling diffusers, as shown in Figure 3.1. The slot diffusers were fixed but the square diffusers could be moved from one location to another. Dampers and orifice plates were installed in the supply, return, outdoor air supply and exhaust ducts to control and measure the air flows through the ducts.

Based on the parameters identified, three different set-ups were considered in this investigation, and a total of 21 tests were carried out, as shown in Table 3.1.

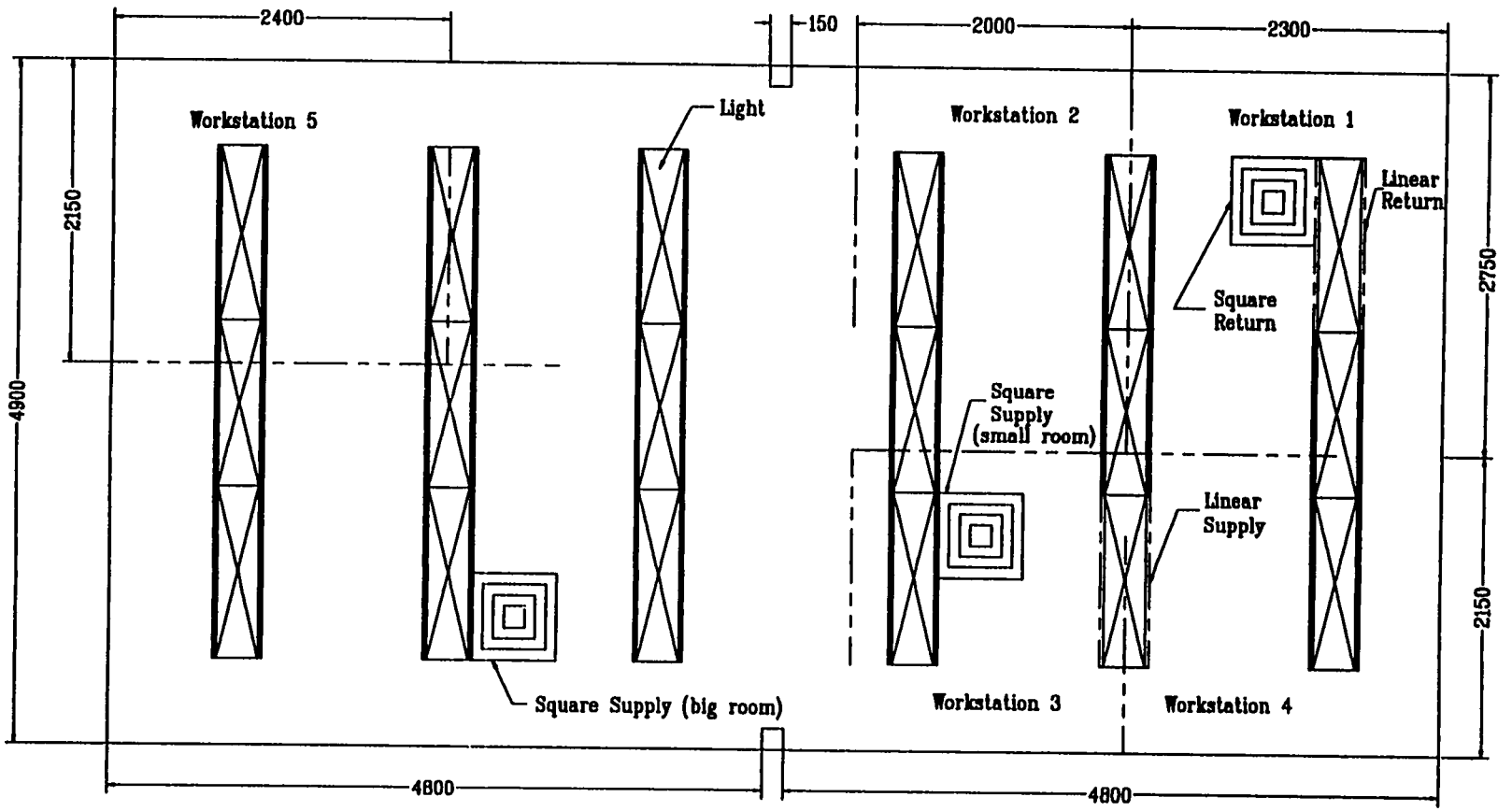

Figure 3.1 Reflected Ceiling Plan of the Test Room

Table 3.1 The Conditions of the Test Cases

Case	Room size	Workstation present	Diffuser type	Supply air flow rate	Outdoor air flow rate	Contaminant source	Partition height (m)	Partition gap size (m)	Heat source	Furniture present	Supply air temp.	Thermal comfort test
001	small	WS#1	linear	30 L/s	10 L/s	#1	1.8	0.15	yes	yes	17 °C	WS#1
002	small	WS#1	square	30 L/s	10 L/s	#1	1.8	0.15	yes	yes	17 °C	WS#1
003	small	WS#1	square	30 L/s	5 L/s	#1	1.8	0.15	yes	yes	17 °C	WS#1
004	small	WS#1	square	73.8 L/s	7.4 L/s	#1	1.8	0.15	yes	yes	17 °C	WS#1
005	small	WS#1	square	100 L/s	10 L/s	#1	1.8	0.15	yes	yes	17 °C	WS#1
006	small	WS#1	square	30 L/s	10 L/s	#1	1.8	0.15	no	yes	17 °C	WS#1
007	small	WS#1	square	30 L/s	10 L/s	#1	1.8	0.15	no	no	17 °C	/
008	small	WS#1	square	30 L/s	10 L/s	#1	0	0	no	no	17 °C	/
009	big	WS#1,2,3,4	square	100 L/s	37.8 L/s	#1	1.8	0.15	yes	yes	17 °C	/
010	big	WS#1,2,3,4	square	100 L/s	37.8 L/s	#3	1.8	0.15	yes	yes	17 °C	WS#2,3
011	big	WS#1,2,3,4	square	100 L/s	37.8 L/s	#2	1.8	0.15	yes	yes	17 °C	WS#1,4
012	big	WS#1,2,3,4	square	100 L/s	37.8 L/s	#2	1.8	0	yes	yes	17 °C	/
013	big	WS#1,2,3,4	square	100 L/s	37.8 L/s	#3	1.8	0	yes	yes	17 °C	WS#2
014	big	WS#1,2,3,4	square	100 L/s	37.8 L/s	#3	1.8	0	yes	yes	30 °C	/
015	big	WS#4	square	100 L/s	37.8 L/s	#3	1.8	0.15	yes	yes	17 °C	/
016	big	WS#4	square	100 L/s	37.8 L/s	#3	1.8	0.15	no	yes	17 °C	/
017	big	WS#1,2,3,4	square	100 L/s	37.8 L/s	#3	1.5	0	yes	yes	17 °C	WS#2
018	big	WS#1,2,3,4	square	100 L/s	37.8 L/s	#2	1.5	0	yes	yes	17 °C	/
019	big	WS#1,2,3,4	square	100 L/s	37.8 L/s	#4	1.8	0.15	yes	yes	17 °C	/
020	big	WS#1,2,3,4	square	100 L/s	37.8 L/s	#4	1.8	0	yes	yes	17 °C	/
021	big	WS#5	square	100 L/s	37.8 L/s	#5	1.8	0.15	yes	yes	17 °C	WS#5

3.2.1 First Set-Up

This study was conducted in one room, and partitions were set up to produce a 2.9m*2.6m workstation (workstation #1), as shown in Figure 3.2(a). The partitions were 1.8 m high with an air gap of 0.15 m at the bottom. The arrangement of furniture included a desk, a 60 W desk lamp, a chair, a table, a book case, a 90 W computer and a file cabinet. A 100 W light bulb was placed on the chair to simulate the sensible heat generated by the office worker. Two types of diffusers, linear and square, were used in this study. The diffusers were placed outside the workstation. A total of 8 experiments, Case 001 to Case 008, were performed for this set-up, as shown in Table 3.1. The experiments were designed to study the influence of (Haghighat et al 1994a):

a) the diffuser type, Case 002 versus Case 001,

b) the outdoor air flow rate, Case 003 versus Case 002,

c) the total air flow rate, Case 003, Case 004 and Case 005,

d) heat source, Case 006 versus Case 002,

e) the furniture, Case 007 versus Case 006, and

f) the partition, Case 008 versus Case 007.

Tracer gas sampling locations were installed at 15 locations within the room as shown in Figure 3.2(b): 10 sampling locations (#4 through #13) within the workstation,

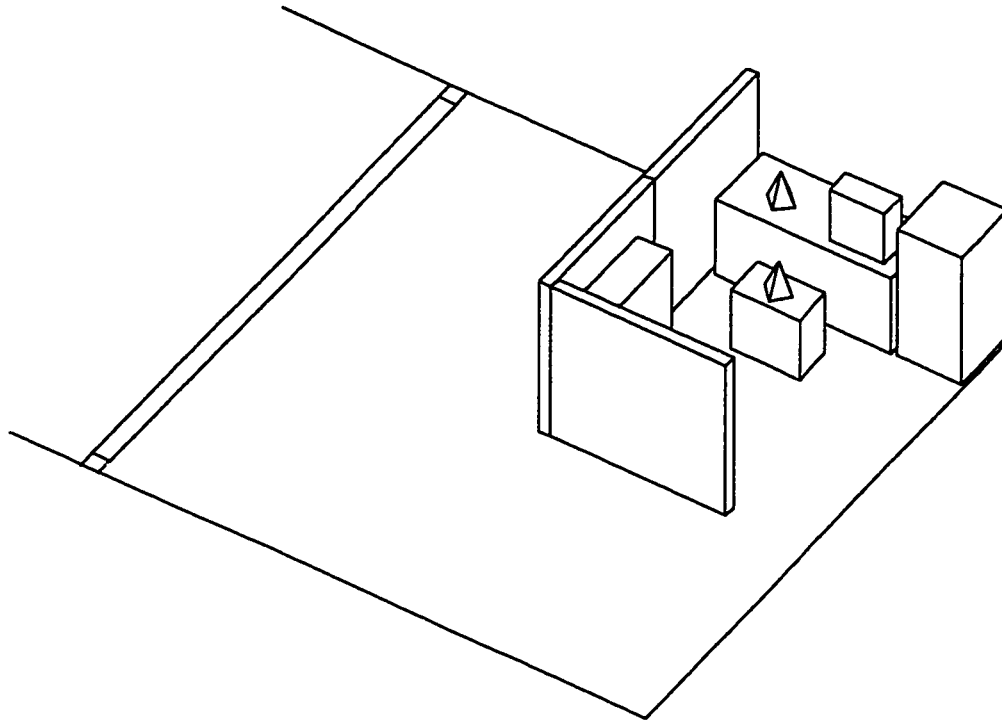

(a) The Test Room Layout of the First Set-up

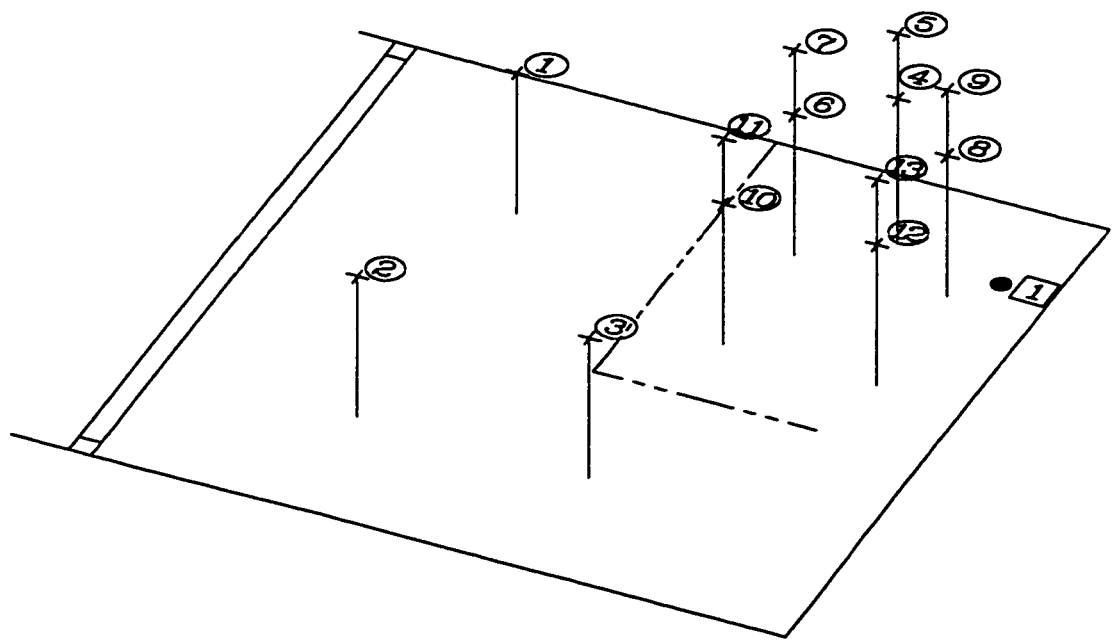

(b) Sample Locations of the First Set-up

Figure 3.2 Test Room Layout and Sample Locations of the First Set-up

three sampling locations (#1,2,3) around the workstation, and two sampling locations in the supply and return air ducts (#14, 15). Inside the workstation, five sampling locations (#5,7,9,11,13) were at a height of 1.6m, which is representative of the breathing height of a standing person, and the others (#4,6,8,10,12) were at the breathing height of a seated adult, 1.1 m. Sampling locations outside the workstation (#1,2,3) were placed at the breathing height of a seated adult.

A contaminant source was placed within the workstation at floor level, see Figure 3.2(b) (black point).

3.2.2 Second Set-Up

In the second set-up, the partition wall between the rooms was removed in order to create a larger space. Three new workstations (#2, 3 and 4) were added adjacent to the former one, and they were furnished with desks and chairs, as shown in Figure 3.3(a). A 100 W light bulb was placed on each chair to simulate the sensible heat generated by each worker. A computer was placed in workstation #3; it generates 100 W.

Only a square diffuser and a return grille were used in this set-up, and their locations are shown in Figure 3.1. A total of 12 experiments were performed for this set-up, Case 009 to Case 020, as shown in Table 3.1. In all these experiments, the supply air flow rate and the outdoor air flow rate were 100 L/s and 37.8 L/s, respectively. These

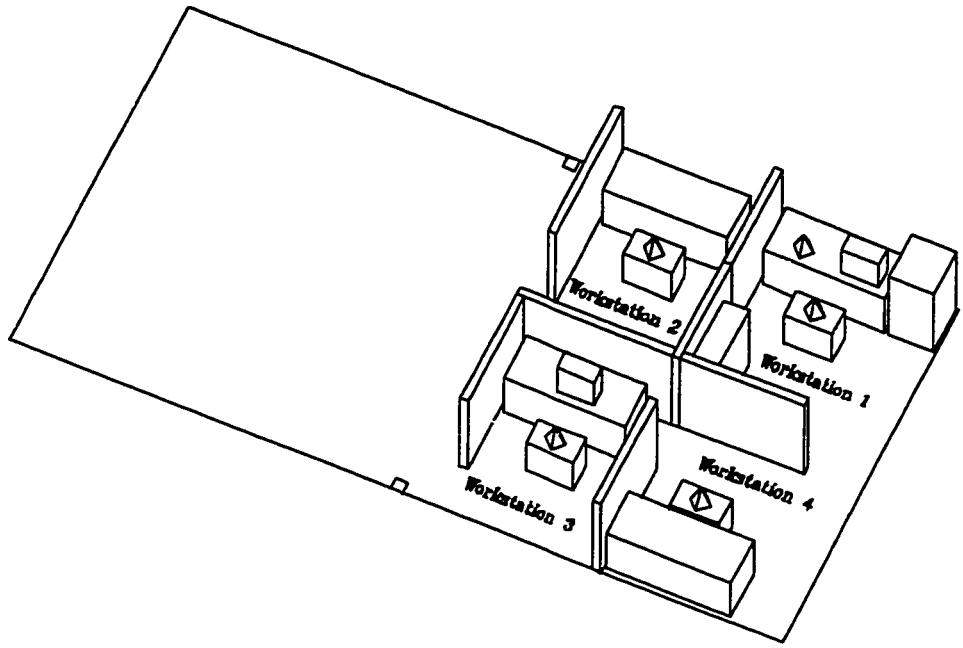

(a) The Test Room Layout of the Second Set-up

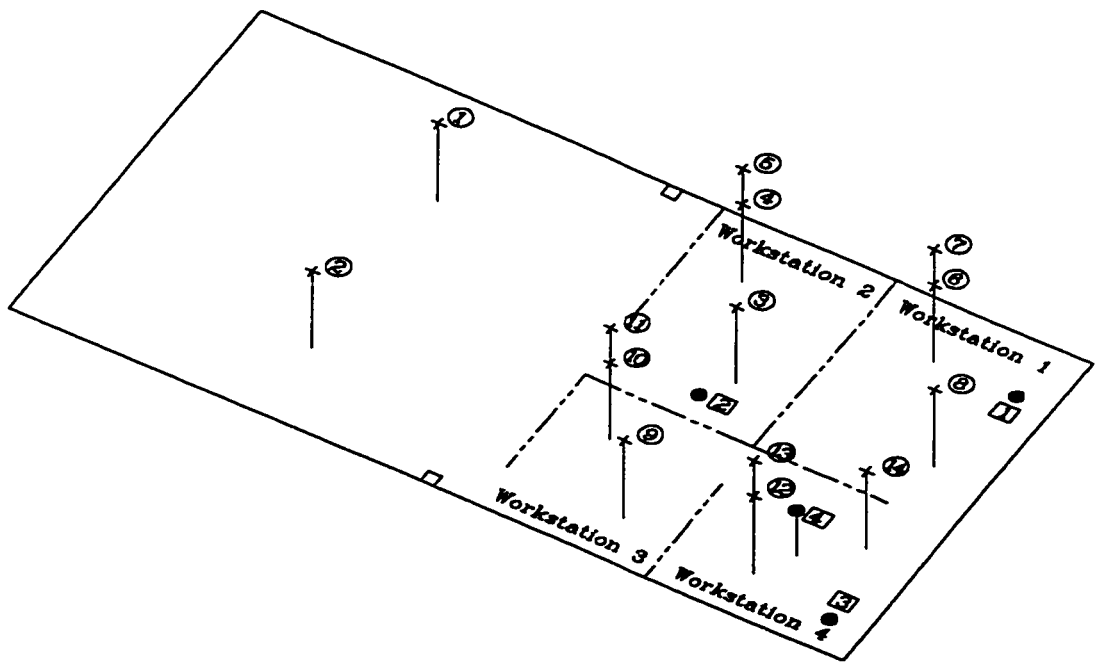

(b) Sample Locations of the Second Set-up

Figure 3.3 Test Room Layout and Sample Locations of the Second Set-up

experiments were designed to study the influence of:

a) contaminant source position for partition with gap, Cases 009, 010 and 011,

b) the partition gap, Case 012 versus Case 011,

c) the contaminant source position for partition without gap, Case 013 versus Case 012,

d) the supply air temperature (heating and cooling mode), Case 014 versus Case 013,

e) adjacent workstations, Case 015 versus Case 010,

f) heat source when it is located outside the workstations, Case 016 versus Case 015,

g) the partition height, Case 017 versus Case 013,

h) the contaminant source position for a short partition, Case 018 versus Case 017, and

I) the relative position between supply and return grilles and the individual workstations, Case 009 to Case 020.

Tracer gas sampling locations were installed at 16 locations: 12 sampling locations (#3 through #14) inside the workstations (three sampling locations per workstation), two sampling locations (#1,2) around the workstations, and two sampling locations in the supply and return air ducts. As shown in Figure 3.3(b), two of the sampling locations in each workstation were at the breathing height of a seated person (#3,4,6,8,9,10,12,14) , and the others (#5,7,11,13) were at the breathing height of a standing person. The two

sampling locations (#1,2) around the workstation were at the breathing height of a seated person.

Four contaminant sources (black points #1 - #4), in Figure 3.3(b), were placed inside the workstations. Source #1 was at the same position as in the first set-up. Sources #2 and #3 were placed on the floor within workstations #2 and #4, respectively, while Source #4 was located at a height of 1 m above the floor within workstation #4.

3.2.3 Third Set-Up

The purpose of this experiment, Case 021, was to study the impact of critical supply diffuser and return grille positions relative to the workstation. For this purpose, the workstation (# 5) was placed in, what is most likely, the worst position, as shown in Figure 3.4(a). As in the former set-ups, the workstation was furnished with a desk, a chair, a 60 W desk lamp, a 100 W computer and a 100 W light bulb on the chair to simulate the sensible heat generated by the office worker. The air supply diffuser and return grilles had the same position as in the previous set-up, and the supply air flow rate and the outdoor air flow rate remained the same with the second set-up. The results were compared with the results obtained from the second set-up cases.

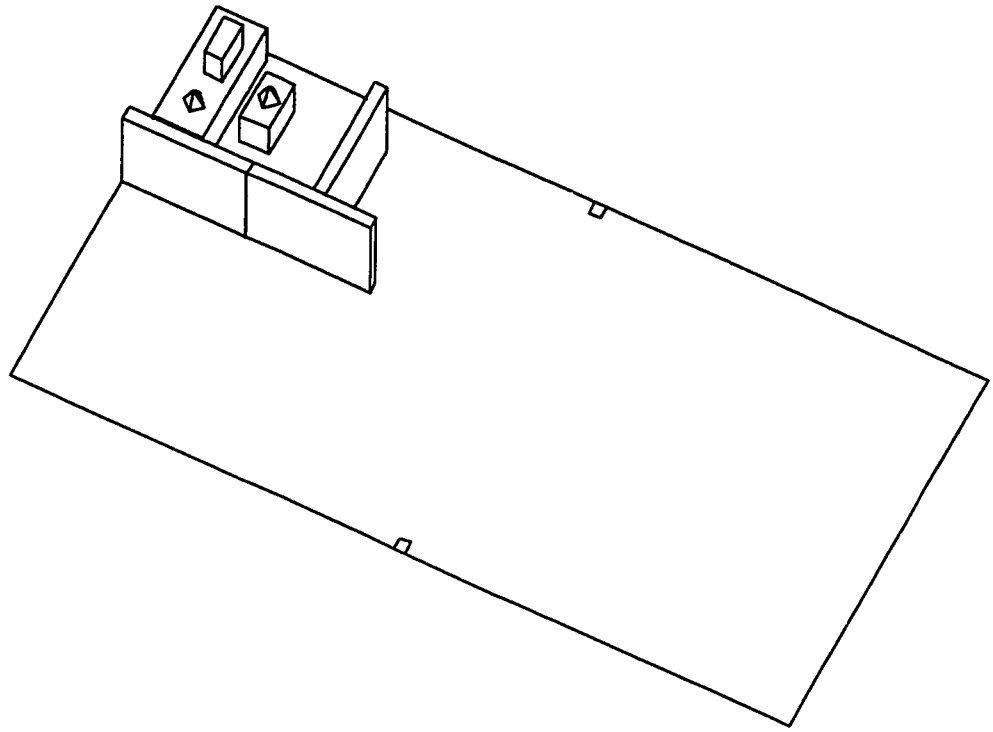

(a) The Test Room Layout of the Third Set-up

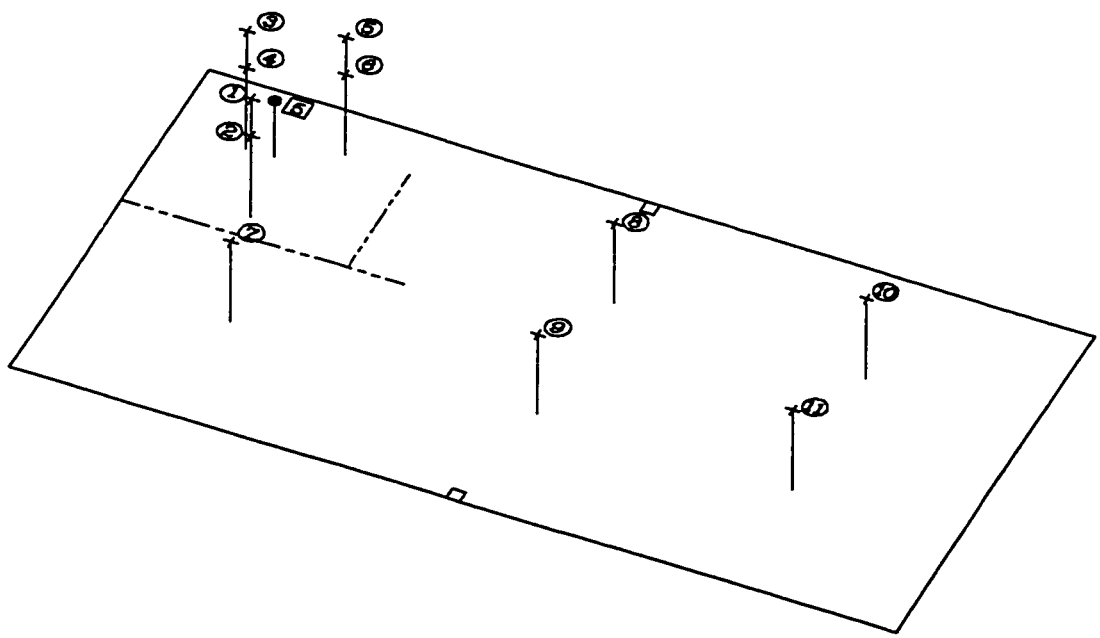

(b) Sample Locations of the Third Set-up

Figure 3.4 Test Room Layout and Sample Locations of the Third Set-up

Thirteen sampling locations were used for this experiment: six sampling locations (#1 through #6) inside the workstation, five locations (#7 through #11) around the workstation, and two locations in the supply and return air ducts (#12,13). As shown in Figure 3.4(b), the sampling locations inside the workstation were at two different aforementioned heights. Contaminant source #5, the black point in Figure 3.4(b), was placed within workstation #5 at a height of 1 m above the floor.

Each sampling location, in all experiments, consisted of two tubes; one used to collect the tracer gas samples (both SF_6 and CH_4) and the other used to inject tracer gas, SF_6, into the room for the mean age of air test.

3.3 MEASUREMENT TECHNIQUES

All experiments were carried out under steady-state conditions. To achieve these conditions, the HVAC system was turned on before the test started and allowed to reach the expected condition for the upcoming experiment.

Since the tracer gas measurement method required that the test room be closed and unoccupied throughout each test, tracer gas tests were performed on different days for each case.

An automated sampling system was used to collect the tracer gas samples. A gas chromatography (GC) and a gas analyzer were used to analyze the samples for tracer gas SF_6 and CH_4, separately.

The tracer gas experimental system consists of a carrier gas supply unit, a sample selection unit, a dual column sampling unit with back flushing and a detection unit (Evans 1988).

The carrier gas supply unit consists of a carrier gas supply tank, a pressure regulator, an oxygen trap and a moisture trap. The carrier gas should be of the type recommended by the detector manufacturer. The flow rate varies with the detector used and is controlled by a two-stage pressure regulator with a stainless steel diaphragm. For this detector, the gas flow rate is controlled at 30 ml/min. An oxygen trap is installed to reduce the oxygen level in the carrier gas. This is recommended because the presence of oxygen in the carrier gas will decrease the standing current and hence, reduce the sensitivity of the detector. A molecular sieve moisture trap is also installed to decrease the deterioration of the column due to moisture accumulation.

The sample selection unit consists of a 16 port multi-position sampling valve, an electro-pneumatic actuator, a timer, an exhaust and a sampling pump, a by-pass valve and a drier. The exhaust pump draws the samples from the 16 port multi-position valve continuously. At the same time, the timer and the actuator control the valve to allow one

sample at a time to be supplied to the sampling unit. To minimize the gas traveling time from the sampling valve to the drier, a by-pass valve is installed upstream of the drier to maintain a high flow rate up to the drier. For the same reason, the volume of the drier and the sample line between the drier and the inlet of the sampling valve is kept to a minimum. A drier (Drierite) is used to reduce the amount of moisture entering the column.

The sampling unit consists of a ten-port sampling valve, an electro-pneumatic actuator, a timer, a flow meter, a sampling loop, and two molecular sieve columns. The timer controls the actuator to switch the sampling valve form position A to B or vice versa in a timed sequence. The sample loop is made of 1.6 mm O.D. stainless tubing and has an internal volume of 0.5 ml. A constant sample flow of 50 ml/min through the sample loop is maintained by adjusting the by-pass valve. Their lengths are 450 mm and 300 mm respectively. Three needle valves are used to maintain equal carrier gas flow rates through the two columns when the sample valve is switched from one position to the other. One of these valves is located on the carrier gas line upstream of the sampling valve, the second one immediately upstream of the vent and the third one upstream of column II. Equal carrier flow rates are necessary to minimize the baseline drift.

The detection unit consists of an electron capture detector and an integrator which measures the SF_6 peak height of the sample from the outlet of the detector.

The GC was calibrated prior to the test and 20 different SF_6 concentrations of 0 to 400 ppb were used for the calibration. The CH_4 gas analyzer was also calibrated before the test.

Three tests were conducted for each case. In the first test, to measure the air distribution, a pulse of SF_6 was injected into the supply air duct. For the second test, to study the mean age of air, a pulse of SF_6 was injected into the room at the sampling locations. In the last test, to determine the contaminant removal efficiency, tracer gas CH_4 was continuously injected at the contaminant source position. All the injections were performed remotely from outside the test room, and the tracer gases were delivered from the injection point to the desired position through tubes. Each test took between three to seven hours.

SF_6 and CH_4 are different tracer gases, therefore their tests can be conducted at the same time. The samples could contain both SF_6 and CH_4, since the GC only collects and analyzes the SF_6, while the CH_4 gas analyzer only collects and analyzes the CH_4. Thus, the air distribution test and the contaminant removal efficiency test were performed simultaneously.

Contaminant removal efficiency tests were conducted for all 21 cases. Air distribution and mean age of air tests were not performed for all cases, because in some

cases the set-up remained unchanged. As an example, in Cases 009, 010 and 011, only the contaminant source position was changed.

3.3.1 Air Distribution

For assessing the air distribution within the space, a small amount of SF_6 (14 ml in the small room and 20 ml in the large room) was injected into the supply air duct to create a point source. Immediately following the injection, tracer gas samples were taken at all the sampling locations at half minute intervals for a period of two to three hours. The spatial uniformity of the tracer gas concentrations can be used to assess the effectiveness of the HVAC system in distributing the ventilation air.

The uniformity of tracer gas concentrations at time t can be calculated from the following expression (Shaw et al. 1993a):

$$U_{rm}(t) = 1 - \frac{C_{std}(t)}{C_{avg}(t)} \qquad (3.1)$$

where, $U_{rm}(t)$ is uniformity of tracer gas concentration at t,

$C_{std}(t)$ is standard deviation of tracer gas concentration at t, ppb,

$C_{avg}(t)$ is average tracer gas concentration at t, ppb.

A linear interpolation technique was used to calculate the concentrations at the different locations, at the time t, in order to compute the $U_m(t)$ from the measured concentration data.

3.3.2 Local Mean Age of Air

The age of air concept was used to evaluate the ventilation efficiency and the spatial variability of the ventilated space. To measure the mean age of air, the tracer gas was injected into the test room from the sampling locations. Several small mixing fans were used to assist in uniformly mixing the tracer gas with the room air. Five minutes after tracer gas injection, the mixing fans were turned off and tracer gas samples were taken at all sampling locations at 4-minute intervals for a period of approximately three hours.

The results obtained were used to calculate the local mean age of air at all sampling locations in the room (within the workstations, and around the workstations), and at the supply and return air ducts using the Nordtest method (NTVVS019 1983):

$$< t >= \frac{(\Sigma C_i)\delta t + C_M / \beta_e}{C_0} \qquad (3.2)$$

where, β_e is the exponential decaying constant,

C_i is the concentration reading number i,

C_o is the initial concentration reading,

C_M is the final concentration reading,

δt is the sampling interval, and

3.3.3 Contaminant Removal Efficiency

To measure the contaminant removal efficiency, the tracer gas, CH_4, was injected continuously into the workstation at a predetermined location to simulate a point contaminant source. The CH_4 flow rate was very small and the outlet was capped with a perforated ping-pong ball to minimise the effect of the injection on the surrounding airflow. Tracer gas samples were taken, from all the sampling locations and at the supply and return ducts, at 4-minute intervals for a period of approximately four hours. The contaminant removal efficiency was calculated from the equation (Liddament 1987):

$$E = \frac{C_{ra} - C_s}{C - C_s} \qquad (3.3)$$

where, C_{ra} is the steady state concentration at the return air duct,

C is the steady state concentration at the sampling location,

C_s is the steady state concentration at the supply duct, and

E is the contaminant removal efficiency.

Time average data in the steady state region were used for the calculation.

3.3.4 Thermal Comfort

Temperature and air velocity were measured inside the workstation. A climate analyzer (B&K) was placed at the working area of one workstation to record the data when the tracer gas test was underway. The samples were automatically recorded every 24 minutes for four hours. Additional parameters, such as air velocity standard deviation and relative humidity were also measured.

The thermal comfort tests were performed within workstation #1 in the first set-up, Case 001 to Case 006, to examine the influence of diffuser type, outdoor air flow rate, total air flow rate and furniture inside the workstation. In the second set-up, Cases 009, 010 and 021, measurements were performed individually within workstations #1, 2, 3, 4 and 5 to examine the influence of workstation position relative to the diffuser and return grille positions. In addition, tests were also performed within workstation #2 in Cases 010, 013 and 016 to examine the influence of partition height and partition gap.

The following mathematical model was used to assess the local uncomfortable due to draught based on the measurement results (Fanger, 1989):

$$PD = (34 - T_a)(V - 0.05)^{0.6223}(3.143 + 0.37VT_u) \qquad (3.4)$$

where, T_a is the air temperature, °C,

V is the mean air velocity, m/s,

T_u is turbulence intensity, %, and

PD is the percentage of dissatisfied people due to draught (%).

3.3.5 Air Flow Visualization

Flow visualization tests were performed for both linear and square diffusers to study the air flow pattern around the diffuser, return grille and partition gap areas. The visualization tests were conducted after the air distribution tests. Helium bubbles were used for this purpose. The helium bubbles were injected into each studied area through tubes. Several slide projectors were used at different heights to form a strong vertical plane of light to highlight the bubbles. The results were recorded using video tapes, pictures and slides.

CHAPTER 4

ANALYSIS OF MEASUREMENT RESULTS

4.1 RESULTS TO BE DISCUSSED

The results discussed in this chapter are in terms of air distribution, mean age of air, contaminant removal efficiency, thermal comfort level and air flow visualization.

4.2 AIR DISTRIBUTION

Air distribution inside the office is an important parameter to show the ventilation efficiency. It is basic for the ventilation system to provide a good air distribution in the entire ventilated area. Poor distribution indicates that the ventilation system was either not well designed or not well maintained.

4.2.1 First Set-Up

A total of eight tests (Cases 001 to 008) were conducted with linear and square diffusers in the first set-up. The details of these tests results are given in Table 4.1. The uniformity of air distribution was calculated using Equation 3.1. For this series of tests, the air supply temperature was 17 °C (cooling mode). With the exception of Case 008 (empty room), the partition height and gap were 1.8 m and 0.15 m, respectively.

Table 4.1 Uniformity of Air Distribution for the First Set-up

Case	001	002	004	005	006	007	008
Time(min.)							
10	0.970	0.985	0.979	0.969	0.957	0.968	
15	0.963	0.981	0.992	0.980	0.972	0.958	0.984
20	0.967	0.978	0.992	0.984	0.966	0.955	0.978
25	0.961	0.981	0.992	0.987	0.974	0.960	0.966
30	0.959	0.975	0.995	0.989	0.964	0.968	0.969
35	0.971	0.977	0.992	0.989	0.955	0.967	0.964
40	0.963	0.978	0.991	0.989	0.958	0.957	0.970
45	0.977	0.972	0.992	0.988	0.958	0.952	0.972
50	0.962	0.970	0.994	0.989	0.955	0.952	0.968
55	0.970	0.961	0.991	0.990	0.959	0.960	0.971
60	0.975	0.966	0.990	0.992	0.966	0.966	0.974
65	0.975	0.975	0.990	0.991	0.965	0.970	0.974
70	0.968	0.976	0.987	0.991	0.959	0.966	0.975
75	0.968	0.969	0.984	0.994	0.954	0.963	0.979
80	0.974	0.973	0.976	0.985	0.955	0.968	0.977
85	0.983	0.980	0.972	0.986	0.962	0.965	0.968
90	0.968	0.974	0.983	0.990	0.964	0.964	0.973
95	0.972	0.973	0.988	0.989	0.961	0.965	0.985
100	0.963	0.971	0.991	0.965	0.982		
105	0.971	0.971	0.991	0.962	0.975		
110	0.976	0.978	0.989	0.958	0.972		

Case 001 – Linear diffuser,

Case 002 – Square diffuser,

Case 003 – Lower outdoor air flow rate,

Case 004 – Higher supply air flow rate,

Case 005 – Highest supply air flow rate,

Case 006 – With partition and furniture, without heat source,

Case 007 – With partition, without furniture and heat source,

Case 008 – Empty room.

Figure 4.1 shows the air distribution pattern within the workstation and its surrounding area for the case with linear diffusers. It shows that the tracer gas concentrations were uniformly distributed throughout the room (inside and outside the workstation) and were almost the same as the tracer gas concentration measured in the return duct. Similar air distribution patterns were observed for the other cases listed in the first set-up. The results suggest that the type of diffuser (Case 001 vs. 002), the supply air flow rate (Case 002 vs. 004 and 005), the presence of heat sources (Case 002 vs. 006), the presence of furniture (Case 006 vs. 007), and finally the presence of a partition (Case 007 vs. 008), had no significant effect on the air distribution patterns within and around the workstation. The results also show that, for all tests, the tracer gas concentration in the return duct was almost the same as the tracer gas concentration within the workstation and its surrounding area; no short circuiting occurred between the supply and return grilles.

Table 4.1 compares the air distribution profiles for these tests in terms of the uniformity of air distribution, calculated using Equation 3.1. The results show the uniformity was similar for all cases.

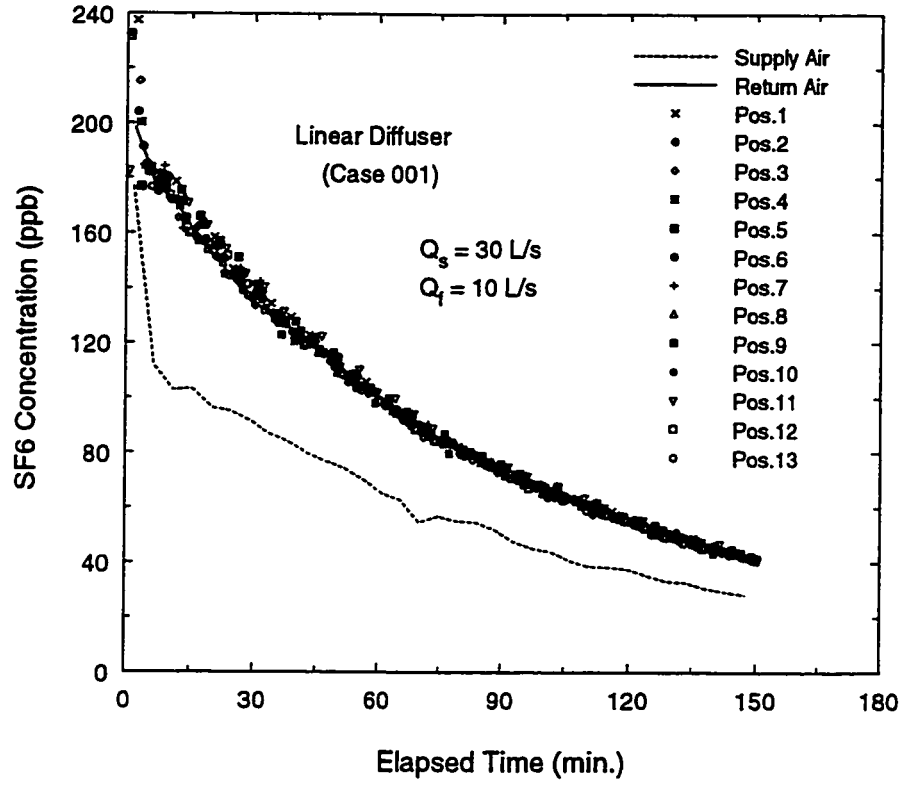

Figure 4.1 Air Distribution Test Results for Case 001

4.2.2 Second and Third Set-Ups

In the second and third set-ups, Cases 009 through 021, the supply and outdoor air flow rates were 100 L/s and 37.8 L/s respectively, and only a square diffuser was used. The supply air temperature was 17°C (cooling mode), except for Case 014, where it was 30 °C (heating mode). Two partition heights were tested, 1.5 m and 1.8 m. The 1.5 m

partition had no air gap, while the 1.8 m partition was tested with the 0.15 m air gap and with no air gap.

Figure 4.2 shows the air distribution pattern within the workstation and its surrounding area for Case 012. The results show that the tracer gas concentrations were uniformly distributed throughout the room (inside and outside the workstation) and were almost the same as the tracer gas concentration in the return duct. Figure 4.3 shows a typical air distribution pattern for Case 014. The results indicate that the operation mode (heating or cooling) had some influence on the air distribution pattern. When the supply air temperature was higher than the room temperature, the air distribution was worse than in the cooling case. This may be because both the supply diffuser and return grille were on the ceiling. In the heating case, the air temperature near the ceiling was higher, thus, buoyancy effects cause stratification in the room whereby the warmer air remains near the ceiling and the colder air remains at floor level. This makes the uniformity of the air distribution poorer than in the cooling case, although it had a high uniformity which was close to 0.9. More evidence is needed for this conclusion.

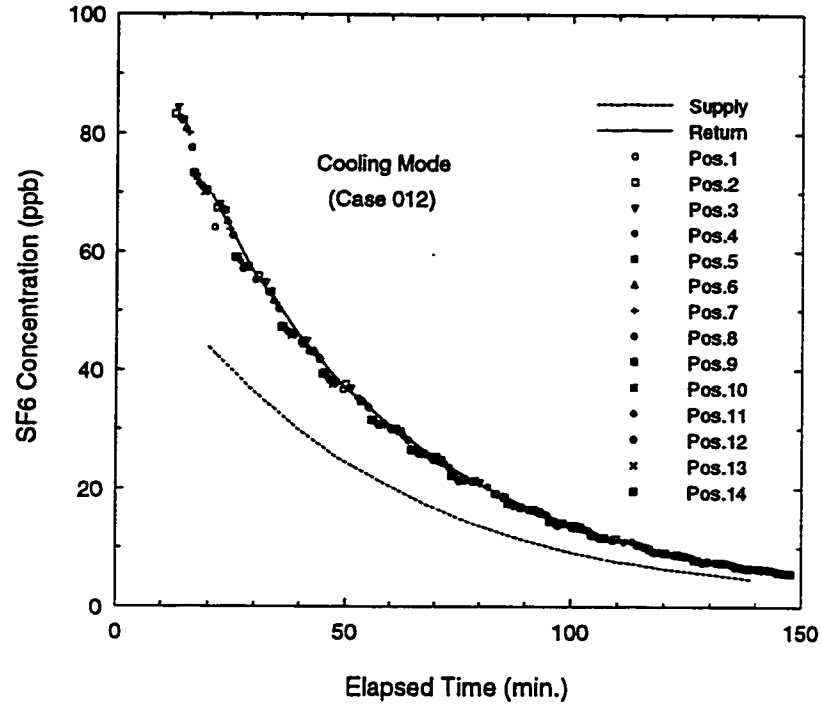

Figure 4.2 Air Distribution Test Results for Case 012

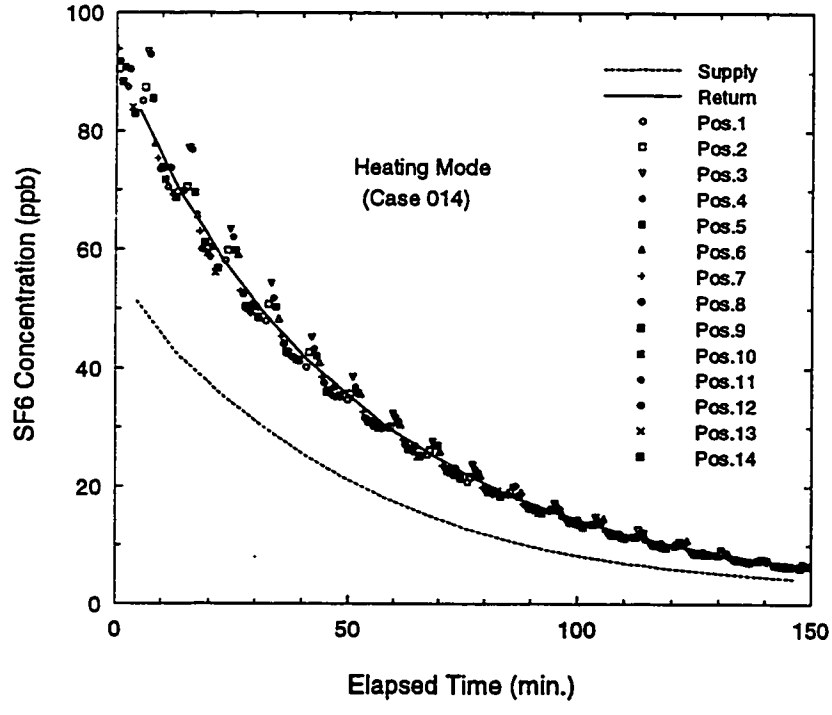

Figure 4.3 Air Distribution Test Results for Case 014

Table 4.2 compares the air distribution profiles for these two set-ups in terms of the uniformity of air distribution. It shows that all cases have more than 0.95 uniformity (calculated using Equation 3.1) except for the heating mode (Case 014). The results suggest that the partition gap (Case 011 vs. 012), the partition height (Case 013 vs. 017), the adjacent workstations (Case 015 vs. 010), the presence of heat sources outside the workstation (Case 015 vs. 016) and finally the workstation position or the relative position of supply diffuser and return grille (Case 009 to 020) have no significant effect on the air distribution patterns within and around the workstation.

Table 4.2 Uniformity of Air Distribution for the Second and Third Set-ups

Case	009	012	014	015	016	017	021
Time(min.)							
10	0.971	0.861	0.982	0.974	0.931		
15	0.965	0.979	0.865	0.979	0.981	0.966	0.996
20	0.961	0.947	0.866	0.983	0.978	0.962	0.966
25	0.964	0.943	0.878	0.979	0.978	0.958	0.973
30	0.967	0.947	0.873	0.979	0.982	0.961	0.975
35	0.968	0.952	0.878	0.978	0.982	0.959	0.972
40	0.967	0.956	0.882	0.978	0.981	0.962	0.976
45	0.967	0.955	0.887	0.984	0.979	0.963	0.976
50	0.962	0.954	0.889	0.986	0.979	0.966	0.974
55	0.967	0.886	0.987	0.981	0.967	0.972	
60	0.968	0.892	0.985	0.984	0.970	0.976	
65	0.888	0.981	0.971	0.977			
70	0.887	0.971					
75	0.972						
80	0.971						

Case 009 – With partition gap, contaminant source #1,

Case 012 – Without partition gap, contaminant source #2,

Case 014 – Without partition gap, contaminant source #3, heating mode,

Case 015 – One workstation, with heat source,

Case 016 – One workstation, without heat source,

Case 017 – Lower partition, contaminant source #3,

Case 021 – Third set-up.

4.3 LOCAL MEAN AGE OF AIR

Local mean age of air shows the outdoor air amount in a room and its distribution. When the mean age of air is long, it indicates that the amount of outdoor air provided inside the room is not enough.

Table 4.3 shows the local mean age of air, for the first set-up, at different locations within the workstation and its surroundings. It indicates that the local mean ages of air measured throughout the room and the local mean age of air at the return duct are similar; the differences are less than 2%. The results also indicate that the mean age of air increased with decreased outdoor air flow rate, suggesting that the mean age of air is very sensitive to the outdoor air flow rate. Other parameters such as diffuser type, supply air flow rate, heat source, furniture and partition, appeared to have little influence on the local mean age of air.

Table 4.3 Mean Age of Air Test Results for the First Set-up

Case	001	002	003	004	006	007	008	
Location								
1	84.42	97.26	220.96	114.81	84.33	98.99	97.47	min.
2	87.31	97.60	220.54	115.30	84.77	99.81	98.49	min.
3	83.67	97.97	220.50	115.00	80.30	99.37	97.78	min.
4	85.00	98.05	221.25	115.52	80.42	94.23	99.46	min.
5	80.74	98.41	221.21	111.09	80.67	94.97	99.33	min.
6	83.86	98.83	219.77	111.43	81.37	95.58	99.88	min.
7	83.84	98.61	221.63	111.52	81.47	95.47	100.43	min.
8	84.76	99.42	221.29	112.00	81.94	96.00	99.85	min.
9	86.03	99.86	217.70	112.39	82.26	96.20	100.17	min.
10	87.60	100.03	222.64	112.50	82.70	96.83	100.21	min.
11	83.66	100.38	223.63	112.82	82.32	96.98	100.61	min.
12	86.57	95.64	222.71	112.89	82.72	97.23	101.14	min.
13	82.35	96.47	223.06	113.33	82.90	97.32	101.70	min.
supply	84.06	96.85	226.39	114.33	84.62	95.96	98.79	min.
return	87.47	97.26	222.29	114.63	84.17	98.25	101.83	min.

Case 001 – Linear diffuser,

Case 002 – Square diffuser,

Case 003 – Lower outdoor air flow rate,

Case 004 – Higher supply air flow rate,

Case 006 – With partition and furniture, without heat source,

Case 007 – With partition, without furniture and heat source,

Case 008 – Empty room.

The results of the mean age of air for the big room (second set-up) are shown in Table 4.4. It indicates that the mean age of air in almost all cases were very close since the same outdoor air flow rate was used for all the tests. Parameters such as partition gap,

partition height, heating or cooling mode and different workstation positions, did not significantly influence the mean age of air.

Table 4.4 Mean Age of Air Test Results for the Second Set-up

Case	009	012	014	015	016	017	019	020	
Location									
1	62.09	61.84	58.80	65.37	64.47	64.24	66.15	65.73	min.
2	62.61	62.53	58.57	65.55	65.07	64.53	66.60	65.84	min.
3	62.90	57.89	58.49	65.61	59.41	64.55	62.11	65.88	min.
4	62.18	57.99	58.79	66.03	59.85	64.60	62.57	66.86	min.
5	58.28	58.40	54.60	65.74	60.30	64.74	62.92	66.91	min.
6	59.07	58.65	55.95	66.15	60.47	64.88	62.84	61.86	min.
7	59.25	58.75	55.02	66.37	60.95	65.21	63.16	62.17	min.
8	59.84	59.19	55.62	66.91	61.32	65.70	63.46	62.59	min
9	59.52	59.81	56.24	67.11	61.34	65.90	63.90	62.80	min.
10	60.27	60.13	56.25	67.54	62.04	61.88	64.14	63.52	min.
11	60.52	60.66	56.62	68.01	62.36	62.18	64.59	63.95	min.
12	60.78	60.69	56.97	62.87	62.44	62.44	64.69	63.92	min.
13	61.05	60.95	56.76	63.18	63.09	62.55	64.78	64.21	min.
14	61.04	61.39	57.24	63.46	63.04	62.84	65.40	64.56	min.
supply	62.75	61.85	57.38	64.75	63.81	64.28	65.35	64.77	min.
return	61.95	61.68	58.14	64.61	63.80	63.34	66.12	65.26	min.

Case 009 – With partition gap, contaminant source #1,

Case 012 – Without partition gap, contaminant source #2,

Case 014 – Without partition gap, contaminant source #3, heating mode,

Case 015 – One workstation, with heat source,

Case 016 – One workstation, without heat source,

Case 017 – Lower partition, contaminant source #3,

Case 019 – With partition gap, contaminant source #4,

Case 020 – Without partition gap, contaminant source #4.

4.4 CONTAMINANT REMOVAL EFFICIENCY

The contaminant removal efficiency describes the ability of a ventilation system to remove or dilute the contaminant from the ventilated area. Even when the air distribution is good, the contaminant removal efficiency could be low. Low contaminant removal efficiency indicates that the air flow inside the room is not well organized for removing or diluting the contaminant from a particular pollution source.

4.4.1 First Set-Up

The values of contaminant removal efficiency for the first set-up are shown in Table 4.5. As mentioned, the results show a large variation in these values for different locations in a given case, and for different cases. An attempt was made to identify the reasons for these differences, by comparing the results and test conditions of some of the cases.

Table 4.5 Contaminant Removal Efficiency Test Results for the First Set-up

Case	001	002	003	004	005	006	007	008
Location								
1	1.15	1.27	1.63	1.80	1.88	1.46	2.45	1.31
2	1.16	1.23	1.54	1.81	2.11	1.34	2.17	1.11
3	1.10	1.22	1.47	1.84	2.09	1.31	2.04	1.11
4	0.99	1.21	1.41	1.47	0.99	0.96	0.94	1.17
5	0.80	1.08	1.07	1.13	0.98	0.97	1.09	1.17
6	0.66	0.95	1.32	0.71	0.67	0.62	1.43	1.13
7	0.69	1.07	1.52	0.88	0.79	0.66	1.35	0.99
8	0.92	1.29	1.53	1.59	1.73	0.95	0.67	0.94
9	1.08	1.24	1.44	1.51	1.34	1.18	1.02	0.98
10	0.93	1.16	1.57	1.07	0.94	0.51	1.55	0.82
11	0.94	1.16	1.43	1.27	1.06	0.66	1.55	0.80
12	1.05	1.26	1.50	1.50	1.62	1.19	1.21	0.59
13	1.13	1.25	1.41	1.63	1.47	1.19	1.79	0.68

Case 001 – Linear diffuser,

Case 002 – Square diffuser,

Case 003 – Lower outdoor air flow rate,

Case 004 – Higher supply air flow rate,

Case 005 – Highest supply air flow rate,

Case 006 – With partition and furniture, without heat source,

Case 007 – With partition, without furniture and heat source,

Case 008 – Empty room.

As an example, Case 001, linear diffuser, and Case 002, square diffuser, had a similar set-up. Figure 4.4 shows the contaminant removal efficiency for Cases 001 and 002 in several sampling locations. Case 002, square diffuser, has a consistently higher efficiency than the case with linear diffuser. Figures 4.5 and 4.6 show the concentration

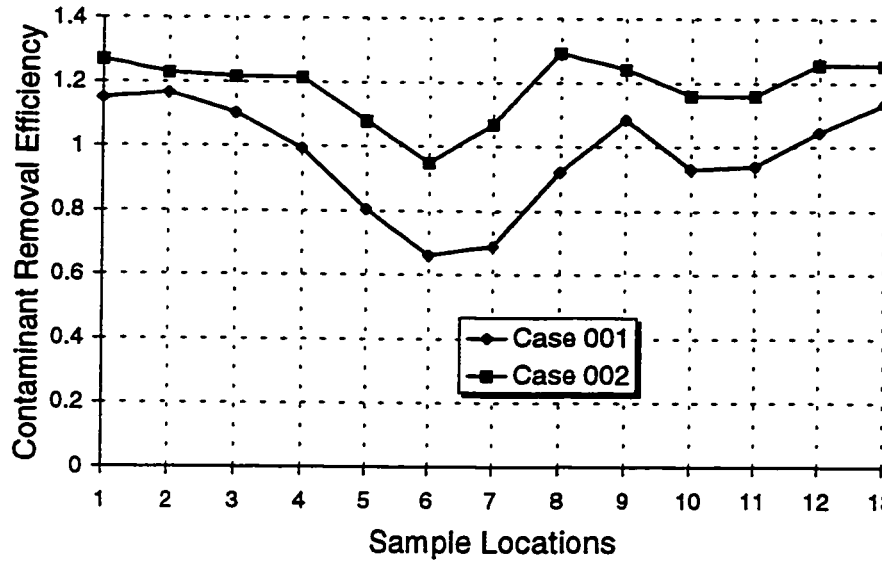

Figure 4.4 Contaminant Removal Efficiency of Case 001 and Case 002

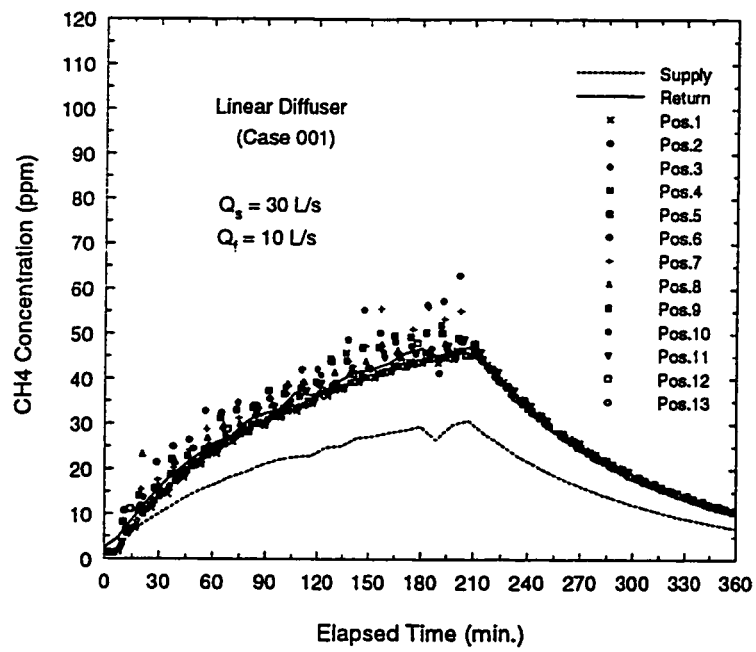

Figure 4.5 Contaminant Concentration of Case 001

profiles of CH_4 for Cases 001 and 002, respectively. As shown in Figures 4.5 and 4.6, there are much greater variations in the CH_4 concentrations within the workstation and its surroundings in Case 001 than in Case 002. In general, the square diffuser obtained a 10% greater efficiency.

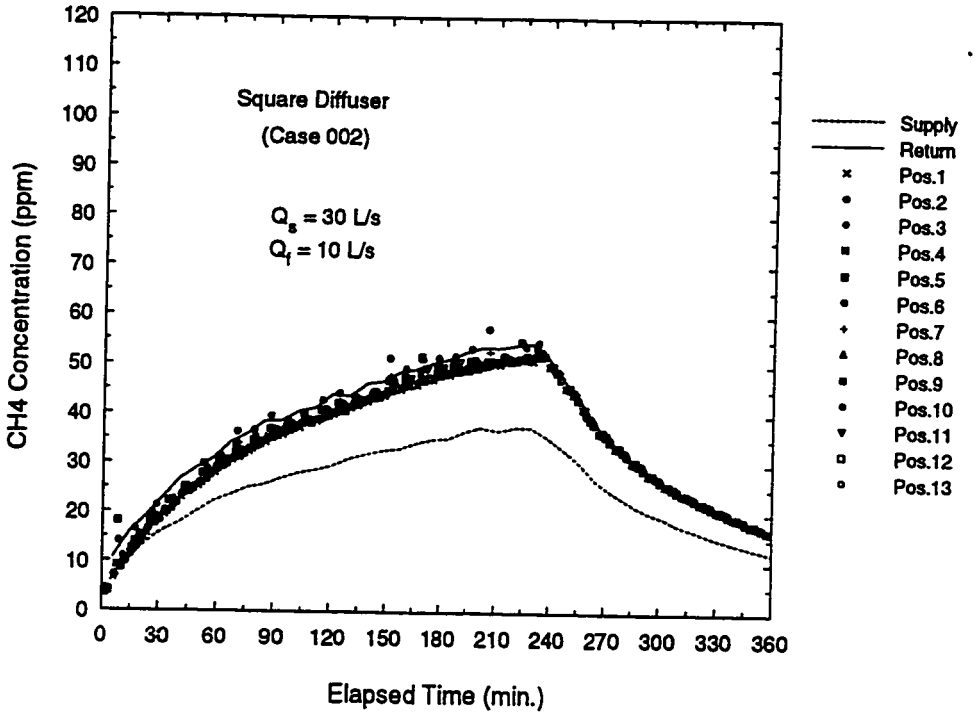

Figure 4.6 Contaminant Concentration of Case 002

As indicated in Table 4.5, the higher supply air flow rate (Case 005) did not improve the efficiency inside the workstation area. The efficiency was improved only for the sampling locations close to the diffuser, locations #2 and #3, as compared to Case 002.

When there were heat sources inside the workstation, the efficiency for the sampling locations inside the workstations improved. A comparison between the ventilation efficiency of the square diffusers with heat sources (Case 002), and without heat sources (Case 006), as shown in Figure 4.7, indicates that the efficiency for the sampling locations outside the workstation deteriorated when heat sources were present. There was a greater variation in contaminant removal efficiency in Case 006 than in Case 002. This indicates that the heat source accelerates the contaminant's removal to outside the workstation. This causes the contaminant removal efficiency to decrease at the sampling locations outside the workstation. Figures 4.6 and 4.8 show the concentration profiles for Cases 002 and 006.

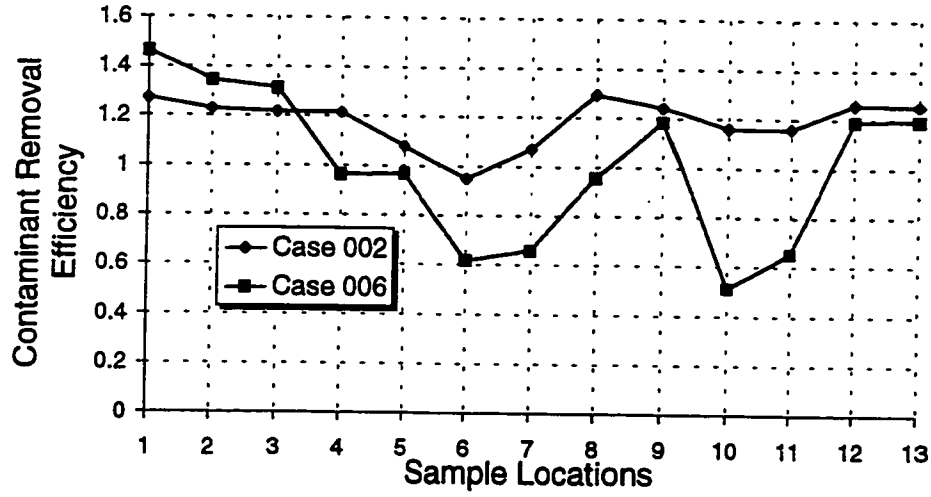

Figure 4.7 Contaminant Removal Efficiency of Case 002 and Case 006

The furniture inside the workstation influences the contaminant distribution. Table 4.5 shows the contaminant removal efficiency results of Cases 006 and 007. The only difference between these two cases is the presence of furniture inside the workstation, Case 006, and the absence of furniture, Case 007. Figures 4.8 and 4.9 show the CH_4 concentration profile for these two cases. As shown, the contaminant distribution inside the workstation was significantly different in these two cases. When furniture was present, Case 006, the sampling locations 6 and 10 had a higher contaminant concentration, when no furniture was present, the sampling location 8 had a higher contaminant concentration. The contaminant concentration in the surrounding area also changed when furniture was present inside the workstation. The furniture changed the contaminant distribution in the test room.

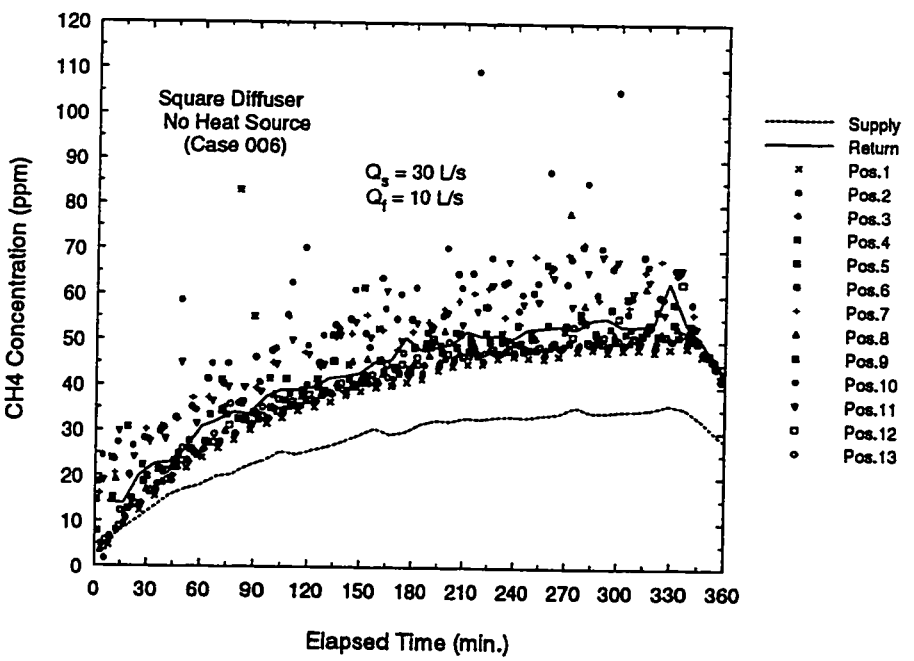

Figure 4.8 Contaminant Concentration of Case 006

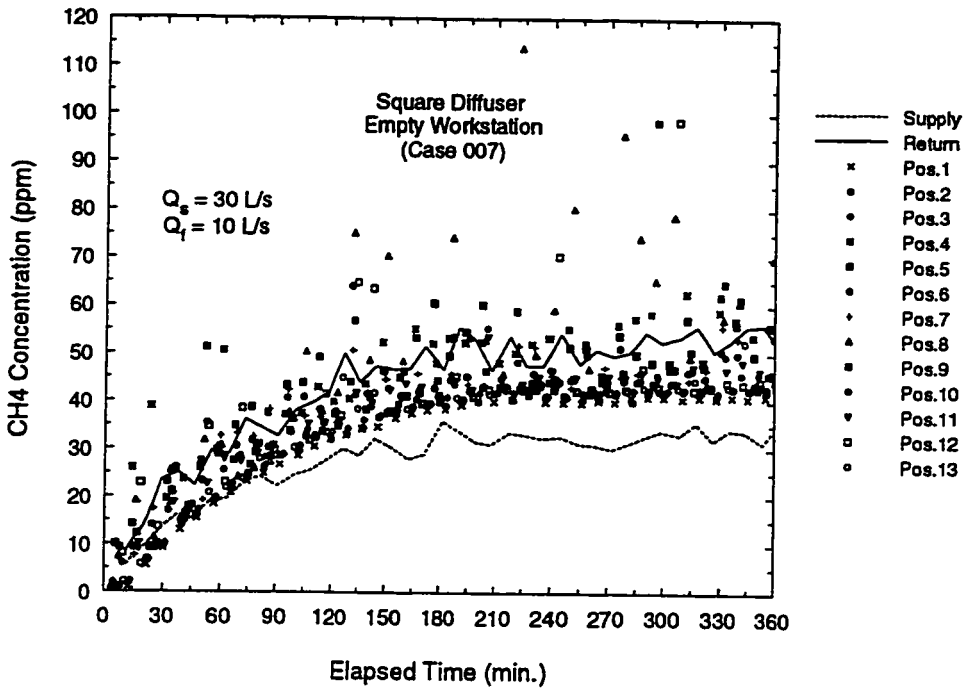

Figure 4.9 Contaminant Concentration of Case 007

Comparing the contaminant removal efficiency of Cases 007 and Case 008 in Table 4.5, it could be concluded that the presence of partitions in the workstation also influenced the contaminant distribution. The contaminant could be blocked by the partitions.

The difference between Case 002 and Case 003 is the outdoor air flow rate. They should have similar results for contaminant removal efficiency according to Equation 3.3. The difference of the results showed in Table 4.5 may be because that the steady state condition was not reached in the measurement of Case 003. Shaw (1992) studied the accuracy of tracer gas experimental method. Most of their tests were in 5% accuracy and a few of the tests were in 10% accuracy.

4.4.2 Second Set-Up

The values of contaminant removal efficiency for the second set-up are shown in Table 4.6. As in the first set-up, the values in Table 4.6 indicate a large variation between different cases.

Cases 009, 010 and 011 were designed to study the influence of the contaminant source positions. Each case had a similar set-up; the only difference was that the contaminant source was located in workstation #1 for Case 009, in workstation #4 for Case 010, and in workstation #2 for Case 011. Figure 4.10 compares the contaminant removal efficiency of these three cases. It indicates that no matter where the contaminant source was located, the sampling locations in workstation #1 had a low efficiency. This is because the return grille was located directly above the workstation #1. The contaminant was removed to the return grille through workstation #1. The relative position of the return grille is very important when there is a contaminant source present in the office. The closer the contaminant source is to the return grille, the less the contaminant source will be spread to other parts of the office. Similar results could be found by comparing the results of Case 012, 013 and 020 in Table 4.6, which was designed to study the influence of contaminant source location for partitions with a gap.

Table 4.6 Contaminant Removal Efficiency Test Results for the Second Set-up

Case	009	010	011	012	013	014	015	016	017	018	019	020
Location												
1	1.63	2.23	1.81	1.25	2.65	2.56	1.25	1.65	2.38	1.40	1.61	2.75
2	1.64	2.17	1.80	0.85	2.57	2.55	1.23	1.61	2.34	1.38	1.57	3.09
3	1.73	2.10	1.83	0.67	2.52	2.47	1.01	1.26	2.28	0.85	1.57	2.52
4	1.75	2.14	1.86	0.96	2.53	2.56	1.16	1.42	2.35	0.69	1.59	2.48
5	1.74	2.08	1.85	0.68	2.49	1.94	1.10	1.42	2.26	0.62	1.57	2.50
6	0.47	1.42	0.70	0.95	1.11	0.52	1.03	1.23	1.03	1.05	1.02	1.11
7	0.78	0.99	0.85	0.77	1.36	1.28	1.02	1.28	1.29	0.77	0.65	1.46
8	1.05	1.05	1.42	1.01	0.92	0.41	0.96	1.22	0.86	1.38	0.76	1.21
9	1.71	1.57	1.84	1.26	1.95	2.60	0.83	1.11	1.55	1.48	1.17	2.84
10	1.75	1.79	1.88	1.23	2.32	2.61	1.00	1.18	1.94	1.50	1.37	2.26
11	1.74	1.81	1.88	1.22	2.34	2.46	0.84	1.10	1.95	1.48	1.35	3.65
12	1.72	0.33	1.84	1.28	0.48	0.58	0.36	0.51	0.47	1.50	0.63	1.93
13	1.69	0.35	1.78	1.26	0.86	1.25	0.54	0.54	0.69	1.49	0.60	2.05
14	1.71	1.05	1.84	1.26	0.85	0.30	0.81	1.09	0.76	1.49	0.36	1.35

Case 009 – With partition gap, contaminant source #1,

Case 010 – With partition gap, contaminant source #3,

Case 011 – With partition gap, contaminant source #2,

Case 012 – Without partition gap, contaminant source #2,

Case 013 – Without partition gap, contaminant source #3,

Case 014 – Without partition gap, contaminant source #3, heating mode,

Case 015 – One workstation, with heat source,

Case 016 – One workstation, without heat source,

Case 017 – Lower partition, contaminant source #3,

Case 018 – Lower partition, contaminant source #2,

Case 019 – With partition gap, contaminant source #4,

Case 020 – Without partition gap, contaminant source #4.

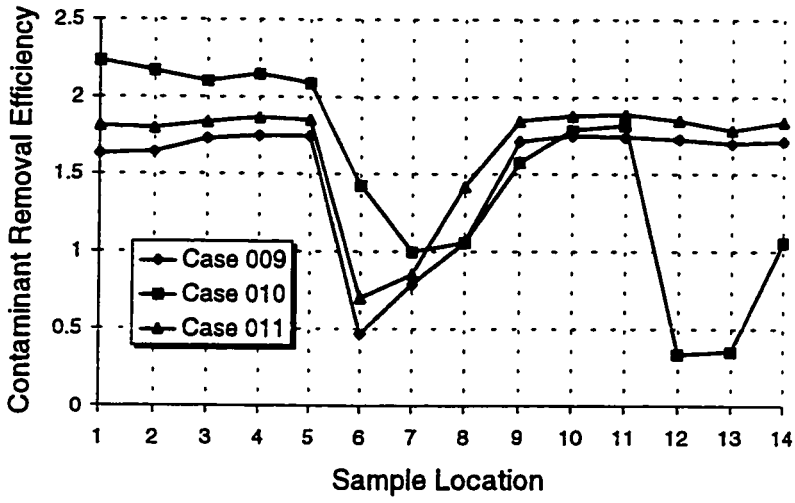

Figure 4.10 Contaminant Removal Efficiency of Case 009, 010 and 011

The partition gap influences the contaminant removal efficiency. Cases 010 and 013 had the same set-up, except the partition in Case 010 had a 0.15 m air gap while the partition in Case 013 had no gap. Figure 4.11 compares the contaminant removal

efficiency of these two cases. As shown, the contaminant removal efficiency was not effected on workstation #4 (the contaminant source located inside it) and in workstation #1 (the return grille located above it). The efficiency improved in other places when the partition had no gap. This indicates that the contaminant was moved to other parts of the office through the partition gap. The CH_4 concentration in the return duct was slightly higher for the case without the gap than with the gap. This is because the CH_4 was not spread out through the gaps, but was moved to the return grille directly. Comparing the results of Case 011, with gap, and Case 012, without gap, in Table 4.6, a similar conclusion can be reached.

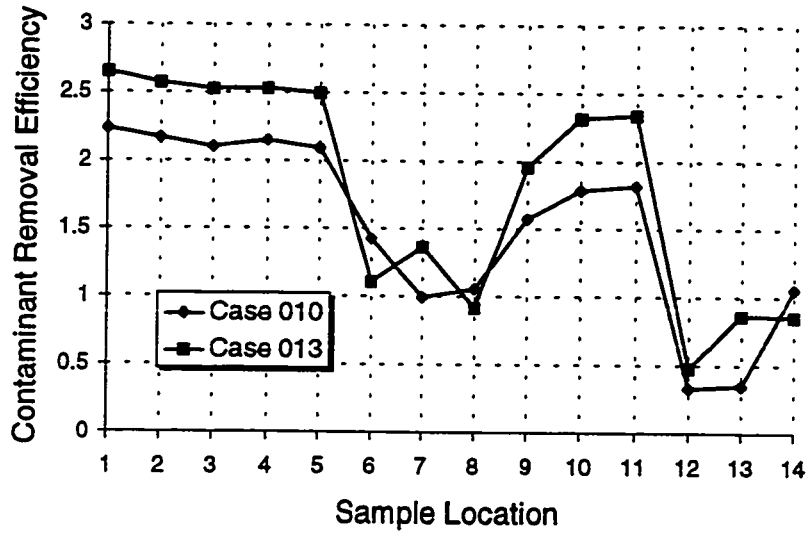

Figure 4.11 Contaminant Removal Efficiency of Case 010 and Case 013

The short partition (1.5m) appeared to provide better conditions for removing the contaminant from inside the workstation. The difference between Case 012, with a 1.8 m

partition, and Case 018, with a 1.5 m partition, was the partition height; the partitions in these two cases had no gap at the bottom. As indicated in Table 4.6, the contaminant removal efficiency for the workstation with a short partition, Case 018, was higher than that of the tall partition, Case 012. Similar conclusions can be make by comparing the results of Case 013 and Case 017 in Table 4.6.

Figure 4.12 compares the contaminant removal efficiency for Cases 010, 015 and 016. The contaminant source was placed on the floor of workstation #4 in all these three cases. In Cases 015 and 016 only workstation #4 was located in the test room. There were heat sources located outside workstation #4 in Case 015 while no heat sources were present outside workstation #4 in Case 016. The results show that, whether or not other workstations or heat sources outside the workstation were present, the contaminant removal efficiency in workstation #4 hardly changed in these three cases. The presence of the other workstations and outside heat sources did not influence the contaminant in the workstation which contained the contaminant source. The results also show that the contaminant removal efficiency in other parts of the test room changed dramatically. The partitions and heat source influenced the contaminant distribution. This confirms the results of the tests from the first set-up.

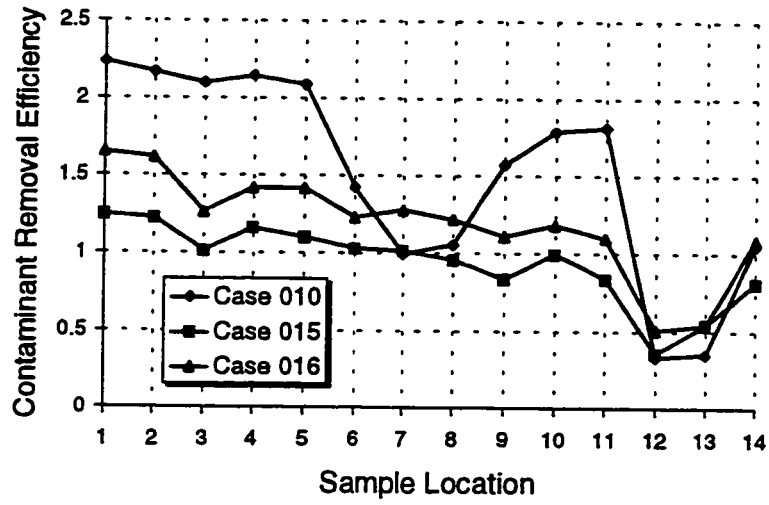

Figure 4.12 Contaminant Removal Efficiency of Case 010, 015 and 016

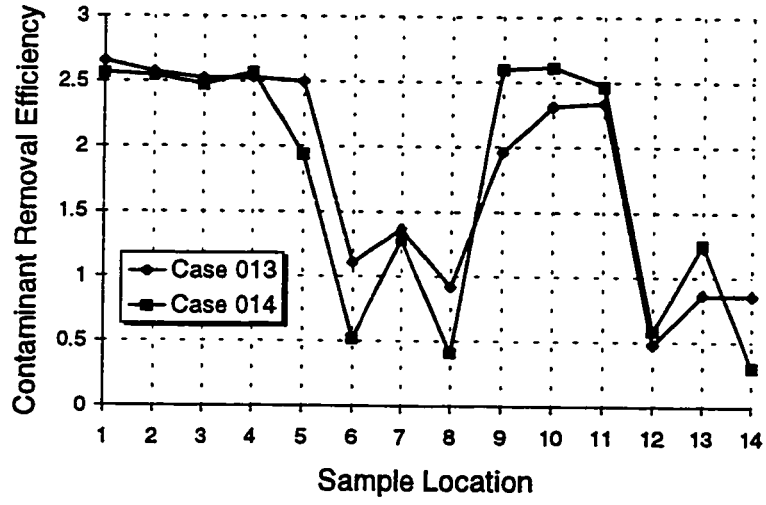

Figure 4.13 Contaminant Removal Efficiency of Case 013 and Case 014

The contaminant removal efficiency for different supply air temperatures, Case 013 (cooling mode) and Case 014 (heating mode) are compared in Figure 4.13. A slight difference could be found between these two cases. The supply air temperature had some influence on the contaminant distribution, but not strong.

4.4.3 Third Set-Up

Figure 4.14 shows the CH_4 concentration profile for Case 021. In this case, workstation #5 was placed in where is most likely the worst position. It can be seen that the CH_4 concentration at all locations inside the test room was higher than the CH_4 concentration in the return duct. This indicates that at this particular workstation location, the contaminant inside the workstation would not be removed as efficiently as a workstation placed at other locations inside the test room; this suggests the contaminant was distributed throughout the test room and diluted before it was removed to the return duct.

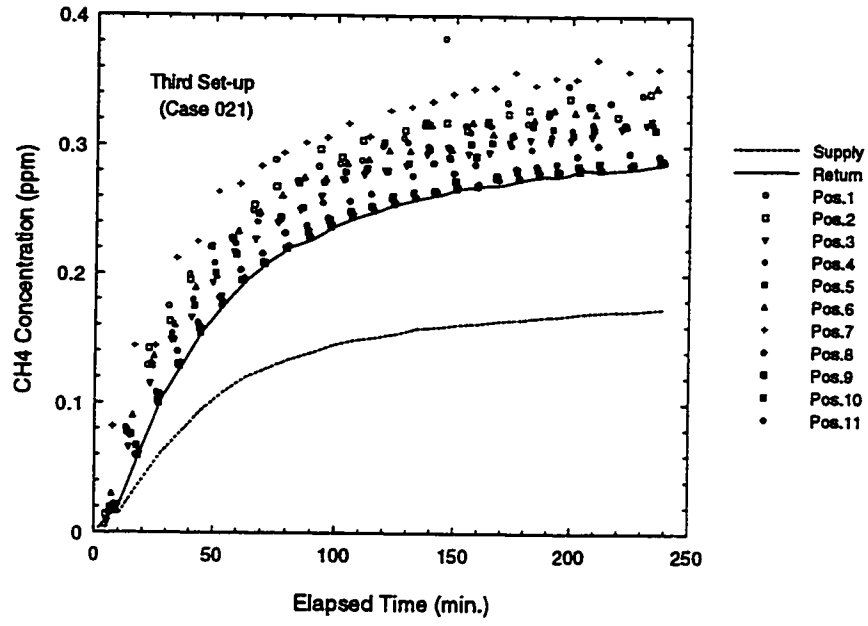

Figure 4.14 Contaminant Concentration of Case 021

4.5 THERMAL COMFORT

Table 4.7 shows the thermal comfort test results.

where, T is the room air temperature,

V is the room air velocity,

V_std is the standard deviation of the velocity,

RH is the relative humidity,

PD is the percentage of dissatisfied people due to draught.

Table 4.7 Thermal Comfort Test Results

Case	T (C)	V (m/s)	V_std (m/s)	RH (%)	PD (%)
001	23.6 – 24.7	0.13 – 0.16	0.05 – 0.09	33 – 38	6.8
002	24.7 – 25.5	0.12 – 0.13	0.02	34 – 37	5.4
003	24.7 – 25.4	0.12 – 0.13	0.02	35 – 36	5.2
004	23.8 – 24.2	0.14 – 0.16	0.04 – 0.05	42 – 43	8.0
005	23.2 – 23.7	0.16 – 0.18	0.04 – 0.05	41 – 44	9.4
006	24.7	0.05 – 0.07	0.02	37 – 38	1.7
009	23.5 – 23.7	0.10 – 0.13	0.03 – 0.05	41 – 43	5.7
011	23.9 – 24.3	0.08 – 0.14	0.02 – 0.08	40 – 43	5.0
013	24.0 – 24.3	0.09 – 0.10	0.03 – 0.04	42 – 44	4.2
017	23.9 – 24.0	0.07 – 0.09	0.03 – 0.04	43 – 44	3.6
021	23.2	0.09 – 0.12	0.03 – 0.04	46 – 47	5.3

When comparing the influence of linear diffuser (Case 001) and square diffuser (Case 002), it can be found that the air flow in the test room created by the linear diffuser was more fluctuating (V and V_std were higher). The linear diffuser caused a higher PD value than the square diffuser.

When no heat sources were present in the test room (Case 006), the PD value was very low because of the stable air flow inside the test room.

When Case 003 (supply air flow rate 30 L/s), Case 004 (supply air flow rate 73.8 L/s) and Case 005 (supply air flow rate 100 L/s) were compared, it can be concluded that the higher flow rate brought higher air velocity inside the test room, which caused a higher PD value.

At the same time, all the thermal comfort test results, including temperature, relative humidity and air speed within the workstation for all the cases were within the limits of ASHRAE Standard (55-1992). The air temperature and relative humidity were very stable. The temperature change in the working area was ±1°C. The relative humidity change in the working area was ±3%. The air flow speed in the working area was less than 0.2 m/s in all cases. The PD values (the percentage of dissatisfied people for draft) for all cases were less than 10%, which indicates that the thermal comfort condition based on PDs was good for all the cases.

4.6 AIR FLOW VISUALIZATION

The flow visualization results based on the recorded video tapes show that the air flow around the diffuser area experienced a strong turbulence phenomena. The fluctuation of the air in this area was very strong. For the square diffuser, the air attached to the ceiling when it was leaving the diffuser. The flow pattern in this area is very complicated.

The air flow pattern around the return grille is simple. The return grille influences the air flow in a very small region. This indicates that the return grilles do not have a strong influence on the air distribution in the room.

In recent years, many questions have been raised regarding whether or not the gaps at the bottom of privacy partitions would have a significant influence on the air flow patterns in a room. The results suggest that when both the supply diffuser and the return grille were located on the ceiling, the air flow through the partition gap was very small. Such little air movement was not expected to have a significant influence on the air distribution within the workstation. However, if a contaminant source was located close to the partition gap, the small air flow through the partition gap could have a significant influence on the contaminant distribution in the room.

4.7 SUMMARY AND RECOMMENDATIONS

The following conclusions and recommendations could be made according to the test results:

1. Under the test conditions, the air distribution within the test workstation was not affected by the following parameters: diffuser type, air flow rate, workstation partitions, partition heights, partition bottom gap, adjacent workstations, the locations of diffuser and return grille relative to the workstation.
2. Under the test conditions, the mean age of air in the test workstation was not affected by the following parameters: the diffuser type, diffuser and return grille position, total supply

air flow rate (with a constant outdoor air supply), heat source, furniture, workstation partition height and partition bottom gap.

3. The mean age of air was strongly influenced by the outdoor air flow rate. Adequate outdoor air should be introduced into each office to maintain acceptable indoor air quality.
4. Under the test conditions, the contaminant removal efficiency was affected by the following parameters: the diffuser type, heat source and furniture in the workstation, the partitions themselves, partition height, heating or cooling mode and different workstation locations.
5. Supply air flow rate (with the same percent of outdoor air flow rate) did not have a significant influence on the contaminant removal efficiency, although it did affect the contaminant concentrations in the workstation.
6. The air flow pattern had a significant influence on the contaminant distribution. The partition gap had a significant effect on the contaminant movement inside a partitioned office when the contaminant source is located close to the gap.
7. The workstation closest to the return grille appeared to have poor contaminant removal efficiency compared to the adjacent workstations, even if the contaminant source was not located inside this workstation, due to the migration of contaminants from adjacent areas. Efforts should be made to place known contaminant sources in workstations where the return grille is located.
8. Under the test conditions, thermal comfort was acceptable for all the cases studied.

4.8 NEED FOR NUMERICAL SIMULATION

The measurement results showed that, when the supply diffuser was located on the ceiling of the partitioned office, the air distribution in the partitioned office did not encounter any problems. The supply air could be evenly distributed through all workstations. However, when a contaminant source was present somewhere inside the office, the distribution of the contaminant was influenced by nearly all investigated parameters in the office. Many factors affect the contaminant flow pattern inside a partitioned office. The contaminant distribution in a partitioned office is strongly case dependent. Considering the cost of measurement techniques, it is nearly impossible to do the measurement for every case of concern. The more feasible numerical method should be applied to simulate the air and contaminant distributions inside partitioned offices.

CHAPTER 5

NEW DIFFUSER DESCRIPTION METHOD DEVELOPMENT

5.1 INTRODUCTION

Numerical modeling is one way to assess the air distribution in a ventilated room. From the conclusion of Chapter 4, contaminant distribution in a ventilated room is case dependent. Applying measurement in each case studied is not practical. It is necessary to apply a numerical analysis method for contaminant distribution study. Computational Fluid Dynamics (CFD) is one of the numerical prediction methods which can be applied for air distribution and contaminant distribution analysis in a ventilated room. It is less expensive than the experimental method and can be easily applied to a specific case.

As described in Chapter 2, the supply air flow condition is an important parameter affecting the air flow distribution in the room. Real supply diffusers often have a very

complicated geometry. Because of this and limited computer capacity, which limits the number of grids to accurately describe all the details of the diffuser geometry, the conventional method of describing the supply air diffuser boundary conditions in CFD simulation is difficult to use and may give incorrect results for some cases. When the supply diffuser boundary is not well defined to correctly express the air inflow condition, the simulation of the air flow inside the room could lead to totally unrealistic results. It is basic and very important to correctly describe the supply air flow condition when the CFD simulation is used for indoor air distribution analysis.

Although several methods of specifying complicated diffuser boundaries have been studied, as discussed in Chapter 2, more practical method is needed for CFD simulation application. A new supply diffuser boundary conditions specification method was proposed in this thesis.

The new method takes advantage of the existing diffuser characteristic equations (ASHRAE Fundamentals, 1993). The specification of the complicated diffuser boundary is transferred to the specification of the jet main region. This method is proven to be applicable. The new method can also save computational time.

5.2 DIFFUSER AIR JETS CLASSIFICATION

The supply air diffuser's characteristics need to be carefully studied before trying to correctly and practically describe its boundary conditions in CFD simulation.

In a ventilated room, the air supplied into the room through the various types of diffusers (e.g., grille-like, ceiling diffusers, perforated panels) is distributed by turbulent air jets. These air jets are the primary factors affecting room air motion (ASHRAE Fundamentals, 1993).

Diffuser air jets have different characteristics when they are supplied from different types of diffusers or under different conditions (initial air temperature, room geometry and size, supply direction, etc.). When the temperature of the supplying air jet is equal to the temperature of the air in the room, the jet is called an isothermal jet. When there is a temperature difference between the incoming air jet and the room air, the air jet is called a non-isothermal jet. When the jet is discharged into a large open space and not influenced by walls and ceilings, the jet is called a free jet. Whereas, when the incoming air jet is attached to a ceiling or wall, it is called an attached jet. Furthermore, if the incoming air jet is affected by the reverse flow in the room caused by the jet itself, it is called a confined jet.

Depending on the types of diffusers, diffuser air jets can be classified as follows:

1. Compact jets: formed by cylindrical tubes, nozzles, square or rectangular openings with a small aspect ratio, unshaded or shaded by perforated plates, grilles etc. Compact air jets are three-dimensional and axis-symmetric at least at some distance from the diffuser opening. The maximum velocity in the cross section of the compact jet is on the axis.
2. Linear jets: formed by slots or rectangular openings with large aspect ratio. These jet flows are approximately two-dimensional. Air velocity is symmetric in the plane at which air velocities in the cross section are maximum.
3. Radial jets: formed when the ceiling cylindrical air diffusers with flat discs or multi-diffusers direct the air horizontally in all directions.
4. Conical jets: formed by cone or regulated multi-diffuser ceiling air distribution devices. They have an axis of symmetry. The air flows parallel to the conical surface (the angle at the top of the cone is 120°) with the maximum velocities in the cross section perpendicular to the axis.
5. Incomplete radial jets: formed by outlets with grilles having diverging vanes and a forced angle of expansion.
6. Swirling jets: forced by diffusers with vortex-forming devices. These devices create rotation, which has besides the axial component of velocity vectors, tangential and radial ones.

5.3 DIFFUSER AIR JET EXPANSION REGIONS

The full length of an air jet (compact, radial, linear, or conical), can be divided into four regions in terms of the maximum or centerline velocity and temperature differential at the cross section (ASHRAE Fundamentals, 1993):

Initial region: A short core region. The maximum velocity (temperature) of the air stream remains practically unchanged.

Transition region: A short region. The centerline velocity and temperature are predictable. The profile of the velocity in this region cannot be normalized. No predictable velocity and temperature profiles can be obtained in this region.

Main region: A region of fully established turbulent flow with velocity profile similarity. The velocity and the temperature can be determined with accuracy from the characteristic equations. The velocity and the temperature profile can be expressed by a single curve in terms of dimensionless coordinates. Temperature and density differences have little effect on cross-sectional velocity profiles (ASHRAE Fundamentals, 1993).

Terminal region: A region of diffuser jet degradation. It is relatively far from the

diffuser and it will not be considered in the diffuser boundary conditions study of this thesis.

The initial and transitional regions are small. The focus of the study in this thesis is on the main region. The characteristic equations in the main region is discussed in the next. It is adequate to apply the diffuser characteristic equations only in the jet main region for the new proposed diffuser description method in CFD simulation. Figure 5.1 shows the first three regions (Abramovich 1960).

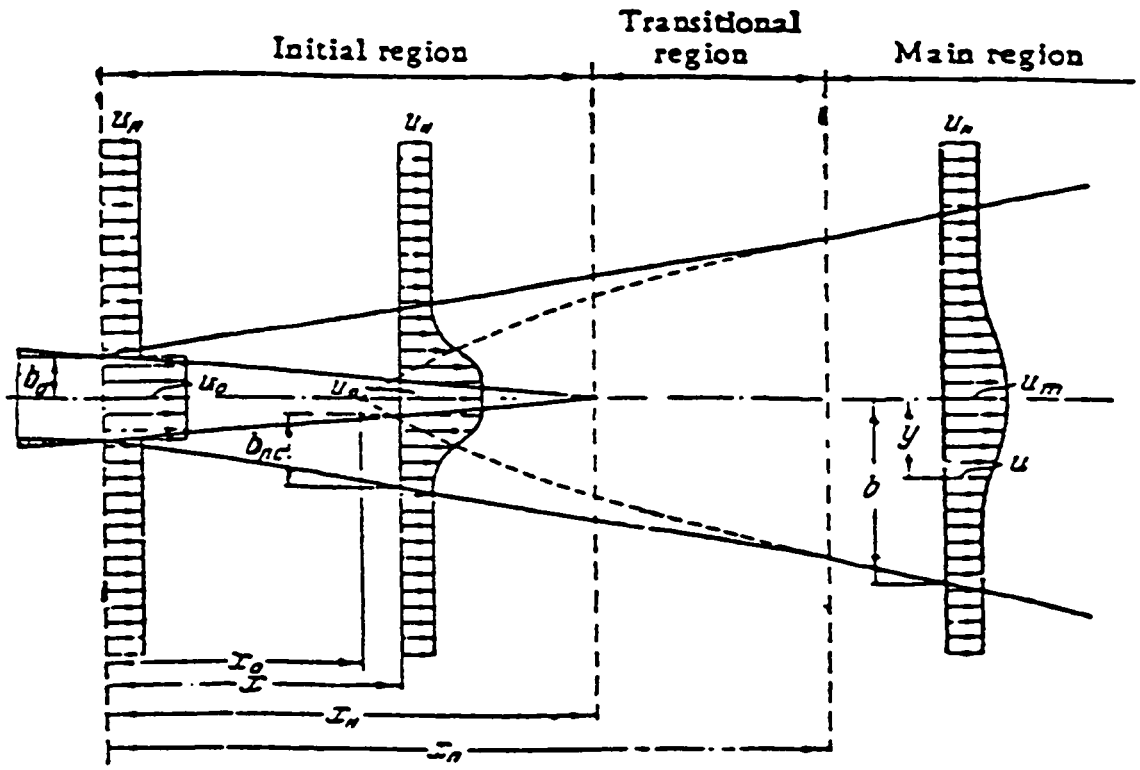

Figure 5.1 Diffuser Jet Regions

5.4 DIFFUSER CHARACTERISTIC EQUATIONS

5.4.1 Velocity Decay of Isothermal Free Jets

The centerline velocity decay of linear jets in the main region can be described by Equation 5.1, and the velocity decay of compact and radial jets can be described by Equation 5.2 (Shepelev 1961):

$$\frac{u_m}{u_0} = K_1 \sqrt{\frac{H_0}{x}} \qquad (5.1)$$

$$\frac{u_m}{u_0} = K_1 \frac{\sqrt{A_0}}{x} \qquad (5.2)$$

where, u_m is the centerline velocity,

u_0 is the average velocity at discharge,

x is the distance to the diffuser face on the jet centerline,

K_1 is the centerline velocity decay constant,

H_0 is the effective width of the linear diffuser jets,

A_0 is the effective area of the diffuser, $A_0=C_d*A_c$,

C_d is the discharge coefficient (usually between 0.65 and 0.90), and

A_c is the diffuser free opening area.

5.4.2 Velocity Decay of Non-isothermal Free Jets

When the temperature of supply air is different from the room air temperature, the behavior of the diffuser air jet is affected by the thermal buoyancy due to the difference on air density. The centerline velocity of a non-isothermal jet introduced vertically and the trajectory of a non-isothermal jet introduced horizontally are influenced by the Archimedes number (Baturin 1972):

$$Ar = \frac{g\Delta t_0 L_0}{Tu_0^2} \qquad (5.3)$$

where, g is the acceleration due to gravity,

Δt_0 is the temperature difference between the supply and return air,

L_0 is the length scale of hydraulic diameter of the diffuser outlet,

T is the mean absolute temperature of the room air, and

u_0 is the average velocity at discharge.

5.4.2.1 Vertically Discharged Non-isothermal Free Jets

For vertically discharged linear diffuser jets, it was found that the calculation of velocity decay can be performed using the following equations (Shepelev 1961):

$$\frac{u_m}{u_0} = K_1 \sqrt{\frac{H_0}{x}} K_n \qquad (5.4)$$

$$K_n = [1 \pm \frac{1.8 K_2}{K_1^2} Ar(\frac{x}{H_0})^{\frac{3}{2}}]^{\frac{1}{3}} \qquad (5.5)$$

where, K_2 is the temperature decay constant of the jets. The "±" sign should be positive when the buoyant force is in the same direction with the initial force, and negative when they are not in the same direction.

For other vertically discharged non-isothermal free jets, such as compact and radial, the following equations can be applied (Shepelev 1961):

$$\frac{u_m}{u_0} = K_1 \frac{\sqrt{A_0}}{x} K_n \qquad (5.6)$$

$$K_n = [1 \pm \frac{2.5 K_2}{K_1^2} Ar(\frac{x}{\sqrt{A_0}})^2]^{\frac{1}{3}} \qquad (5.7)$$

5.4.2.2 Trajectory and Drop of Non-isothermal Supply Air Jets

For horizontally declined compact free jets, with a decline angle, α, of not more than 45°, the trajectory of the centerline can be described as (Shepelev 1961):

$$\frac{z}{A_0} = \frac{x}{\sqrt{A_0}} tg\alpha \pm \Psi \frac{K_2}{K_1} Ar(\frac{x}{\sqrt{A_0}})^3 \qquad (5.8)$$

where, z is the distance below the ceiling at which the maximum velocity in the jet occurs;

x is the horizontal distance to the jet; and

ψ is a coefficient determined by diffuser type, size etc. ψ=0.47±0.06.

Zhang G. (1996) and Zhivov (1993) studied in details the trajectory and characteristics of inclined jets. Their work made it possible to apply the characteristic equations to inclined

diffuser jets.

5.4.3 Velocity Profile of the Jets in the Main Region

The velocity at other points within the jet main region can be calculated by Equation 5.9 (ASHRAE Fundamentals, 1993):

$$\left(\frac{r}{r_{0.5}}\right)^2 = 3.3 \log \frac{u_m}{u} \qquad (5.9)$$

where, u is the velocity at the point being considered,

u_m is the centerline velocity in the same cross-sectional plane,

r is the radial distance of the point under consideration from the centerline of the jet, and

$r_{0.5}$ is the radial distance in the same cross-sectional plane from the axis to the point where the velocity is one-half of the centerline velocity, i.e. $u=0.5u_m$.

5.4.4 Temperature Decay of Non-isothermal Free Jets

The temperature decay in the centerline of the jet was calculated using the following equations (Shepelev 1961):

For linear jets, horizontally projected:

$$\frac{T_m - T_r}{T_0 - T_r} = K_2\sqrt{\frac{H_0}{x}} \qquad (5.10)$$

For linear jets, vertically projected:

$$\frac{T_m - T_r}{T_0 - T_r} = K_2\sqrt{\frac{H_0}{x}}\frac{1}{K_n} \qquad (5.11)$$

For compact, radial and conical jets, horizontally projected:

$$\frac{T_m - T_r}{T_0 - T_r} = K_2\frac{\sqrt{A_0}}{x} \qquad (5.12)$$

For compact, radial and conical jets, vertically projected:

$$\frac{T_m - T_r}{T_0 - T_r} = K_2\frac{\sqrt{A_0}}{x}\frac{1}{K_n} \qquad (5.13)$$

where, T_0 is the supply temperature at the diffuser,

T_r is the return air temperature,

T_m is the temperature along the centerline of the jet main region, and

K_2 is the temperature decay constant.

5.4.5 Temperature Profile in the Jet Main Region

The relation between the velocity distribution and temperature distribution in the cross section of non-isothermal jets could be expressed as follows (ASHRAE Fundamentals, 1993):

$$\left(\frac{r}{r_{0.5}}\right)^2 = 4.7\log\frac{T_m - T_r}{T - T_r} \qquad (5.14)$$

where, T is the actual air temperature at the point being considered,

T_m is the centerline air temperature in the same cross-sectional plane, and

T_r is the return air temperature.

5.4.6 Effects of Ceilings and Walls

Jets discharging parallel to a surface with one edge of the outlet coinciding with the surface take the form of one-half of an axial jet discharging from an outlet twice as large, similar to radial jets from ceiling plaques. Entrainment takes place almost only along the surface of a half cone, and the maximum velocity remains close to the surface (ASHRAE Fundamentals, 1993).

Isothermal ceiling jets were found to attach to the ceiling and flow along it due to the "Coanda" effect if the initial jet axis was close to the ceiling (Tuve 1953). The spread of the jet in the traversing direction was found to be reduced when the axis of a long jet was too close to the ceiling and parallel to it. The angle of divergence of the jet away from the wall was slightly less than one-half the angle of a free conical jet (Tuve 1953).

It was found that if an edge of the nozzle was in contact with the plane, so long as the axis of the nozzle formed an angle less than 40° to 45° with the plane, the jet would cling to the plane and spread over it. But if the edge of the jet was shifted away from the plane, air entrainment would occur on all sides of the jet, and the jet did not cling anymore (Baturin 1972). If the jet attached to a ceiling or a wall, K_1 became larger than for free jets. The values

of K_1 were approximately those of the free jets multiplied by 1.4 (ASHRAE Fundamentals, 1993). When the temperature of the attached air jet is lower than the temperature of the ambient air, this jet will remain attached to the ceiling until the downward buoyancy force becomes greater than the upward static pressure ("Coanda" force).

5.4.7 Effect of Confinement

The confined centerline velocity u_{mc} and the temperature differential Δt_{mc} caused by the reverse flow in the room can be modified using the coefficient K_c (Grimitlyn and Pozin 1973):

$$u_{mc} = u_m * K_c \qquad (5.15)$$

$$\Delta t_{mc} = \Delta t_m * \frac{1}{K_c} \qquad (5.16)$$

where u_m is the centerline velocity calculated from Equation 5.1, 5.2, 5.4 and 5.6. Δt_m is the temperature difference between the jet centerline and the occupied region calculated from Equation 5.10 to 5.13. The values of K_c are available from graphs (Grimitlyn and Pozin 1973).

5.4.8 Diffuser Characteristic Equation Application

All these above mentioned equations are developed for the main region of the diffuser jet. Since the first two regions are very small, the beginning of the main region is still close to the jet surface compared to the room size. The parameters such as the effective supply area A_0 and the average supply velocity u_0 can be obtained from the diffuser manufacturer product

information data. The velocity and temperature decay coefficient K_1 and K_2 for different diffusers can be obtained from ASHRAE Fundamentals. As long as the supply air flow rate and the supply air temperature are given, the velocity and temperature in the jet main region can be calculated using these diffuser jet characteristic equations. If the jet main region can be correctly described as a boundary condition, the CFD prediction results in the working area could be expected to have better accuracy.

5.5 THE NEW PROPOSED DIFFUSER SPECIFICATION METHOD

The new proposed diffuser boundary conditions specification method is a jet main region specification method. It takes advantage of the existing diffuser characteristic equations. The specification of the complicated diffuser boundary is transferred to the specification of the surfaces of a volume around the diffuser. One volume surface is located in the main region of the diffuser jet (Huo et al 1996).

5.5.1 Selection of the Volume

Figure 5.2 shows the boundary conditions considered for the diffuser using the new proposed method. A two-dimensional air jet (linear air jets are two-dimensional jets) is applied in this Figure. The diffuser jet is installed on the ceiling. The air is introduced into the room at an angle α to the vertical direction. A_1B_1 is the jet opening. O_1 is the centre of the jet opening

and O_1O_2 is the centerline of the supplying jet. A_1A_2 and B_1B_2 are the jet region borders. B_2 is selected such that it is located at the beginning of the jet main region. A_2 is selected to make A_2B_2 parallel to the ceiling. Points C and D are selected to make CA_2DB_1 a rectangular volume.

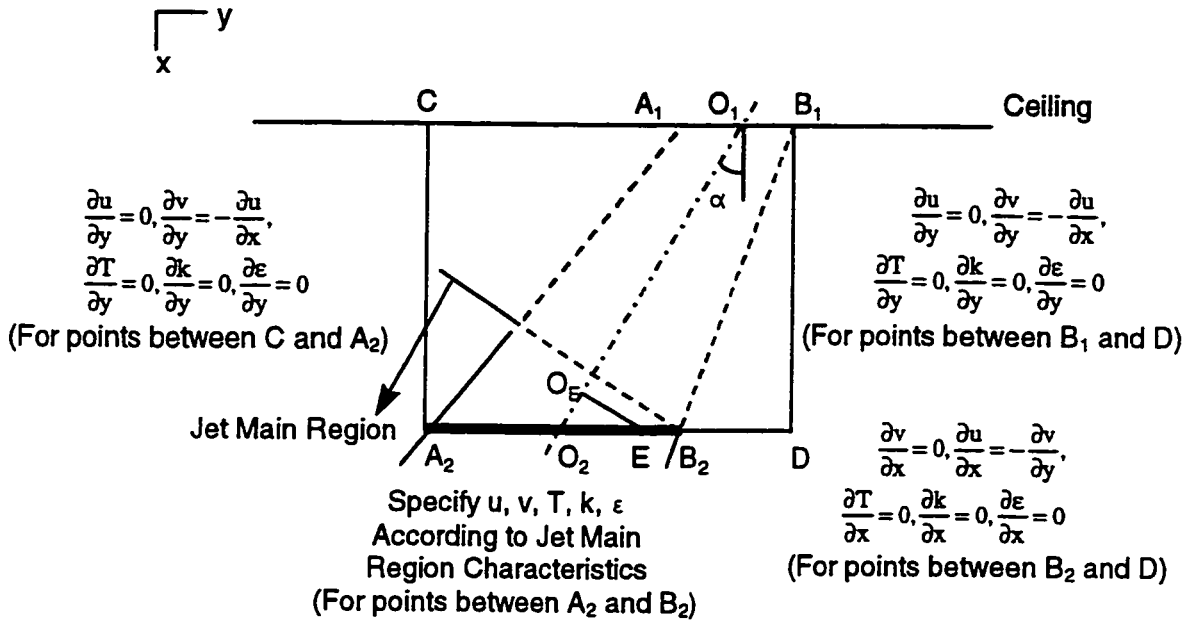

Figure 5.2 Boundary Conditions in the Jet Main Region

Point B_2 decides the height of the volume and points B_1 and A_2 decide the width of the volume in Figure 5.2. As long as A_2B_2 is located inside the jet main region, the volume should be selected as small as possible to minimize the inaccuracy caused by the simplification.

For three-dimensional diffusers (radial, compact etc.), the volume can be selected in a similar manner. The principle is that part of one volume surface needs to be located at the

beginning of the jet main region and the other surfaces should be selected to make a smallest possible volume to eliminate the inaccuracy of the simplification.

The uniqueness of the volume selection is that the jet main region concept is introduced and applied. The surfaces of the volume around the diffuser are divided into two parts, inside the jet main region (A_2B_2) and outside the jet main region (CA_2, B_2D and B_1D), for the boundary conditions specification. One surface of the volume (A_2D) could be partly inside the jet region and partly outside the jet region (Figure 5.2).

5.5.2 Boundary Conditions of the Selected Volume

5.5.2.1 Velocity Boundary Conditions

The velocity boundary conditions of the volume surface inside the jet main region will be calculated using the jet main region characteristic equations.

For two-dimensional cases, as shown in Figure 5.2, when the velocity of a point E on line A_2B_2 (inside the jet main region) is needed, the velocity of its orthogonal projection point O_E on the centerline is calculated first using the velocity decay equations. After the average supply air velocity u_0 is obtained according the supply conditions and the diffuser data from manufacturer's catalog, the velocity decay u_m at the centerline point O_E can be calculated using Equation 5.1 or 5.4.

After calculating the velocity u_m at point O_E, the velocity u at point E can be calculated using the velocity profile equations based on the centerline velocity at point O_E using Equation 5.9. The velocity direction for the points on A_2B_2 is considered the same as the velocity direction of the centerline since the velocity component perpendicular to the centerline is very small compared with the velocity component parallel to the centerline (Baturin, 1972).

For the three dimensional cases, the velocity on the surface located inside the jet main region can be calculated in a similar manner. When the velocity of a point on that surface, u, is needed, the velocity of its orthogonal projection point on the centerline, u_m, is calculated first using Equation 5.2 or 5.6. Then the velocity, u, can be calculated using Equation 5.9. The distance, r, should be a three dimensional distance in Equation 5.9.

When considering the boundary conditions of the other part of the volume surfaces, a zero gradient is assumed based on the fact that the velocity outside the jet main region does not have big changes. Nielsen (1978) applied this assumption in his work. The velocity component parallel to the volume surfaces is assumed as:

$$\frac{\partial V}{\partial n} = 0 \qquad (5.17)$$

where, n is the direction perpendicular to the volume surface; and V is the velocity component parallel to the volume surface. The velocity component perpendicular to the volume surface is determined by using the continuity equation in the simulation. Figure 5.2 shows the equations

for a two dimensional case. The velocity of a three dimensional case can be similarly derived.

5.5.2.2 Temperature Boundary Conditions

Like the velocity boundary conditions, the temperature boundary conditions are also decided depending on whether the surface of the volume is located inside or outside the jet main region.

The jet main region temperature characteristic equations are used for the temperature boundary conditions of the volume surface inside the jet main region. The temperature on the diffuser centerline is calculated first according to the supply air temperature and the diffuser type. When the temperature at a point on the surface inside the jet main region, T, is needed, the temperature of that point's orthogonal projection on the centerline, T_m, is calculated first using Equation 5.10 to 5.13, depending on the diffuser type. Then the temperature at the point, T, can be calculated using the temperature profile (Equation 5.14).

Zero gradient is also assumed for the temperature boundary conditions of the volume surfaces outside the jet main region. Similarly to the velocity boundary conditions simplification. This assumption is based on the fact that temperature outside the jet main region does not have big change. The equation applied is:

$$\frac{\partial \theta}{\partial n} = 0 \qquad (5.18)$$

where, θ is the temperature difference, and n is the direction perpendicular to the volume surface.

5.5.2.3 Boundary Conditions for k and ε

The boundary conditions, k and ε, for the volume surface inside the jet region can be determined based on Rodi and Spalding's (1983) work. They reviewed and studied the turbulence model for the jet. They summarized other researchers' measurement data for k when using different types of diffusers. For the same type of diffusers, the same dimensionless curve can be obtained in the jet main region. In this thesis, k is decided based on the measurement curves they summarized. They also suggested that ε could be calculated using the following equation:

$$\varepsilon = C_D \frac{k^{\frac{3}{2}}}{L} \qquad (5.19)$$

where, C_D is a constant, equal to 0.09 for a plane jet and 0.06 for a round jet,

L is a length scale, equal to 0.075d for a radial jet, 0.052d for a plane jet and 0.033d for a round jet, and

d is the distance from the jet centerline to the edge of the jet region at the location where ε is specified.

The boundary conditions, k and ε, for the other part of the volume surfaces are described in a similar manner as the velocity and temperature boundary conditions. They are

assumed as:

$$\frac{\partial k}{\partial n}=0, \qquad \frac{\partial \varepsilon}{\partial n}=0 \tag{5.20}$$

where, n is the direction perpendicular to the volume surface.

5.6 VALIDATION OF THE PROPOSED METHOD

5.6.1 Simulation Software

The air velocity prediction CFD code, EXACT3 (Kurabuchi 1989), was modified for this study. EXACT3 can simulate three dimensional and non-isothermal cases. The k-ε two equation turbulence model is applied, and an energy equation is added to consider the buoyancy effect in the code.

EXACT3 uses the following equations to simulate the air flow pattern:

$$\frac{\partial u_j}{\partial x_j}=0 \tag{5.21}$$

$$\frac{\partial u_i}{\partial t}+\frac{\partial u_i u_j}{\partial x_j}=-\frac{1}{\rho}\frac{\partial \Pi}{\partial x_i}+\frac{\partial}{\partial x_j}\left\{(\nu+\nu_t)\left(\frac{\partial u_j}{\partial x_i}+\frac{\partial u_i}{\partial x_j}\right)\right\}-\beta g_i \theta \tag{5.22}$$

where, $\Pi = p + 2\rho k / 3$

$$\frac{\partial \theta}{\partial t}+\frac{\partial \theta u_j}{\partial x_j}=\frac{\partial}{\partial x_j}\left\{\left(K+\frac{\nu_t}{\sigma_\theta}\right)\frac{\partial \theta}{\partial x_j}\right\}+h(x_j,t) \tag{5.23}$$

$$\frac{\partial k}{\partial t}+\frac{\partial k u_j}{\partial x_j}=\frac{\partial}{\partial x_j}\left\{\left(\nu+\frac{\nu_t}{\sigma_k}\right)\frac{\partial k}{\partial x_j}\right\}+\nu_t\left(\frac{\partial u_j}{\partial x_i}+\frac{\partial u_i}{\partial x_j}\right)\frac{\partial u_i}{\partial x_j}+\beta g_i\frac{\nu_t}{\sigma_\theta}\frac{\partial \theta}{\partial x_i}-\varepsilon \tag{5.24}$$

$$\frac{\partial \varepsilon}{\partial t}+\frac{\partial \varepsilon u_j}{\partial x_j}=\frac{\partial}{\partial x_j}\left\{\left(\nu+\frac{\nu_t}{\sigma_\varepsilon}\right)\frac{\partial \varepsilon}{\partial x_j}\right\}+\frac{\varepsilon}{k}\left\{C_1\nu_t\left(\frac{\partial u_j}{\partial x_i}+\frac{\partial u_i}{\partial x_j}\right)\frac{\partial u_i}{\partial x_j}-C_2\varepsilon+C_3\beta g_i\frac{\nu_t}{\sigma_\theta}\frac{\partial \theta}{\partial x_i}\right\} \tag{5.25}$$

Eddy viscosity:

$$\nu_t=C_D\frac{k^2}{\varepsilon} \tag{5.26}$$

where, x_i are the Cartesian coordinates,

t is the time,

u_i is the velocity component in the x_i direction,

θ is the temperature difference,

k is the turbulent kinetic energy,

ε is the dissipation rate of the turbulent kinetic energy,

p is the static pressure difference,

ρ is the density of air,

ν is the kinematic viscosity of air,

ν_t is the eddy viscosity of air,

β is the volumetric coefficient of expansion,

g_i is the gravitational acceleration in the x_i direction,

K is the thermal diffusivity, and

h is the heat generation rate.

Empirical constants are:

$C_D = 0.09$, $C_1 = 1.44$, $C_2 = 1.92$, $C_3 = C_1$, $\sigma_k = 1.0$, $\sigma_\varepsilon = 1.3$ and $\sigma_\theta = 0.5$.

The density of air ρ is considered as a constant in EXACT3 to simplify the calculation process.

Finite difference numerical method is applied in EXACT3, and the "Marker and Cell" (MAC) method is implemented to solve these equations (Kurabuchi, 1989). A pseudo time step is used and the simulation reaches a steady state result when the accumulated time step converges.

EXACT3 can only be used to simulate a rectangular region. To apply the new diffuser description method, the boundary condition subroutine of the EXACT3 code was modified to assign the boundary conditions of the volume around the diffuser.

5.6.2 Case Studies

Three cases were designed to validate the new proposed diffuser description method.

5.6.2.1 First Case

In the first case, a simple linear diffuser under a two dimensional isothermal condition was studied. This case is designed to validate whether the new proposed method is applicable. Since the conventional method provides correct predictions for simple geometry diffusers, such as the one applied in this case, the prediction of the conventional method was treated as a correct solution in this case.

The simulation results of the new jet main region specification method and the conventional method for this case are shown in Figures 5.3(a) and 5.3(b). There are no velocity vectors inside the small volume around the supply diffuser in Figure 5.3(a) when the new proposed method is used. For comparison purposes, the velocity vectors were removed in the same volume position when the conventional method was applied in Figure 5.3(b). The results indicate that the air flow pattern predicted using the new method is similar to the air flow pattern predicted by the conventional method.

To further compare these results, the velocity along a vertical line at the supply position is shown in Figure 5.4(a). For this simple case, a calculation curve using the diffuser characteristic equations is also presented, considered to be the correct result. The conventional method provided slightly better results. However, the new method still provided acceptable results.

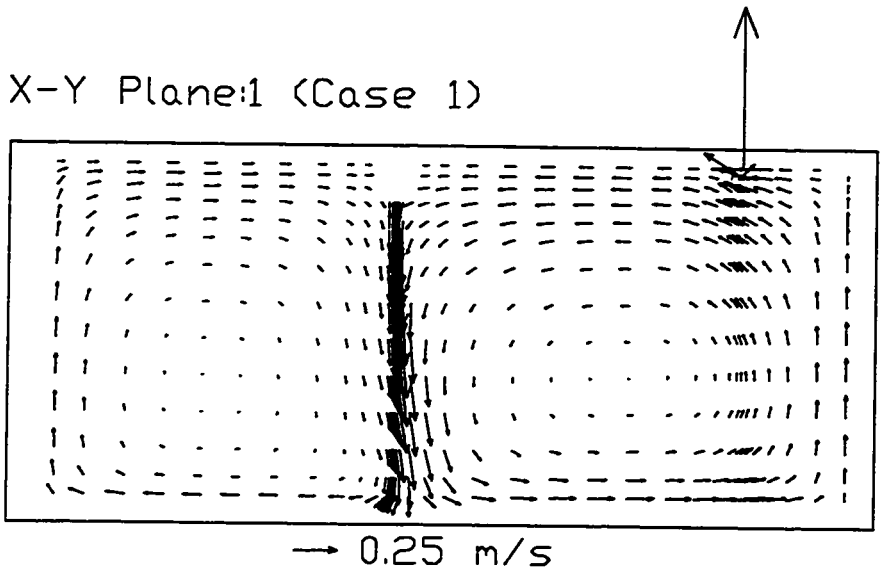

(a) Jet Main Region Specification Method

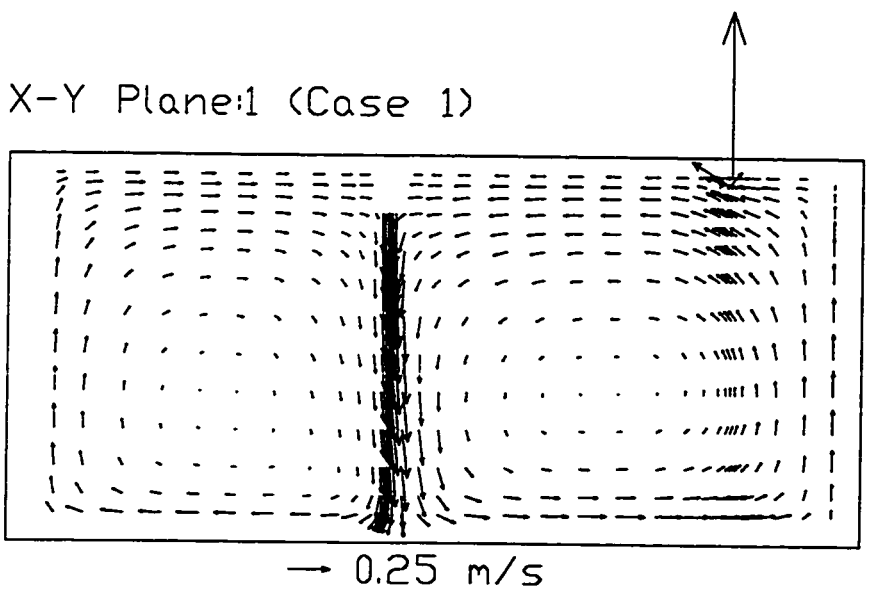

(b) Conventional Method

Figure 5.3 Simulation Velocity Vectors for the First Case

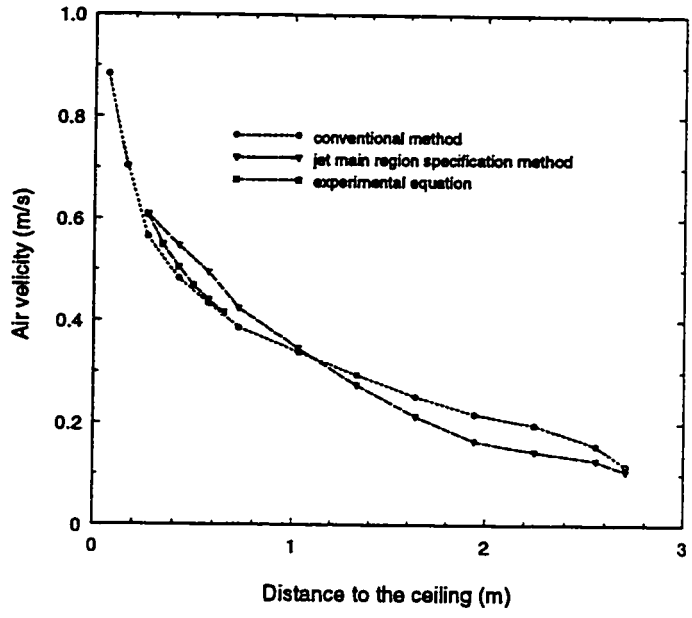

(a) Air Velocity in a Vertical Line (Supply Position)

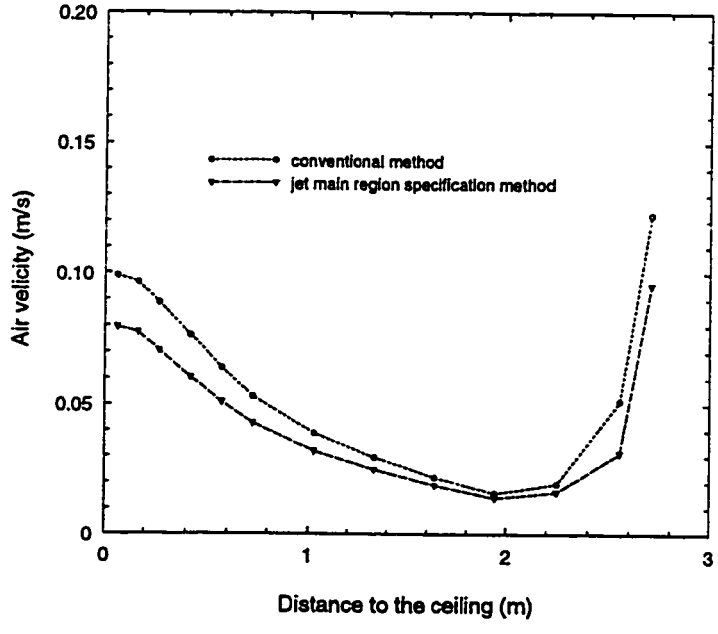

(b) Air Velocity in a Vertical Line (0.75m from the Supply)

Figure 5.4 Detailed Velocity Comparison of the First Case

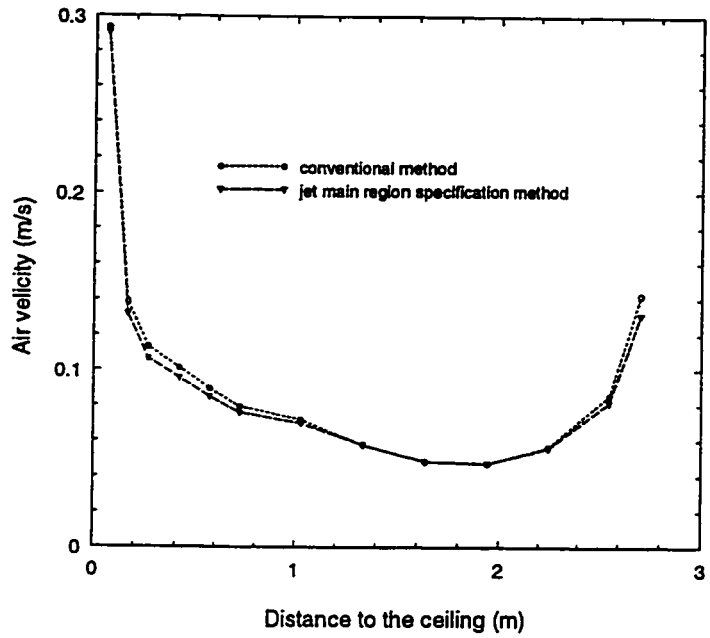

(c) Air Velocity in a Vertical Line (Return Position)

Figure 5.4 Detailed Velocity Comparison of the First Case

The comparison of the velocity along a vertical line 0.75m from the diffuser is shown in Figure 5.4(b). The simulation results using the new method are in good agreement with the results obtained using the conventional method in the working area. There are some differences in the region close to the ceiling. This is due to the inaccuracy caused by the simplification of the volume surfaces which were not located in the jet main region. The largest difference (less than 20%) only occurred in a small region close to the ceiling. The difference at breathing height (1.5 to 2m away from the ceiling) is very small.

A comparison of the velocity along a vertical line at the return position is shown in Figure 5.4(c). The differences between these two methods are negligible.

The simulation results of this case indicate that the new jet main region specification method could be applied. The results are in good agreement with the other methods as shown in Figure 5.4, and no convergence difficulties were encountered.

5.6.2.2 Second Case

The second case was similar to the first one. The only difference was that the direction of the supply air was not perpendicular to the ceiling but at an angle of 60 degrees. In this case, two and a half edges of the volume were located outside the jet main region. Simplification of the boundary conditions had to be applied to all these edges. Furthermore, the simplifications were applied to more than one direction. The boundary conditions of two edges perpendicular to one direction and one edge perpendicular to the other direction need to be simplified. In the simplified part of volume boundaries, the air may move out the volume in one position and move into the volume in another position (see Figure 5.2). In short, many more simplifications were required for this case. This case was designed to examine whether the simplifications under these conditions would cause any problems.

The velocity vector distribution of the simulation using the new jet main region specification method is shown in Figure 5.5(a). It indicates that the air flow pattern inside the room is reasonable. No large discrepancies can be seen directly. No convergence problem and other difficulties were encountered in the simulation when the jet main region specification method was applied for such a case.

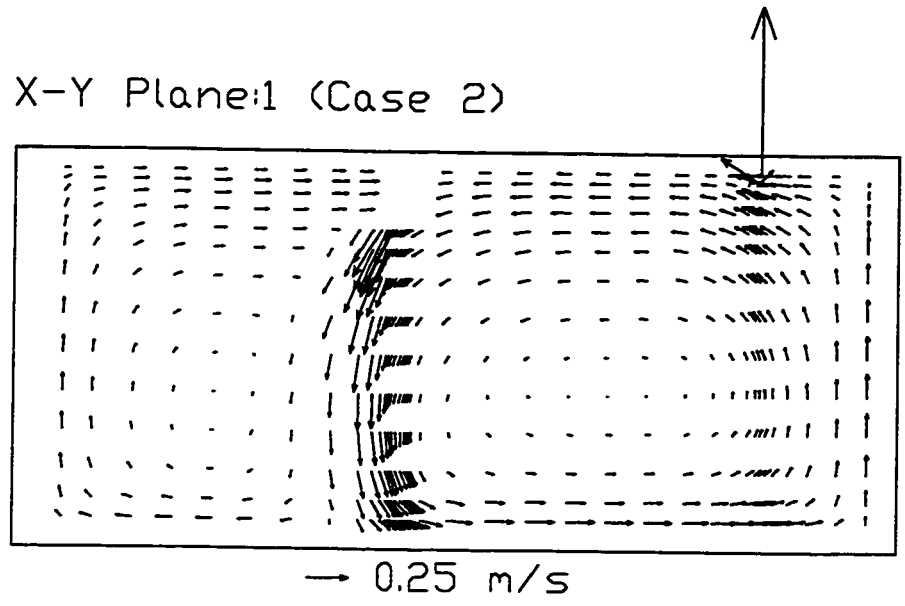

(a) Jet Main Region Specification Method

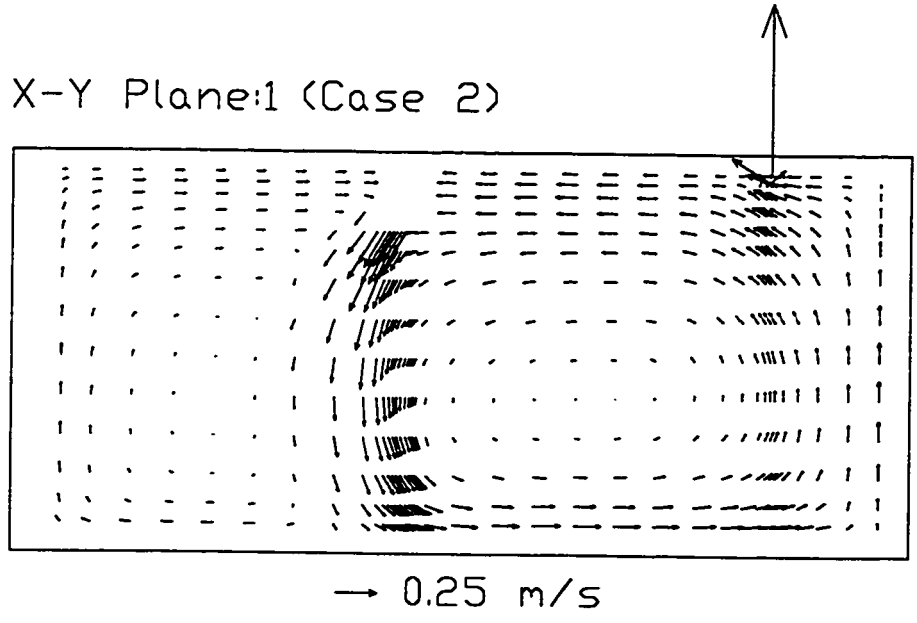

(b) Conventional Method

Figure 5.5 Simulation Velocity Vectors for the Second Case

The simulation results using the conventional method are shown in Figure 5.5(b). Comparing Figure 5.5(a) an 5.5(b), it can be seen that the new proposed jet main region specification method provided the correct air flow pattern prediction.

Even though no measurement data strongly support the results in this case. The results still indicate that the simplification at the three edge of the volume for the new proposed jet main region specification method was acceptable. The new proposed method could, at least, provide the correct air flow pattern in the room.

5.6.2.3 Third Case

In the third case, the data from a detailed measurement which was carried on a test chamber (Christianson, 1994) was used to study the validity of the new diffuser description method. The diffuser used in this study was a square diffuser and the simulation was performed for a three dimensional and non-isothermal situation. This case is designed to compare the predictions made by the new method and those made by the measurement and the conventional method while a complicated geometry diffuser was encountered.

The geometry of the test room and the square diffuser layout are shown in Figures 5.6(a) and 5.6(b), respectively. There were 15*21*16 measurement points in the room to study the velocity and temperature distributions.

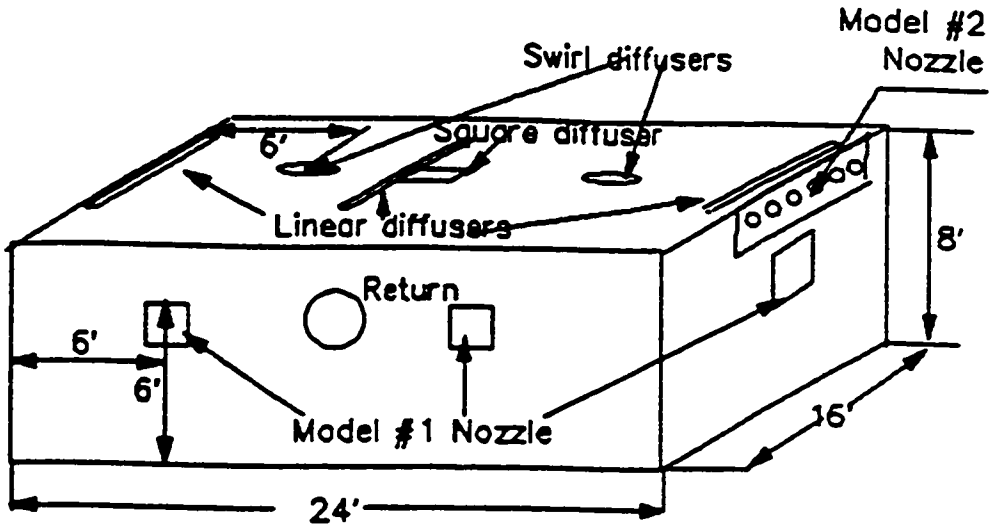

(a) Geometry of Test Room

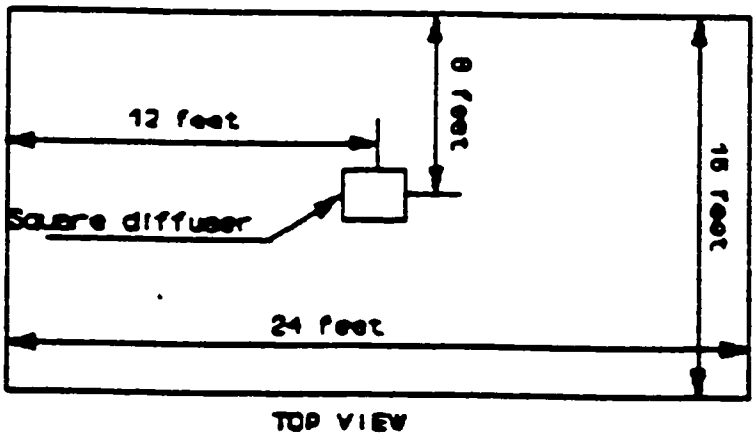

(b) Location of the Square Diffuser

Figure 5.6 Test Room Layout of the Third Case

A 16*26*22 grid was defined in the simulation while using the jet main region specification was applied for this case. A volume was selected around the diffuser. The four surface of the volume perpendicular to the ceiling were located in the jet main region. The boundary conditions on these four surfaces were calculated using jet main region characteristic equations. The boundary conditions on another surface, which parallel to the ceiling was simplified using zero gradient (Equations 5.17, 5.18 and 5.20) for velocity, temperature, k and ε specification.

The simulation took about 12 hours on an IBM system/6000 workstation. The velocity vector and contour along a center vertical plane using the new method are shown in Figures 5.7(a) and 5.8(a), respectively, and the measured velocity contour in the same plane is shown in Figure 5.9.

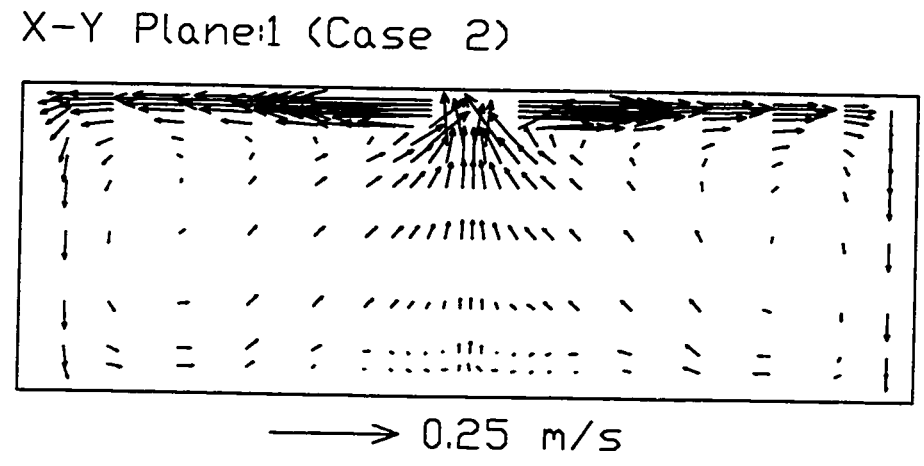

(a) Jet Main Region Specification Method

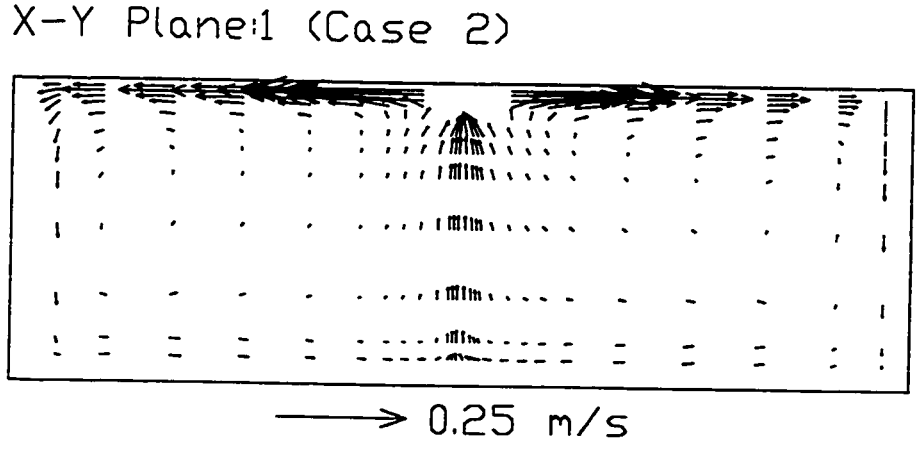

(b) Conventional Method in the Middle Vertical Plane

Figure 5.7 Simulation Velocity Vectors for the Third Case

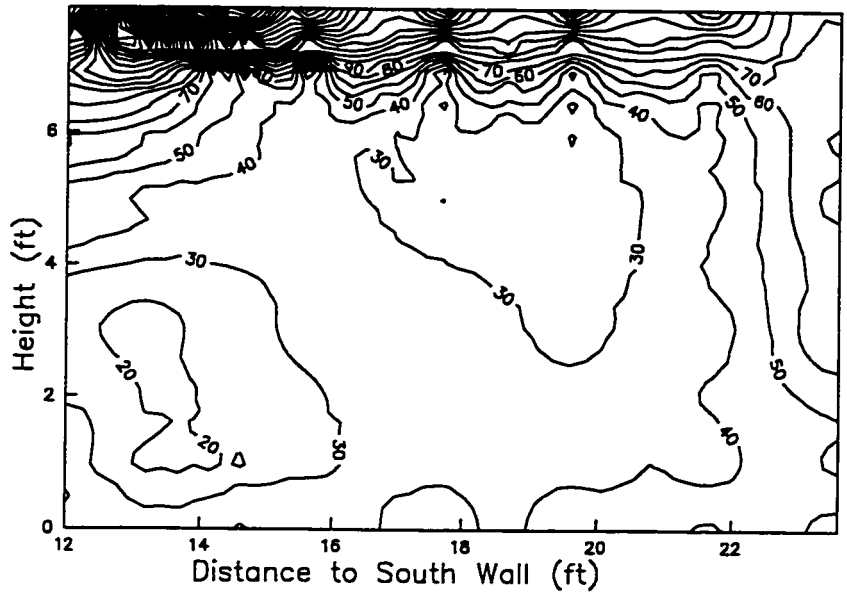

(a) Jet Main Region Specification Method

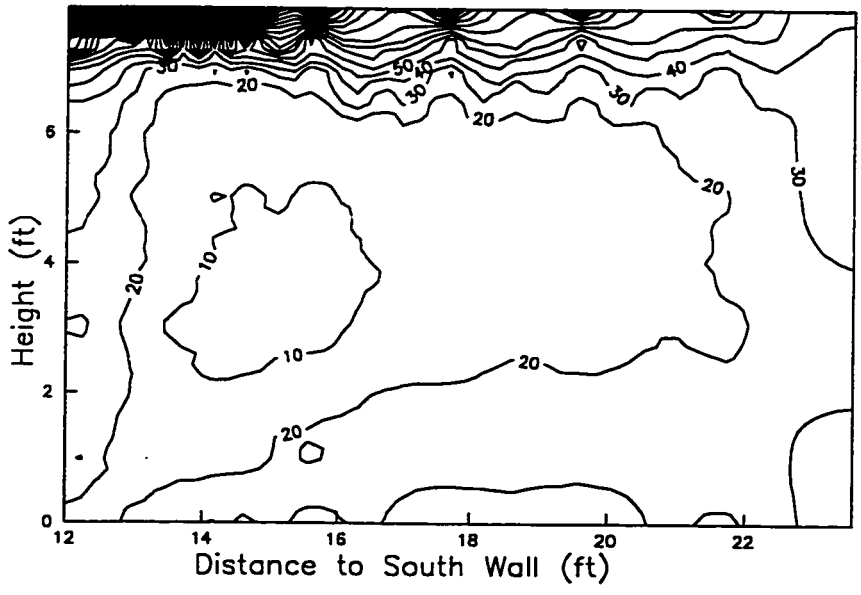

(b) Conventional Method

Figure 5.8 Simulation Velocity Contour in the Middle Vertical Plane

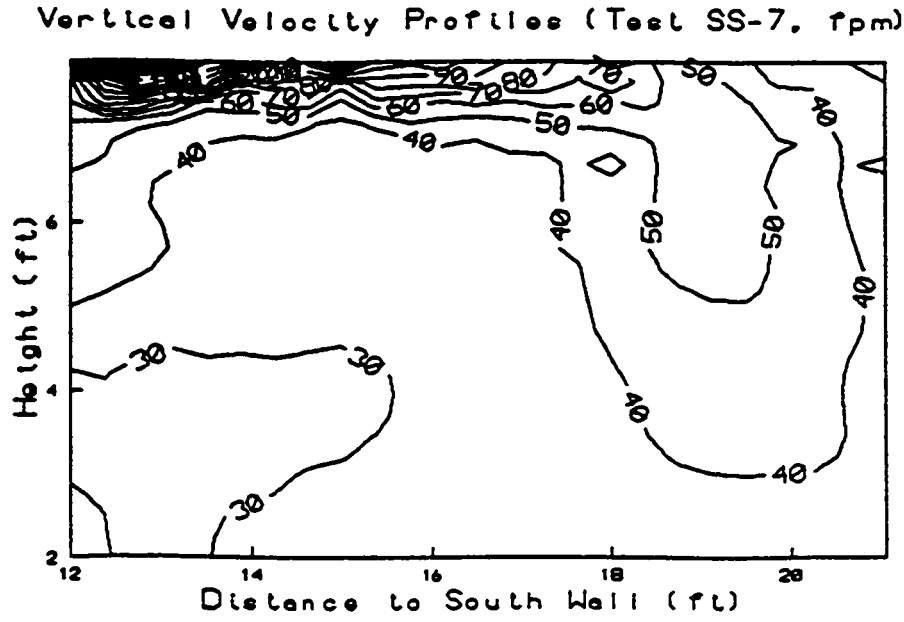

Figure 5.9 Measurement Velocity Contour in the Middle Vertical Plane

While the conventional method was applied for this case, the method used to specify the boundary condition in the conventional method was as follows:

$$u_0 = \frac{Q_s}{A} \qquad v_0,\ w_0 = \sqrt{V^2 - u_o^2} \qquad (5.27)$$

where, u_0, v_0 and w_0 are the supply air velocity component in the x, y and z direction, respectively; A is the area of the diffuser opening, Q_s is the supply air flow rate, and V is the supply air velocity at flow rate Q_s, provided by the diffuser manufacturer manual.

More grids had to be used to specify the square diffuser in the conventional method than in the jet main region specification method. The total number of grids was increased from

8580 (16*26*22) to 11700 (16*30*26). When less grids were applied in the conventional method, the results were very poor compared to the measurement data. The difficulty in reaching convergence also increased in the conventional method. A half time step, as applied in the jet main region specification method, had to be applied to obtain the converged results. In the end, the simulation time under this condition was five times longer than that using the new proposed jet main region specification method.

The velocity vector in the same vertical plane for the simulation results using the conventional method is shown in Figure 5.7(b). The velocity contour at this plane is shown in Figure 5.8(b).

The simulation results obtained by the jet main region specification method (Figure 5.8(a)) yield a similar air flow pattern as the measurement data (Figure 5.9). The flow pattern from the conventional method did not compare well with the measurement data.

A comparison of the velocity at the breathing height along the middle vertical plane for both diffuser specification methods and the measurement data are shown in Figure 5.10. It shows that the new proposed method provided better agreement with the measurement data than the conventional method.

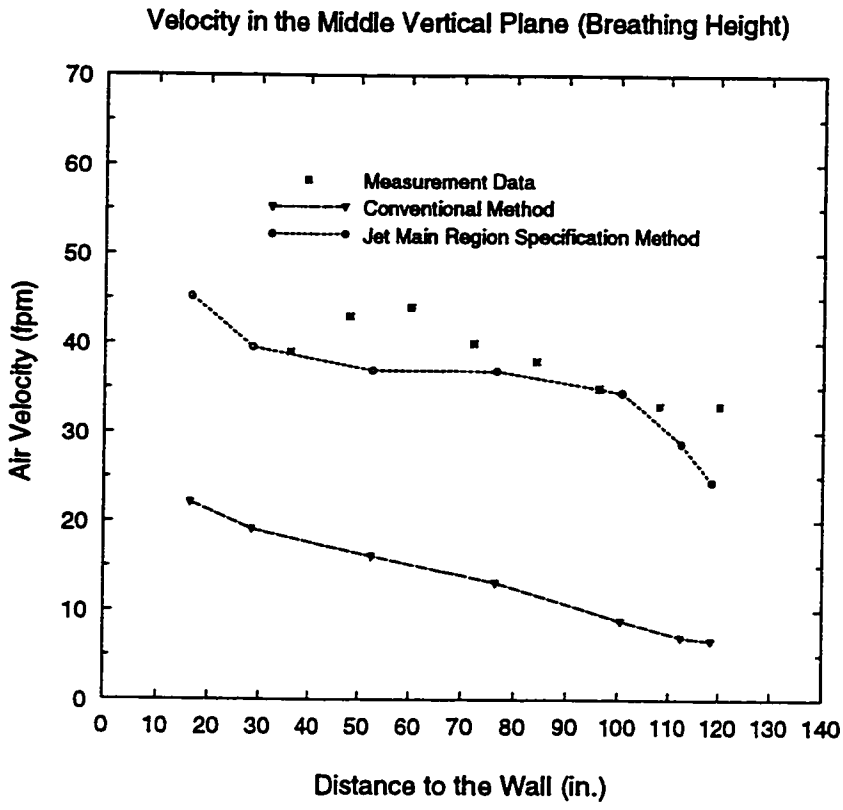

Figure 5.10 Detailed Velocity Comparison of the Third Case

When comparing the contours, Figures 5.8(a) and 5.9, air velocity differences between the new proposed method and the measurement data exist if the entire room is considered. The air velocity in the jet main region, calculated using the jet characteristic equations, was a little higher than the measurement data. This might cause some inaccuracy. It could be improved by developing more accurate jet characteristic equations. In spite of this, the new method provided much better results than the conventional method when compared to the measurement data.

5.7 CONCLUSIONS

Based on the case studies, it can be concluded that the new proposed jet main region specification method provides an applicable and more accurate way to correctly specify the diffuser boundary conditions in CFD simulation. The assumptions used in the new method are reasonable, misleading results will not occur.

The advantages of the new proposed method are:

1. The user can avoid describing the complicated diffuser geometry by using data from manufacturer's catalogs;
2. Correct air flow patterns in a room can be predicted;
3. The method is applicable for different diffusers;
4. A savings in simulation time can be realized since a lower grid density can be used.

It should also be noted that, when the new jet main region specification method is used, it is very important to find the suitable diffuser characteristic equations. Calculation is required for the jet main region boundary conditions specification.

Although the new method is not a perfect one, it leads an acceptable air flow pattern prediction in the room. The conventional method is only applicable for the simple case studied

earlier. It cannot provide the correct air flow pattern prediction in complicated cases. Until computing capacity is significantly improved from today's situation, the new proposed jet main region specification method is an accurate and practical way to specify the diffuser boundary conditions in CFD simulations for studying the air distribution in HVAC and IAQ analyses.

CHAPTER 6

INDOOR AIR QUALITY INDICES STUDY USING CFD METHOD

6.1 INTRODUCTION

The three cases presented in the experimental study of this thesis were simulated using the CFD method, the results of which are presented in this chapter. The new proposed diffuser description method was applied in the CFD simulation for these cases. The same CFD simulation software used in Chapter 5, modified EXACT3, was applied. The contaminant distribution simulation software, CONTAM3, was also applied to analyze the indoor air quality indices. The simulation results were compared with the experimental data to further validate the new proposed diffuser description method and CFD application in indoor air quality analysis.

6.2 THE CASES SELECTED IN THIS STUDY

Three cases were selected in this study; they are Case 008, Case 007 and Case 006 conducted in the experimental study. The test room was empty in Case 008. The partitions were present in the test room in Case 007. Both partitions and furniture were present in the test room in Case 006. The room layout and supply air conditions were the same in all three cases (Table 3.1). The dimensions of the room are 4.9m*4.8m*2.9m high. A square diffuser was used as the air supply device. The total supply air flow rate was 30 L/s and the outdoor air flow rate was 10 L/s. The supply air temperature was 17°C and the room temperature was designed for 23°C. The partitions used in Case 007 and Case 006 were 1.8m high with an air gap of 0.15m at the bottom. The workstation produced by the partitions was 2.9m*2.6m in size (Figure 3.2(a)). The arrangement of furniture in Case 006 include a desk, a chair, a book case and a bookshelf as shown in Figure 3.2(a). A point contaminant source was located at the same position for all the three cases (Figure 3.2(b), black point #1, floor level).

The uniformity of the air distribution, mean age of air and contaminant removal efficiency were measured in the experimental study for these three cases. They were studied using the CFD method in this chapter.

6.3 THE TECHNIQUE TO STUDY THE IAQ INDICES

EXACT3 and CONTAM3 software were used in this study. Using the EXACT3 (or most of the other CFD simulation software), the velocity and temperature distribution in the studied room can be predicted. The CONTAM3 software can predict the contaminant distribution given the input data of the velocity and temperature distribution in the room and the contaminant sources positions and their strength. The indoor air quality indices, such as the uniformity of the air distribution, mean age of air and contaminant removal efficiency, can be predicted using the CONTAM3 software after some derivations (Li 1992). The jet main region specification method was applied to specify the supply boundary conditions in this study.

6.3.1 Air Distribution

The uniformity of the air distribution in a room, U_{rm}, was defined in Equation 6.1, which is the same as the one used in the experimental study (Equation 3.1).

$$U_{rm} = 1 - \frac{C_{std}}{C_{avg}} \qquad (6.1)$$

where, C is the contaminant concentration,

C_{std} is the standard deviation of the C distribution, and

C_{avg} is the average value of C distribution.

In the simulation, the supply air was considered as a "contaminant" source in the supply duct, which kept the contaminant concentration at the supply duct as C_0. When applying the CONTAM3 software, the contaminant boundary condition was considered as $C=C_0$ at the inlet and $\partial C/\partial x = 0$ at the outlet. x is the direction perpendicular to the return grille surface. The distribution of C in the whole room could be calculated using the CONTAM3 software, after the velocity and temperature distribution was predicted using the EXACT3 software. The air distribution uniformity index, U_m, can be calculated based on the simulation results of the C distribution in the room.

6.3.2 Mean Age of Air

The local mean age of air is an important indicator for indoor air quality analysis. It is usually obtained from the experimental data. A derivation could make it easier and more effective to calculate the local mean age of air by using CFD simulation method.

If it is assumed that there is a uniform air concentration C(0) in the whole room at time 0, and at time t the concentration at position p becomes C(t), the definition of the local mean age of air τ_p at position p is (Li 1992):

$$\tau_p = \int_0^{\infty} \frac{C(t)}{C(0)} dt \qquad (6.2)$$

and C(t) satisfies the following contaminant conservation equation:

$$\frac{\partial C}{\partial t}+\frac{\partial Cu_j}{\partial x_j}=\frac{\partial}{\partial x_j}\left\{\left(D+\frac{\nu_t}{\sigma_c}\right)\frac{\partial C}{\partial x_j}\right\} \qquad (6.3)$$

where D is the contaminant diffusion coefficient, and the empirical constant σ_c equals to 0.5. Dividing both sides of Equation 6.3 by C(0) (a constant) and integrating both sides from t=0 to t=∞, the equation will become,

$$\frac{\partial \tau_p u_j}{\partial x_j}=\frac{\partial}{\partial x_j}\left\{\left(D+\frac{\nu_t}{\sigma_c}\right)\frac{\partial \tau_p}{\partial x_j}\right\}+1 \qquad (6.4)$$

This is the steady state contaminant conservation equation used in CONTAM3 with the source term as 1 (which will be related to the supply and return conditions in the non-dimensional form equation). If the boundary condition $\tau_p=0$ is considered at the inlet and $\partial\tau_p/\partial x=0$ at the outlet (Li 1992), the local mean age of air could be calculated directly by using the CONTAM3 software, after the room air velocity and temperature distribution was predicted using the EXACT3 software.

6.3.3 Contaminant Removal Efficiency

The contaminant removal efficiency, E, is defined as:

$$E=\frac{C_r-C_s}{C-C_s} \qquad (6.5)$$

where, C is the contaminant concentration at the point to be analyzed,

C_r is the contaminant concentration in the return air, and

C_s is the contaminant concentration in the supply air.

The contaminant removal efficiency can be calculated with the value of C simulated by the CONTAM3 software, after the air velocity and temperature distribution was predicted using the EXACT3 software.

6.4 MAIN REGION SPECIFICATION METHOD APPLICATION

In all the simulations for indoor air quality indices studies, the jet main region specification method was applied. The velocity and temperature jet region boundary conditions were already discussed in Chapter 5. The contaminant boundary conditions of the jet main region were also calculated using the jet main region characteristic equations when the CONTAM3 software was applied.

When specifying the contaminant concentration boundary conditions for the jet main region, the contaminant concentration was calculated using the temperature characteristic equations in the jet main region. The contaminant distribution was assumed to have the same distribution as the temperature in the jet main region. The assumption is based on the fact that the Lewis number for air is approximately equal to 1. Lewis number, Le, is defined as $Le=\alpha/D$, where α is the dissipation rate of heat (temperature) and D is the dissipation rate of mass (contaminant). When the Lewis number is equal to 1, the

temperature and the contaminant have the same dissipation rate. The non-dimensional equations of the temperature distribution in the jet main region (Equation 5.10 to 5.14) could be used for the contaminant concentration calculation in the jet main region.

6.5 THE FLOW CHART OF THE SIMULATION PROCEDURE

Figure 6.1 shows the flow chart of the CFD simulation procedure for indoor air quality indices analysis.

6.6 SIMULATION RESULTS DISCUSSION

The computer used for the CFD simulation is an IBM system/6000 workstation. The grids applied in the CFD simulation were 25*37*37 for all three cases studied. Approximately thirty hours were spent for each case to obtain the converged results when simulating the air flow using the EXACT3 software. Eight hours were spent for each case to obtain the converged results when simulating the contaminant flow using the CONTAM3 software. The simulation results for the three cases studied are discussed in the following sections.

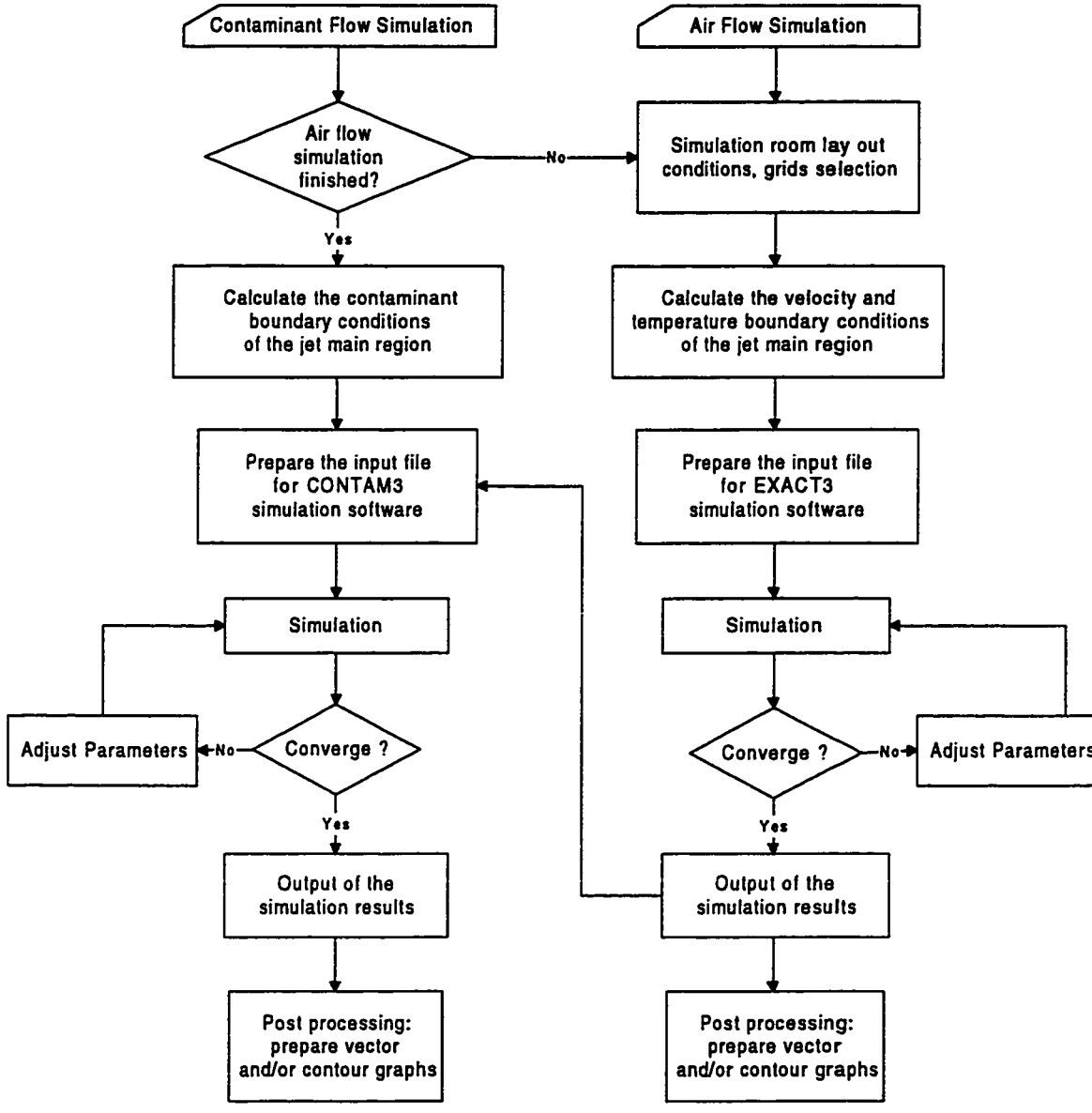

Figure 6.1 Flow Chart of the CFD Simulation Procedure

6.6.1 Simulation Results Of Velocity Distribution

Figure 6.2 and Figure 6.3 show the velocity vectors in the three studied cases.

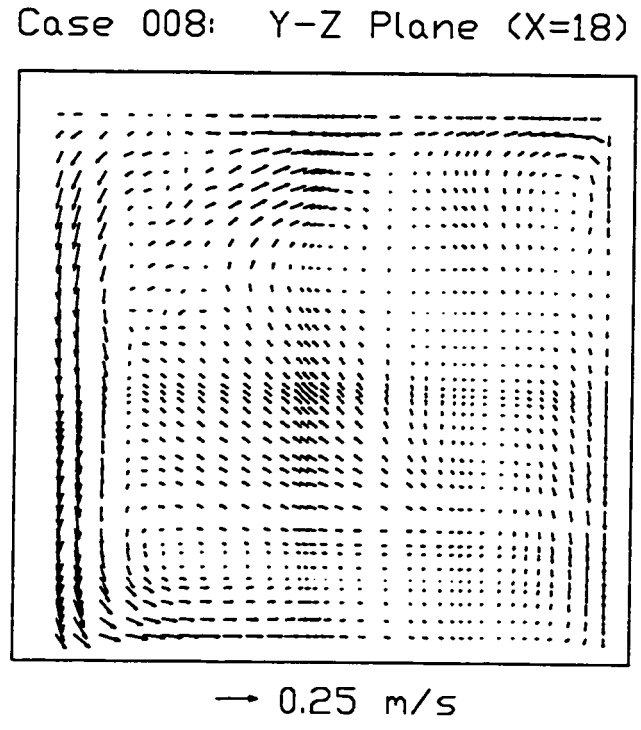

(a) Velocity Vectors in a Horizontal Plane of Case 008

Figure 6.2 Simulation Velocity Vectors in a Horizontal Plane

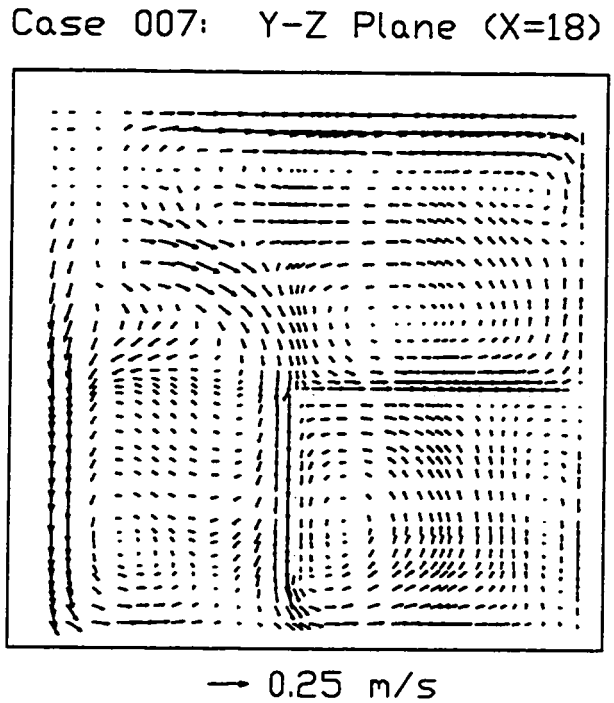

(b) Velocity Vectors in a Horizontal Plane of Case 007

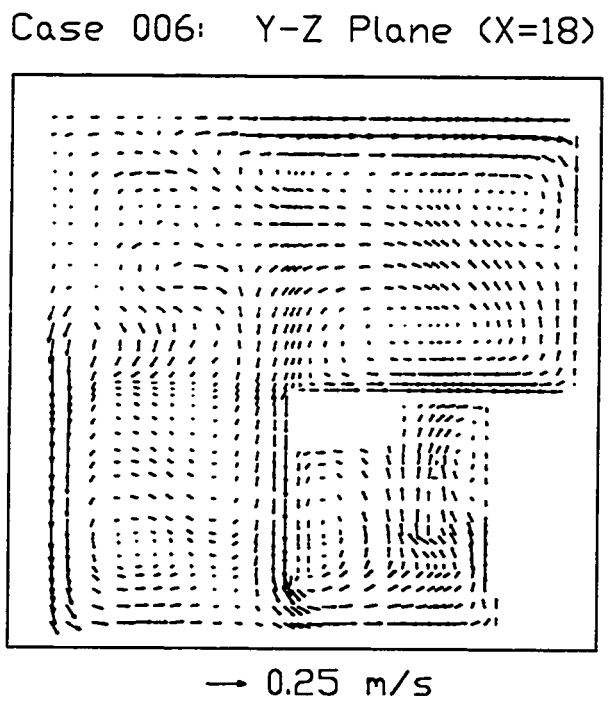

(c) Velocity Vectors in a Horizontal Plane of Case 006

Figure 6.2 Simulation Velocity Vectors in a Horizontal Plane

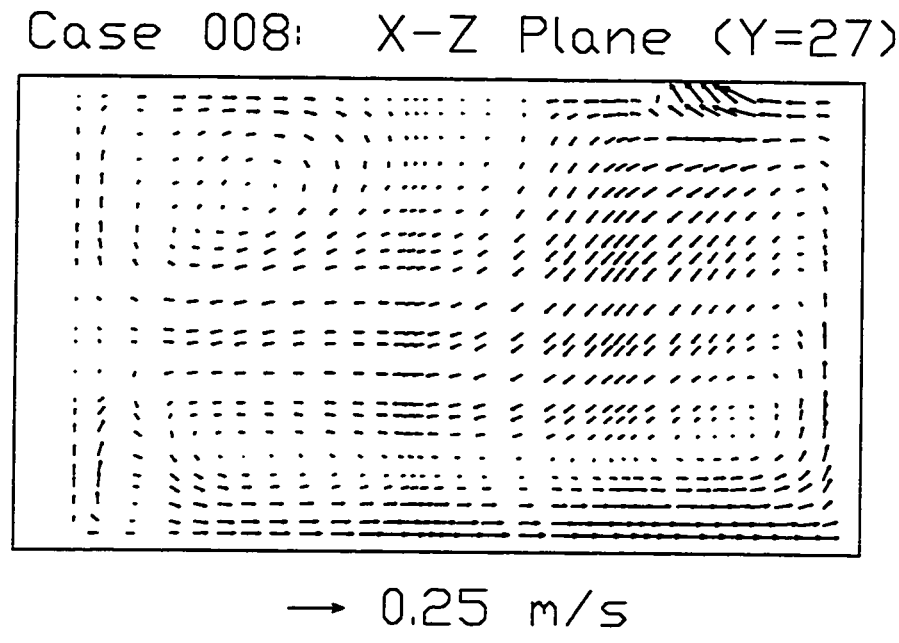

(a) Velocity Vectors in a Vertical Plane of Case 008

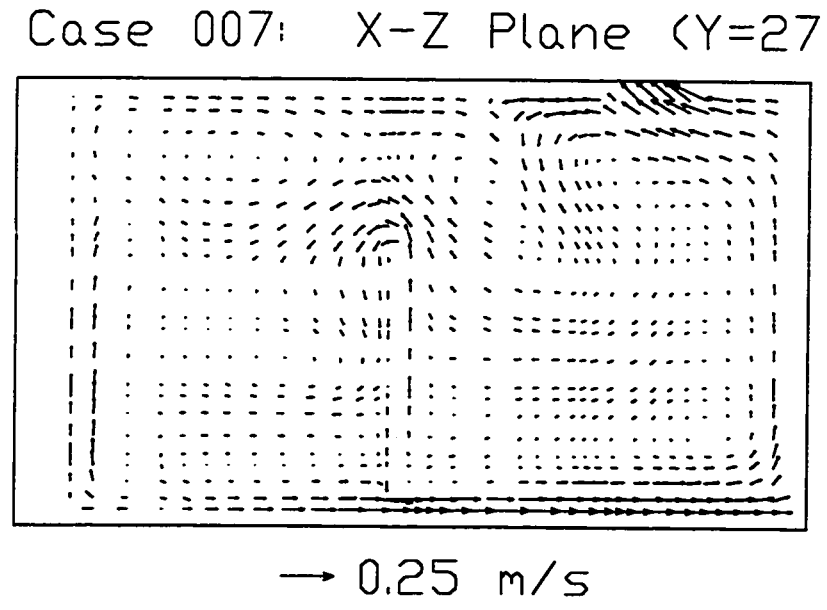

(b) Velocity Vectors in a Vertical Plane of Case 007

Figure 6.3 Simulation Velocity Vectors in a Vertical Plane

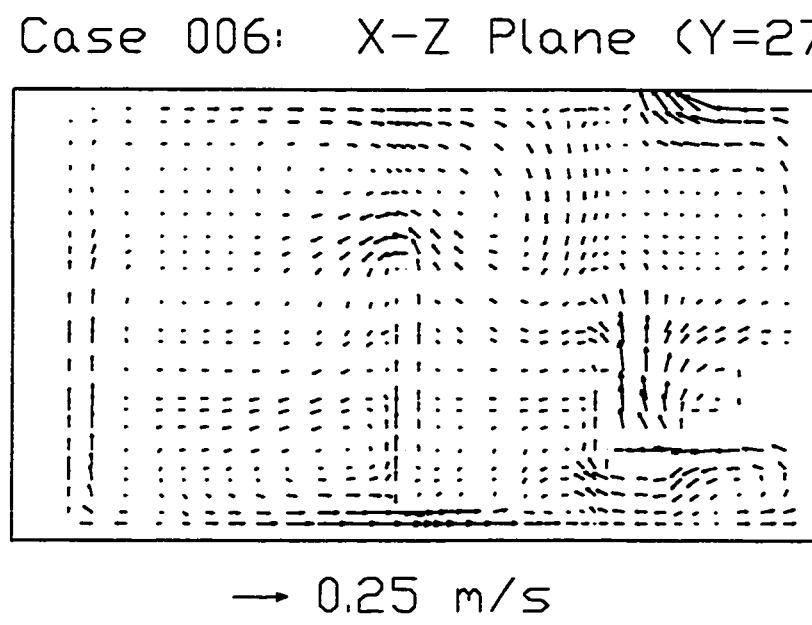

(c) Velocity Vectors in a Vertical Plane of Case 006

Figure 6.3 Simulation Velocity Vectors in a Vertical Plane

Figure 6.2 shows the velocity vectors in a horizontal plane of the test room. Comparing Figures 6.2(a) and 6.2(b), it can be seen that the influence of the partition on the air flow pattern in the room is obvious. Comparing Figures 6.2(b) and 6.2(c), it can be seen that the furniture has a great influence on the air flow pattern inside the workstation.

Figure 6.3 shows the velocity vectors in a vertical plane across the return grille. When comparing Figures 6.3(a) and 6.3(b), the influence of the partition on the air flow pattern in the room can be realized. It also shows that the air is moving over and through the partition gap, which agrees with the flow visualization observation results. This indicates that the partition gap influences the air flow pattern in the room. When comparing Figures 6.3(b) and 6.3(c), it can be realized that the furniture has a great

influence on the air flow pattern inside the room. Even the air flow around the return grille was changed while the furniture was present.

6.6.2 Simulation Results of Indoor Air Quality Indices

6.6.2.1 Air Distribution

Table 6.1 shows the air distribution simulation results. The simulation results agreed well with the experimental data for all three cases. This indicates that CFD simulation is applicable for air distribution analysis.

Table 6.1 Uniformity of Air Distribution Experimental and Simulation Results

	Time(min.)	Case 006	Case 007	Case 008
Experimental Results	10	0.957	0.968	
	15	0.972	0.958	0.984
	20	0.966	0.955	0.978
	25	0.974	0.960	0.966
	30	0.964	0.968	0.969
	35	0.955	0.967	0.964
	40	0.958	0.957	0.970
	45	0.958	0.952	0.972
	50	0.955	0.952	0.968
	55	0.959	0.960	0.971
	60	0.966	0.966	0.974
	65	0.965	0.970	0.974
	70	0.959	0.966	0.975
	75	0.954	0.963	0.979
	80	0.955	0.968	0.977
	85	0.962	0.965	0.968
	90	0.964	0.964	0.973
	95	0.961	0.965	0.985
	Average	0.961	0.962	0.973
Simulation Results	Steady State	0.968	0.972	0.987

The air distribution for the cases studied was quite uniform both in the experimental study and the CFD simulation study. These results yield a very important conclusion that, the air distribution system could not be the cause of indoor air quality problems, if any existed, while the HVAC system is well designed and maintained.

6.6.2.2 Local Mean Age of Air

Figure 6.4 shows the local mean age of air simulation results. Again, they agreed well with the experimental data in all three cases. The simulation results for Case 006 (see Figure 6.4(c)) had the biggest difference with the experimental data compared with the simulation results for the other two cases. Considering that the mean age of air is very sensitive to the outdoor air flow rate (Table 4.3) and a very low outdoor air flow rate was used in Case 006, this difference (approximately 10-15%) is acceptable. The simulation results indicated that CFD simulation is applicable for local mean age of air analysis.

The local mean age of air for the cases studied was uniform in the room and very sensitive to the outdoor air flow rate. This was demonstrated both in the experimental study and the CFD simulation study. Therefore, it can be concluded that it is very important to keep the supply outdoor air at an appropriate level for providing better indoor air quality in the room.

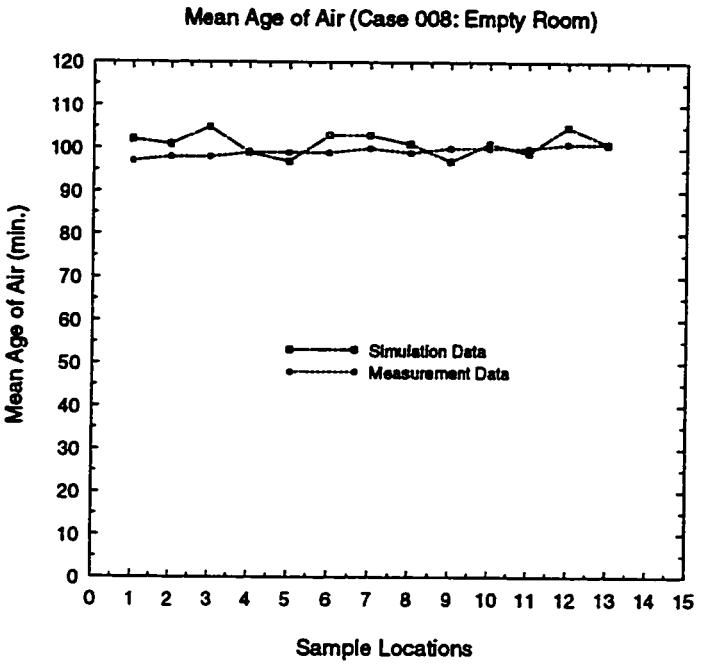

(a) Mean Age of Air Simulation Results for Case 008

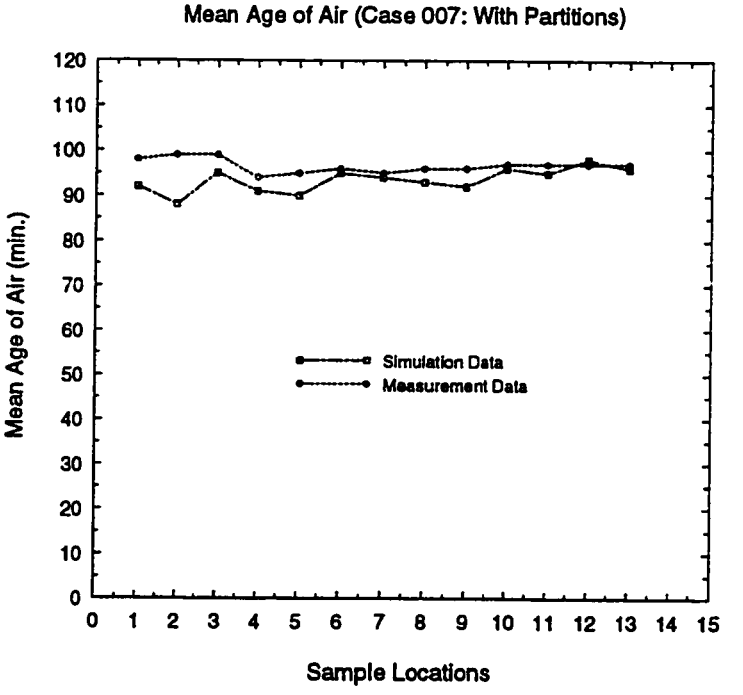

(b) Mean Age of Air Simulation Results for Case 007

Figure 6.4 Mean Age of Air Simulation Results

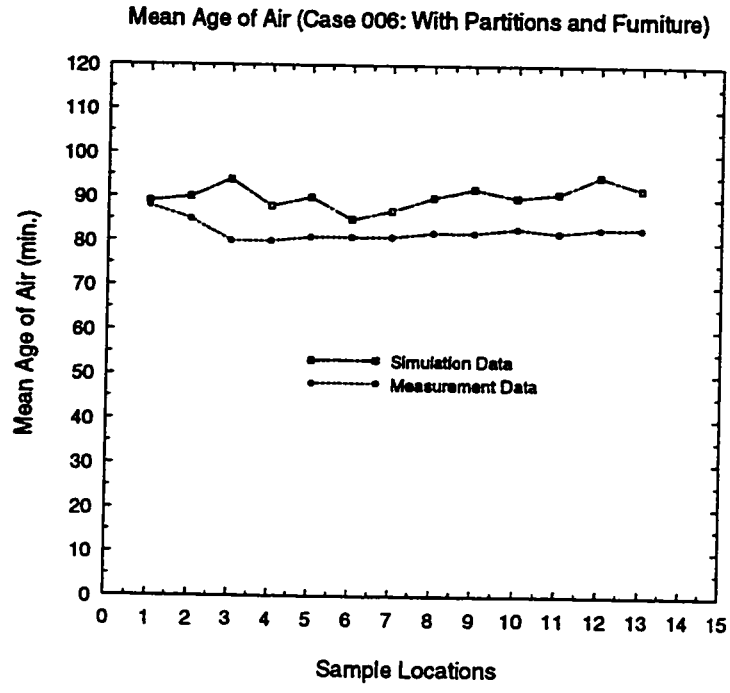

(c) Mean Age of Air Simulation Results for Case 006

Figure 6.4 Mean Age of Air Simulation Results

6.6.2.3 Contaminant Removal Efficiency

Figure 6.5 shows the contaminant removal efficiency simulation results. In general, the simulation result agreed well with the experimental data, even though a few points show greater discrepancy between the results. The trends in all these three cases were the same when comparing the experimental data and the simulation data. Considering the achievable CFD simulation accuracy for reality cases and the fluctuation of the contaminant distribution in the test room, these results were very encouraging. They indicate that the CFD method is applicable for contaminant distribution predictions.

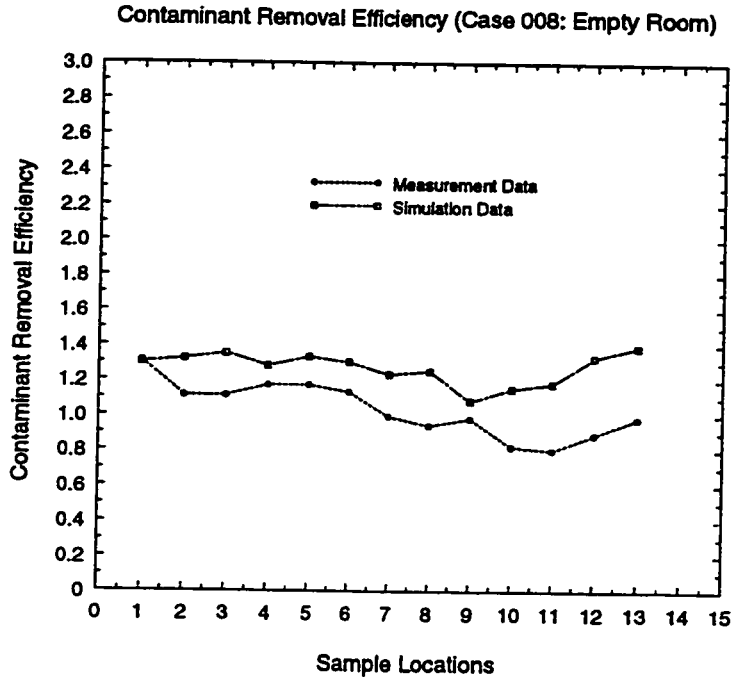

(a) Contaminant Removal Efficiency Simulation Results for Case 008

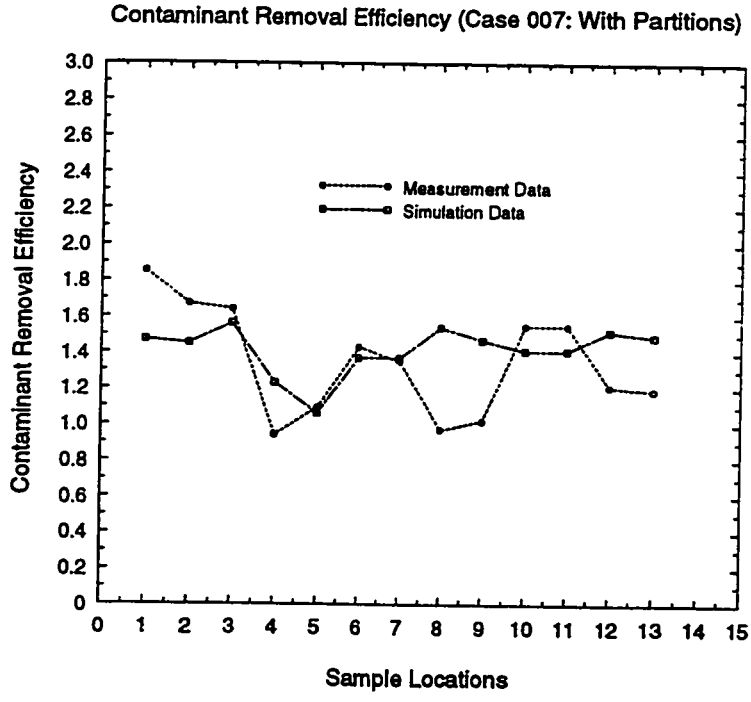

(b) Contaminant Removal Efficiency Simulation Results for Case 007

Figure 6.5 Contaminant Removal Efficiency Simulation Results

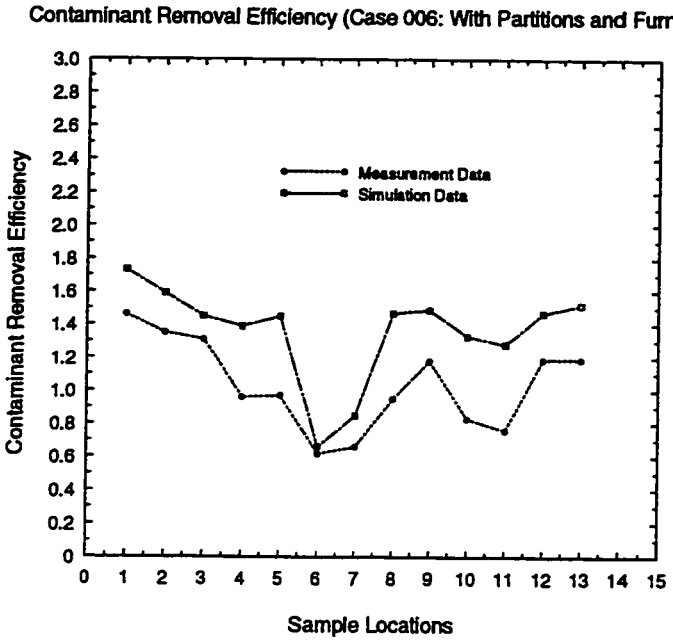

(c) Contaminant Removal Efficiency Simulation Results for Case 006

Figure 6.5 Contaminant Removal Efficiency Simulation Results

The contaminant concentration in the room was influenced by many factors, such as the room layout, the supply air and return air conditions, the partitions and furniture, the heat source in the room, etc. Each case must be studied separately when analyzing the contaminant distribution in a room. A lot of cases need to be studied to collect more information for the contaminant distribution in partitioned offices. The CFD simulation method can provide a very helpful tool for such amount of detailed predictions.

The study in this chapter compared the results of simulation and experiment for a real mechanically ventilated room, in terms of air distribution, mean age of air and contaminant removal efficiency. While the new proposed jet main region specification

method was applied to the supply diffuser description in CFD simulation, there was a good agreement between the simulating and experimental results. This further validated the new proposed diffuser description method. The new method provides a simplified an accurate way to overcome the big difficulty and inaccuracy in CFD simulation while the complicated geometry supply air diffuser is encountered in the studied office.

CHAPTER 7

CONCLUSIONS AND FUTURE WORK

7.1 DIFFUSER DESCRIPTION METHOD FOR CFD SIMULATION

A new jet main region specification method was proposed in this thesis to describe the complicated diffuser boundary conditions for CFD simulation. This new method was proven to be applicable and more accurate than the conventional method when a complicated geometry supply air diffuser was encountered in the study.

When the new jet main region specification method is used, the detailed description of the complicated supply diffuser geometry will be avoided, which is very difficult to be sufficiently described using the CFD simulation software; the air flow pattern in the room studied could be predicted correctly; a significant simulation time saving could be realized; and the new description method could be applied for most of the diffusers available from the industry.

The new jet main region specification method provides an effective and efficient way to apply the CFD simulation method for the analysis of real case indoor air quality problems.

7.2 IAQ CASE STUDIES IN A PARTITIONED OFFICE

Experimental and CFD simulation methods were applied to study the indoor air quality indices for a partitioned office. The important parameters which influence the indoor air quality in a partitioned office were identified.

For the partitioned office studied, the air distribution in the room was quite uniform in all the different conditions. Under the test conditions, the air distribution within the test workstation was not affected by the following parameters: diffuser type, air flow rate, workstation partitions, partition heights, partition bottom air gap, adjacent workstations, the locations of diffuser and return grille relative to the workstation. It indicated that, while the ventilation and air conditioning system is well designed, the air distribution is mostly not the main cause of indoor air quality problems.

The mean age of air was uniformly distributed in the room and was extremely sensitive to the outdoor air flow rate of the ventilation system. The increase of the outdoor

air flow rate can significantly improve the situation to solve the indoor air quality problems.

The air flow pattern has a significant influence on the contaminant distribution although it has very few influence on the supply air distribution in the room. The contaminant distribution was influenced by almost all the parameters in the office. Any changes in the partitioned offices, such as supply and return air conditions, layout of the room and partitions, the partition bottom air gap, the furniture positions in the office, heat source position and strength, the contaminant source positions, etc. will change the contaminant distribution in the room.

The workstation closest to the return grille appeared to have poor contaminant removal efficiency compared to the adjacent workstations, even if the contaminant source was not located inside this workstation, due to the migration of contaminants from adjacent areas. Efforts should be made to place known contaminant sources in workstations where the return grille is located.

There are some arguments among researchers for the partition bottom air gap influence on the indoor air quality problems in partitioned offices. The experimental and CFD simulation results of this thesis indicate that the partition gap has little influence on the supply air distribution but does have an influence on the contaminant distribution in

partitioned offices. When the contaminant source is located close to the gap, the influence of the partition gap on the contaminant movement inside a partitioned office is significant.

Providing the appropriate outdoor air and arranging the contaminant source in a right position will be the key factors to avoid indoor air quality problems in partitioned offices. It is possible to rearrange the contaminant distribution inside the office to resolve indoor air quality problems by changing the office layout, relative position of the heat sources and contaminant sources to the position of supply air and return air grilles.

The CFD simulation results, after applying the new jet main region diffuser description method, agreed well with the experimental data. This proved that the CFD simulation could provide a helpful tool for indoor air quality analysis. It is very important to have such a tool for the contaminant distribution analysis since the contaminant distribution is case based, any changes of office layout or heat source and contaminant source positions will influence the contaminant distribution inside the office. It is not affordable to use the experimental method to study each case separately.

7.3 FUTURE WORK

The new jet main region specification method should be verified for more different types of diffusers. The characteristic equations for these diffusers need to be further

studied and summarized. The CFD simulation application for real room indoor air quality analysis can be improved to be more applicable and reliable by simulating and summarizing more cases.

More detailed studies need to be conducted for the influence of ventilation on partitioned offices. The CFD simulation method can be applied in the work. The correlation of the parameters which influence the contaminant distribution in the offices should be developed. Remedies for improving the indoor air quality inside the partitioned offices should be proposed after these detailed studies.

The CFD simulation (a micro model studying for room air flow) should be combined with the multi-zone simulation models (macro models studying for room air flow) in indoor air quality analysis to study more related rooms. The multi-zone model can provide some input data for CFD simulation in the separated rooms. The CFD simulation can be used for detailed air and contaminant distribution analysis in that room. Cases need to be studied and the combined models need to be verified.

In near future, it is also expected that more innovative approaches are developed for room air distribution in office buildings. These new approaches offer an improved thermal comfort and air quality as well as reduced energy consumption.

The task-ambient air conditioning is one of the promising technologies. The floor-based, desk-based or partition-based air conditioning systems can relax temperature set-points in ambient areas. This technology can be further integrated with a desk displacement ventilation system.

Another innovative approach in improving the thermal environment is the new idea of intermittent air movement. A rotating supply air diffuser can be used to provide an intermittent air movement in the office. The main benefit of this approach is that, higher air temperature becomes acceptable in an air-conditioned space, resulting in significant energy savings.

Further research is needed to study the impact of these new innovative technologies on the quality of indoor environment and the consumption of energy in partitioned offices. This can be an exiting area of future research.

REFERENCES

Abramovich G.N. (1960) "The theory of turbulent jets", Moscow: Fizmatgiz.

AIVC (1991) "A guide to contaminant removal effectiveness", AIVC Tech. Note 28.2, Air Infiltration and Ventilation Centre, UK.

Albright L.D. (1989) "Research needs", Building System: Room Air and Air Contaminant Distribution, ASHRAE, U.S.A., pp. 8-10.

ASHRAE Fundamentals (1993) "Space air diffusion", Chapter 31, ASHRAE, U.S.A.

ASHRAE Standard 62-1989 (1989) "Ventilation for acceptable indoor air quality", ASHRAE, U.S.A.

ASHRAE Standard 55-1992 (1992) "Thermal environmental conditions for human occupancy", ASHRAE, U.S.A.

Baturin (1972) "Fundamentals of industrial ventilation", 3rd Edition, New York: Pergamon Press.

Bauman F.S, Faulker D., Arens E.A., Fisk W.J., Johnston L.P., McNeel P.J., Pih D. and Zhang H. (1991) "Air movement, comfort and ventilation in workstations", Final Report for Contract No. DE-AC03-76SF00098, Indoor Environment Program, Applied Science, Lawrence Berkeley Laboratory, U.S.A.

Brohus H. and Nielsen P.V. (1996) "CFD models of persons evaluated by full-scale wind channel experiments", 5th International Conference on Air Distribution in Rooms, RoomVent'96, Yokohama, Japan, Vol. 2, pp. 137-144.

Byred R.R. (1995) "Indoor air quality frequently asked questions", http://www.elitesoft.com/sci.hvac.

Chaturvedi S.K. et al (1989) "A CFD analysis of effects of vent location on pollutant concentration in rooms", Building System: Room Air and Air Contaminant Distribution, ASHRAE, U.S.A., pp. 158-160.

Chen Q. and Jiang Z. (1996) "Simulation of a complex air diffuser with CFD technique", 5th International Conference on Air Distribution in Rooms, RoomVent'96, Yokohama, Japan, Vol. 1, pp. 227-234.

Chen Q. and Jiang Z. (1992a) "Evaluation of air supply method in a classroom with a low ventilation rate", Proceedings of Indoor Air Quality, Ventilation and Energy Conservation Conference, Montreal, Canada, pp. 412-419.

Chen Q. and Jiang Z. (1992b) "Significant questions in predicting room air motion", ASHRAE Transaction, Vol. 98(1), pp. 929-939.

Chen Q. and Moser A. (1991a) "Simulation of a multiple nozzle diffuser", Proceedings of 12th AIVC Conference, oventry, UK: Air Infiltration and Ventilation Centre.

Chen Q. et al. (1991b) "A database for assessing indoor air flow, air quality and draught risk", Energy System Laboratory, Swiss Federal Institute of Technology.

Christianson L.L. et al (1994) "Low temperature air distribution: jet of low temperature air", Final Report for ASHRAE Project #705, ASHRAE, U.S.A.

Collett C.W. et al (1988) "Changing sick buildings into healthy buildings: improving the ventilation system", Healthy Buildings'88, Vol. 3, p. 55.

Daridge B. et al (1990) "Suggestions for avoiding indoor air quality complaints", Indoor Air'90, Vol. 3, p. 343.

Davidson L. and Nielsen P.V. (1996) "Large eddy simulations of the flow in a three-dimensional ventilated room", 5th International Conference on Air Distribution in Rooms, RoomVent'96, Yokohama, Japan, Vol. 2, pp. 161-168.

Doi S. (1996) "Measurement of multi-zone air flow and experimental house", 5th International Conference on Air Distribution in Rooms, RoomVent'96, Yokohama, Japan, Vol. 1, pp. 55-60.

Eftekhari M.M. (1996) "Air flow measurements in new houses", 5th International Conference on Air Distribution in Rooms, RoomVent'96, Yokohama, Japan, Vol. 1, pp. 35-40.

Emvin P. and Davidson L. (1996) "A numerical comparison of three inlet approximations of the diffuser in Case E1 Annex20", 5th International Conference on Air Distribution in Rooms, RoomVent'96, Yokohama, Japan, Vol. 1, pp. 219-216.

Evans R.G. and Shaw C.Y. (1988) "A multiposition tracer gas sampling system for building air movement studies", Paper 5, AIVC Measurement Techniques Workshop 1988.

Fanger P.O., Melikov A.K., Hanzawa H. and Ring J. (1989) "Turbulence and draft: the turbulence of airflow has a significant impact on the sensation of draft", ASHRAE J., Vol. 31, pp. 18-23.

Grimitlyn M., Zhivov A. and Pozin G. (1973) "Determination of parameters for the jet in a confined space following blocked or through flow pattern", Proceedings of Research Institutes for Labor Protection VTsSPS 91.

Guthrie A. (1996) "Designing for climate control in large volumes", 5th International Conference on Air Distribution in Rooms, RoomVent'96, Yokohama, Japan, Vol. 1, pp. 1-8.

Haghighat F., Huo Y, Zhang J.S. and Shaw C.Y. (1996) "The impact of office furniture, workstation layouts, diffuser types and location on indoor air quality and thermal comfort conditions in workstations", Journal of Indoor Air, No.6, 1996, pp.188-203.

Haghighat F. et al (1994a) "The influence of office furniture, workstation layouts, diffuser types and location on indoor air quality and thermal comfort conditions in workstations", Proceedings of Healthy Building'94, Budapest, Vol. 2, pp. 427-432.

Haghighat F., Jiang J. and Zhang Y. (1994b) "The impact of ventilation rate and partition layout on the VOC emission rate: time-dependent contaminant removal", Indoor Air, No 4, 1994, pp. 276-283.

Haghighat F., Jiang Z and Wang J.C.Y. (1991) "A CFD analysis of ventilation effectiveness in a partitioned room", Indoor Air, Vol. 1(3), pp. 606-615.

Heikkinen J. (1991) "Modeling of a supply air terminal for room air flow simulation", 12th AIVC Conference, Ottawa.

Huo Y., Zhang J. S., Shaw C. Y. and Haghighat F. (1996) "A new method to specify the diffuser boundary conditions in CFD simulation", 5th International Conference on Air Distribution in Rooms, RoomVent'96, Yokohama, Japan Vol. 2, pp. 232-240.

Huo Y., Zhang J. S., Shaw C. Y. and Haghighat F. (1995) "The impact of office furniture, workstation layouts, on indoor air quality in workstations", Proceedings of Healthy Building'95 Vol. 3, pp. 1329-1334.

Int-Hout D. (1981) "Measurement of room air diffusion in actual office environments to predict occpant thermal comfort", ASHRAE Transaction, Vol. 87(2), pp. 495-502.

Jiang Z. et al (1992) "Comparison of displacement and mixing diffusers", Indoor Air Vol. 2(2) p.168.

Kurabuchi T. et al (1989) "A numerical method for calculating indoor air flows using a turbulence model", U.S. Department of Commerce, NISTIR 89-4211.

Li Y.G. (1992) "Simulation of fluid and heat transfer in ventilated rooms", Ph.D. Thesis, Department of Mechanics, Royal Institute of Technology, Sweden.

Li Z. et al (1993) "Characteristics of diffuser air jets and air flow in the occupied regions of mechanically ventilated rooms -- a literature review", ASHRAE Transaction, Vol. 99(1), pp. 1119-1127.

Liddament M.W. (1987) "A review and bibliography of ventilation effectiveness -- definitions, measurement, design and calculation", AIVC, Technical Note 21, Air Infiltration and Ventilation Centre, UK.

Menzies R. et al (1993) "Varying ventilation conditions to provide a more complete assessment of building HVAC operation and indoor air quality", Indoor Air'93, Vol. 6, pp. 551- 556.

Miller P.L. (1971) "Room air distribution performance of few selected outlets", ASHRAE Trasaction, Vol. 77(2), pp. 194 - 204.

Murakami S. et al (1996) "Numerical prediction of flow around a building with various turbulence models: comparison of k-ε EVM, ASM, DSM and LES with wind tunnel tests", ASHRAE Transactions, Vol. 102(1), pp. 741-753.

Namiesnik J. et al (1992) "Indoor air quality (IAQ), pollutants, their sources and concentration levels", Building and Environment, pp. 339-356, No.3.

Nielsen P.V. (1992) "Description of supply openings in numerical models for room air distribution", ASHRAE Transaction, Vol. 98(1), pp. 963-971.

Nielsen P.V., Restivo A. and Whitelaw J.H. (1978) "The velocity characteristics of ventilated rooms", Journal of Fluid Engineering, Vol. 100, pp. 291-298.

Nordtest Method NTVVS019 (1983) "Buildings: local mean age", Nordtest, Finland.

Ohishi J. et al (1989) "Numerical prediction of room air distribution -- effects of calculation procedures at fluid-solid interfaces", Building System: Room Air and Air Contaminant Distribution, ASHRAE, U.S.A., pp. 161-168.

Peng S., Davidson L. and Holmberg S. (1996) "Performance of two-equation turbulence models for numerical simulation of ventilation flows", 5th International Conference on Air Distribution in Rooms, RoomVent'96, Yokohama, Japan, Vol. 2, pp. 153-160.

Rodi W. and Spalding D.B. (1983) "A two-parameter model of turbulence and its application to free jets", Numerical Prediction of Flow, Heat Transfer, Turbulence, and Combustion: Selected Works of Professor D. Brian Spalding, Oxford; New York: Pergamon Press, pp. 22-32.

Schiller G. et al (1990) "Air movement and comfort in workstations", Scientific Report, The University of California, Berkeley and Lawrence Berkeley Laboratory, U.S.A.

Shaw C.Y., Zhang J.S., Said M.N. and Vaculik P.E. (1993a) "Effect of air diffuser layout on the ventilation conditions of a workstation -- part I: air distribution patterns", ASHRAE Transaction, Vol. 99(2), pp. 125-132.

Shaw C.Y, Zhang J.S., Said M.N. and Vaculik F. (1993b) "Effect of air diffuser layout on the ventilation conditions of a workstation -- part II: air change efficiency and ventilation efficiency", ASHRAE Transaction, Vol. 99(2), pp. 133-142.

Shaw C.Y. (1992) "Application of tracer gas techniques to ventilation and indoor air quality investigations", Proceedings of Indoor Air Quality, Ventilation and Energy Conservation Conference, Montreal, Canada, pp. 235-245.

Shepelev I. (1961) "Air supply ventilation jets and air fountains", Proceedings of the Academy of Construction and Architecture of the USSR 4.

Takai T., Jacobson L.D., Morsing S., Madsen P. And Dahl P. (1996) "The analytical accuracy of multiple tracer gas techniques for measuring inter-zonal air flows", 5th International Conference on Air Distribution in Rooms, RoomVent'96, Yokohama, Japan, Vol. 1, pp. 69-76.

Tuve G.L. (1953) "Air velocity in ventilating jets". ASHRAE research report No.1467, ASHRAE Transaction Vol. 59, p. 261.

Valbjorn O. et al (1990) "Indoor climate and air quality problems -- investigation and remedy", SBI Report 212, Danish Building Research Institute.

Woods J.E. et al (1988) "Recent developments for heating, cooling and ventilation buildings: trends for assuring healthy buildings", Healthy Buildings'88, Vol. 1, p. 99.

Zhang G., Strom J.S. and Morsing S. (1996) "Jet drop models for control of cold air jet trajectories in ventilated livestock buildings", 5th International Conference on Air Distribution in Rooms, RoomVent'96, Yokohama, Japan, Vol. 1, pp. 305-316.

Zhang J.S. et al (1992a) "An experimental evaluation of a numerical simulation model for prediction room air motion", Proceedings of Indoor Air Quality, Ventilation and Energy Conservation Conference, Montreal, Canada, pp. 360-371.

Zhang J.S. et al (1992b) "Detailed measurements of room air distribution for evaluating numerical simulation models", ASHRAE Transaction, Vol. 98(1), pp. 58-63.

Zhang Y. (1996) "A study of the mechanisms of contaminant emissions from building materials", Ph.D. Thesis, Centre for Building Studies, Concordia University, Montreal, Canada.

Zhivov A. (1993) "Theory and practice of air distribution with inclined jets", ASHRAE Transaction, Vol. 99(1), pp. 1152-1159.